DESIGN AND PERFORMANCE OF TWO SPEED RELUCTANCE MOTOR

A DISSERTATION
Submitted in partial fulfilment
of the requirements for the award of the Degree
of
MASTER OF ENGINEERING
in
ELECTRICAL ENGINEERING
(Advanced Electrical Machines)

By
YOGESH KUMAR PANDEY

DEPARTMENT OF ELECTRICAL ENGINEERING
UNIVERSITY OF ROORKEE
ROORKEE (U.P.)
INDIA

August, 1974

CERTIFICATE

CERTIFIED that the dissertation entitled " DESIGN AND PERFORMANCE OF TWO SPEED RELUCTANCE MOTOR" which is being submitted by Shri Yogesh Kumar Pandey in partial fulfilment for the award of the Degree of Master of Engineering in Electrical Engineering (Advanced Electrical Machines) of the University of Roorkee, is a record of the student's own work carried out by him under my supervision and guidance. The matter embodied in this dissertation has not been submitted for the award of any other degree or diploma.

This is further to certify that he has worked for a total period of seven months from January 1974 to July, 1974 for preparing the dissertation for the Master of Engineering at the University of Roorkee.

SNSingh

(S.N. SINGH)
LECTURER
Electrical Engineering Deptt.,
University of Roorkee, Roorkee.

Roorkee
August , 1974.

ACKNOWLEDGEMENTS

I am deeply indebted to Shri S.N. Singh, Lecturer, Department of Electrical Engineering , University of Roorkee for his able guidance and sustained encouragement throughout this work.

I am thankful to Shri J.D. Sharma, Lecturer, Department of Electrical Engineering, University of Roorkee for his guidance in solving the optimisation problem.

I express my sincere thanks to Dr. T.S.M. Rao, Professor and Head of the Department of Electrical Engineering, University of Roorkee, for providing necessary facilities in department workshop, central workshop, Mechanical Engineering Departmental workshop and pilot Production cum Training Centre.

Thanks are also due to staff of the workshops and P.C. Laboratory for their assistance in fabricating and testing of the reluctance motor.

YOGESH KUMAR PANDEY

CONTENTS

Contents (Contd..)

V	Line voltage
ω	Angular velocity
X_d	Direct axis reactance
X_q	Quadrature axis reactance
x	Displacement
X_{ad}	Direct axis magnetising reactance
X_{aq}	Quadrature axis magnetising reactance
X_1	Leakage reac tance
$\alpha_2, \alpha_2', \alpha_3, \alpha_3'$	Flux Barrier parameters
α	Angular displacement round the air gap
δ	Mechanical load angle
δ_e	Electrical load angle.
μ_o	Permeability of free space
ϕ	Power factor angle
ϕ	Flux
θ	Instantaneous position of rotor
λ_o	Permeance constant
λ_{4p}	Permeance constant

S Y M B O L S

A, B, C, D, E	Channel parameters
B	Flux density
D	Rotor diameter
E	Generator emf
f	Supply frequency
g	Minimum air gap length
G	Maximum air gap length
H	Reluctance
H_d	Direct axis reluctance
H_q	Quadrature axis reluctance
h	Ratio G/g
I	Maximum value of current
i	Instantaneous value of current
J	Moment of inertia
K_ω	Winding factor
K	A constant defined within
M	MMF
m	Number of phases
p	Permeance
P	Rotor magnetic potential
p	Number of pole pairs
p	Derivative d/dt
r	Phase winding resistance
S	Slip
T	Torque
T_{po}	Pull out torque
T_a	Asynchronous torque
T_l	Load torque
T_r	Reluctance torque
t	Time

ABSTRACT

In the dissertation work the principle of flux barriers is extended to multispeed operation of reluctance motors. Analysis has been carried out for a two speed rotor incoorpprating essential as well as auxiliary barrier alongwith the interpolar channels.

A three phase reluctance motor is designed, fabricated and tested for different rotor designs. A search has been made for optimum value of the rotor interpolar channel parameters, to give equal maximum power factors for two speeds of operation with lower stator input current. An alternative method is suggested to predict the performance of a reluctance motor having only interpolar channels on the periphery of its rotor.

Test results of three rotor designs, for the same reluctance motor stator with analytical as well as optimised channel parameters have been recorded. Their performances are satisfactory and compare favourably with the suggested method of predicting the performance.

The pull-in criterion has been further generalised to include the viscous friction and coupling rigidity.

It is believed that if a rotor is designed incorporating the flux-barrier principle the performance of the motor at each speed, will become comparable to induction motor performance for the same frame and the reluctance motor may be preferred to all existing machines, in a large number of applications.

CHAPTER I

INTRODUCTION.

1.1 GENERAL

Reluctance motors were known to exist for over one and half a century. But they occupied very low position in the general family of rotating electric machines because of their poor performance as compared to the squirrel-cage induction motors of same size. But with the progressive increase in the demand of constant multi-speed drives in the industry, the research workers have been prompted to further improve the design of these motors with respect to both synchronous and asynchronous performances.

The reluctance motor operates on the principle of variable reluctance and has been defined by ASA as "a synchronous motor similar in construction an induction motor in which the member carrying the secondary circuit has salient poles without d.c. excitation. It starts as an induction motor but operates normally at synchronous speed".

1.2 [illegible] DEVELOPMENT

Significant improvements have been achieved in the past decade in the performance of reluctance motors. Lawrenson[1] (1964) proposed a segmental rotor which was superior to the previous salient pole rotors in all respec-ts except that it was mechanically a complicated structure to be fabricated. Kostko's[2] flux-barrier principle was also employed to increase the asymmetry in the magnetic circuit. Fong[3] (1967) extended the idea of pole amplitude modulation to two speed operation of the reluctance motor. Lawrenson[4] (1968) then extended his segmental rotor to multi speed operation. Again it was Fong[5] (1970) who applied the flux-barrier principle to obtain widely differing axes-reactances and achieved significantly high X_d/X_q ratio and hence far better single speed operation.

The synchronisation process was also a subject of study simultaneously. Lawrenson[6,7,8] has many papers to his credit which deal with different aspects of synchronisation. K. Burian[9] also studied the pull-in phenomenon and he gave a generalised analogue representation to search for the boundaries for inertia, slip etc. for successful synchronisation. Lawrenson[10] (1973) derived a pullin criterion which gave the values of inertia which could be synchronised if the induction motor action be strong enough to bring the rotor to a maximum speed corresponding to a fixed minimum slip.

1.3 SCOPE OF DISSERTATION WORK

In the dissertation work, the principle of flux barriers suggested by Fong[5] for single speed operation has been extended to multispeed range. Analysis has been carried out to obtain the ratio X_d/X_q for p- pair of poles. To facilitate the design, the same analysis has been repeated for (i) rotor structure having no barriers (ii) rotor structure having only essential barrier. In the first case analysis has been done in two ways (a) by the conventional analysis (b) by the employment of principle of net flux accumulation.

A suitable design procedure is then suggested to determine the optimum location and dimension of the interpolar channels, the essential barrier and the auxiliary barrier. Optimisation has accordingly been carried out to obtain simultaneously maximum values of X_d/X_q ratio for the two speeds of operation, thus deriving maximum possible torques for equal power factors. The experimental results are compared with the analytical results to establish the authenticity of the derived expressions. This established that the suggested method of analysis for determining the performance of a salient pole rotor gives better prediction of the performances of reluctance motor.

The pull-in criterion has also been modified to include the rigidity of the coupling and the viscous friction which have been shown to affect the pulling in significantly, by K. Ruzien[9]. Lawrenson[10] (1973) did not include these in his criterion.

As the pulling into step of a reluctance motor can be more easily studied by Lawrenson criterion, it is further generalised to also include the viscous friction and coupling rigidity constant.

CHAPTER II

THEORY OF OPERATION AND MAGNETIC CIRCUITS OF RELUCTANCE MOTOR

2.1 PRINCIPLE OF OPERATION

The stator of a reluctance motor is identical to that of an induction motor. It's speed being exactly related to the frequency of supply and the number of poles for which the armature winding is wound. Rotor of the machine, is in principle, similar to that of a squirrel-cage induction motor, excepting that the rotor punching is given such a shape that the fabricated rotor has got widely differing magnetic reluctances along different axes. The axis of least reluctance is known as the direct-axis; that of largest reluctance is known as the quadrature-axis. The revolving magnetic field produced in the stator causes the rotor to start revolving and to come upto near synchronous speed, by induction motor action. If now the mechanical load on the shaft of the machine is comparatively light, the slip would be negligibly small and the flux entering from the stator into the rotor tends to align itself to the path of least reluctance . Thus the rotor experiences a torque which tends to move the rotor so that the direct-axis coincides with the rotating flux axis, in the process, locking itself with the stator poles and the machine then operates at synchronous speed.

When the machine is operating without load, the rotating flux and the direct-axis of the rotor are exactly aligned (assuming losses in the machine to be negligible). If the machine is loaded, the rotor is displaced backwards relative to flux by a small angle known as the load angle. This load angle increases as the load increases, and if it exceeds a value of one half of a pole pitch, the motor is pulled out of synchronism. The value of load torque which is necessary to cause this pull-out is known as the pull-out torque. After being pulled-out of synchronism the motor continues to run with a slip in induction motor mode, until the load can be reduced sufficiently for the motor to again pull back into synchronism. The maximum resistive torque against which the motor is capable of pulling into synchronism is known as the pull-in torque and is a function of the load inertia, the saliency of rotor and the minimum slip which is attainable under the induction motor mode.

2.2 EXPRESSION FOR RELUCTANCE TORQUE

The reluctance torque is produced due to saliency of rotor only. It can be shown that the torque required to move the armature of an electrical machine through an angle $d\theta$ is given by

$$T = - \frac{1}{2} \phi^2 \frac{d R}{d\theta}$$

The expression clearly shows that the force set up in the system tends to decrease the reluctance and move the mechanical part towards the position of minimum reluctance [3]. The principle of operation of reluctance motor.

It has been shown in Appendix 9.1 that the motor torque T could be expressed in terms of flux and reluctance as

$$T = \frac{1}{8} \phi^2_{max.} (R_q - R_d) \sin 2\delta \qquad (2.1)$$

where R_q and R_d signifies the quadrature-axis and direct-axis reluctance respectively, ϕ_{max} is the maximum flux and δ is known as the load angle.

5 The same torque T can be written in terms of d-axis and q-axis reactances as

$$T = \frac{MV^2}{2\omega_s} \left(\frac{1}{X_q} - \frac{1}{X_d} \right) \sin 2\delta \qquad (2.2)$$

If now the frequency and magnitude of the supply voltage remain constant, the flux in the air-gap would also remain constant. The reluctances R_d and R_q are constant for a particular machine as these depend on the geometry of the magnetic circuit. Thus the only variable is the rotor phase angle δ.

When the load on the motor changes, load angle δ adjusts itself so that the electromagnetic torque developed by the motor becomes sufficient to drive the mechanical load connected to its shaft and the torque required to overcome the losses in the motor. If the load increases, the motor would momentarily slow down, thereby increasing the angles δ until sufficient electromagnetic torque is developed to carry the increased load. The operation is resumed at synchronous speed after a brief transient period. The maximum value of electromagnetic torque occurs at $\delta = 45^\circ$ for which expression for the torque becomes:

$$T_{max} = \frac{mV^2}{2\,\omega_s}\left(\frac{1}{X_q} - \frac{1}{X_d}\right) \qquad (2.3)$$

2.3 RATIO X_d/X_q

The expsessions for power factor and pull-out torque (sec. 3.6) suggest that the operation of reluctance motor depends primarily on the ratio of the direct-axis to quadrature-axis reactances, X_d/X_q ; the higher the ratio, the better is the performance. This can be achieved by increasing X_d and reducing the value of X_q. The direct-axis and quadrature-axis reactances are associated with the direct and quadrature-axes of the rotor. So by guiding the path of the flux along these axes, appropriate value of the two reactances can be obtained. It has also been established that the guiding of flux is mainly dependent on the asymmetry in the magnetic circuit, which therefore led to the investigation of various kinds of asymmetry in the magnetic circuit.

2.4 MAGNETIC CIRCUITS OF RELUCTANCE MACHINE

Since the date invented, reluctance machines have been built in varying degree of magnetic circuit proportions and have been used in a variety of applications . The earliest form of reluctance motor rotor was produced by simply milling out from the periphery of a squirrel-cage rotor two channels as shown in Fig. 2.1. The pole axis is the direct-axis of magnetisation. The path of direct-axis flux is shown by continuous lines. If the rotor is turned through an angle 90° from the original position, keeping the position of stator field same, it occupies the least favourable position with regard to the position of the flux. This is the position of quadrature-axis and the dotted line shows the path of the quadrature-axis flux.

The same motor could be operated for more than two poles on rotor. But the performance of the motor deteriorates as the number of poles, for which the stator is wound, increases. ~~This~~ It was due to very low value of X_d/X_q ratio made available by the magnetic circuit for higher pole numbers. It was later observed that for successful operation at higher pole numbers the rotor must have equal number of channels (or poles).

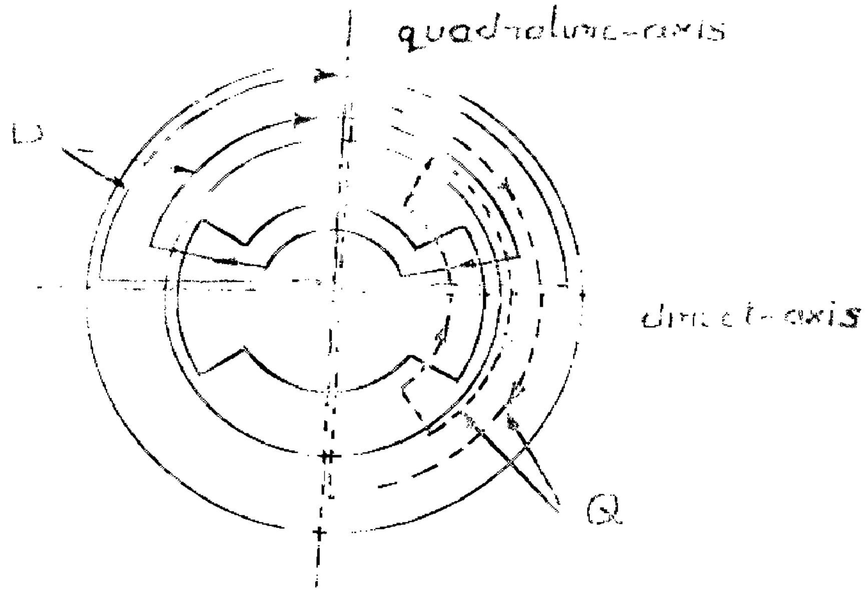

FIG. 2.1. Magnetic circuit of conventional reluctance motor.

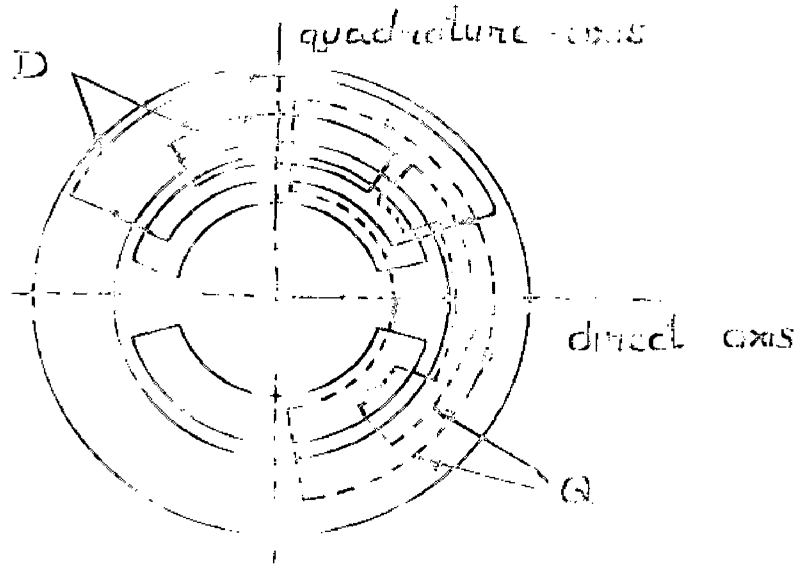

FIG. 2.2. Magnetic circuit of segmental rotor reluctance motor

The earlier designs, however, suffered from following disadvantages :

1. Low efficiency,
2. Low power factor,
3. Low output
4. High magnetising current.

The reason behind the above stated drawbacks being the inadequacy of the magnetic circuit to provide larger reluctance to the quadrature-axis flux which would lead to low qudrature-axis reactance and hence higher X_d/X_q ratio.

Though the very next form of the suggested rotor was a crude form of the present day single speed design, yet it was exploited for research work and commercial application only after another form of rotor called the segmental rotor came into existance. This type of rotor resulted in significant improvements in performance compared with the earlier designs.

The segmental rotor consists, magnetically, of a number (equal to number of magnetic poles for which stator is excited) of circumferentially extending pole segments. The shape along with magnetic circuit is as shown in Fig. 2.2, where lines marked D and Q are associated with direct and quadrature-axis fluxes respectively. As in the previous designs, direct-axis is the axis of minimum reluctance and the quadrature-axis that of maximum reluctance but as is clear from Fig. 2.2, that the direct axis coincides, not with the pole centre line (Fig.2.1)

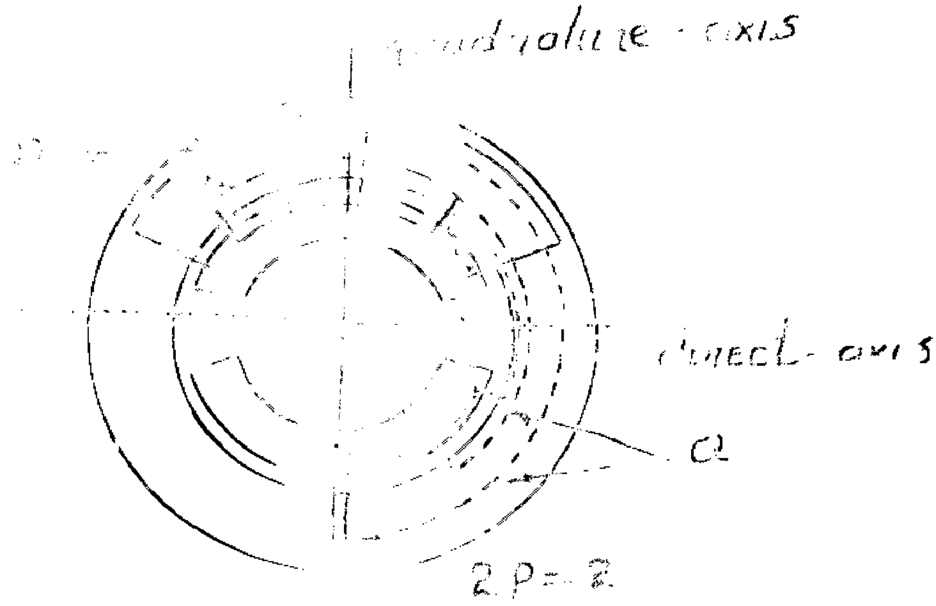

FIG 2.8 Improved segmental rotor type
(a)

Fig 2.8 Improved segmental rotor type
(b)

but with the centre of the interpolar space.

Consideration of the corresponding flux paths shows the advantage of the new circuit. The radially extending interpolar space has only a slight effect on the direct-axis paths it lies across, and has a much greater effect on the quadrature-axis paths. Consequently even with larger values of the pole arc and hence low magnetising current, larger value of ratio X_d/X_q could be attained. Thus, advantage of the geometry of this rotor lamination is the improvement in both synchronous and asynchronous performances . The success of segmental rotor further led to the milling out of channels on the pole segment (Fig. 2.3) and thereby reducing the quadrature-axis reactance and giving still higher ratio of direct-axis to quadrature-axis reactances.

The segmental form, however, posed problems with mechanical design as the combined magnetic and centrifugal forces on each segment may become considerable . Also, these rotors require non-magnetic steel shafts and non-magnetic steel bolts. These drawbacks cleared the way for employment of flux barriers (or guides).

The ideal for a reluctance motor is to produce strongly directional rotor while maintaining a standard type of construction. The principle of flux guides employ one such system per pole. Each system is comprised of one essential barrier and one auxiliary barrier. Various rotor

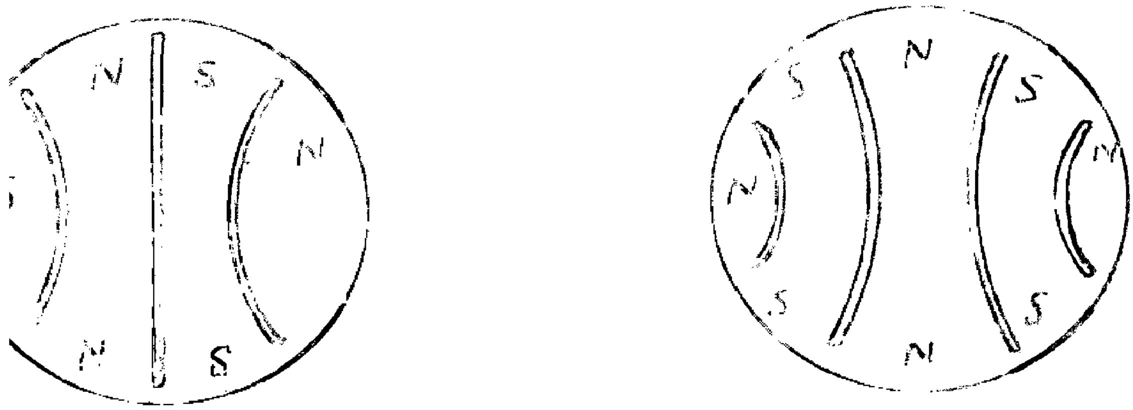

p = 3.   p = 4.

FIG. 2.[illegible].

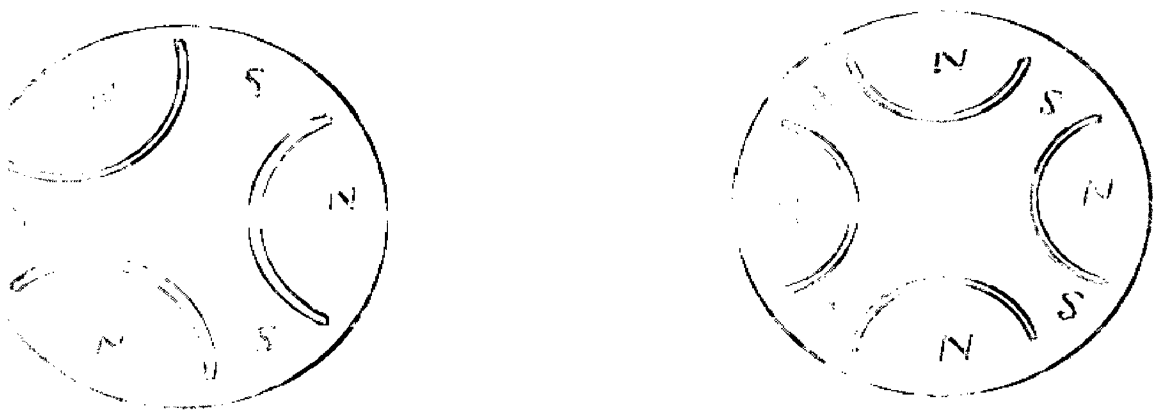

p = 3   p = 4

FIG. 2.5. Rot[illegible] employing flux barr[illegible]
(with [illegible] per pole pair)

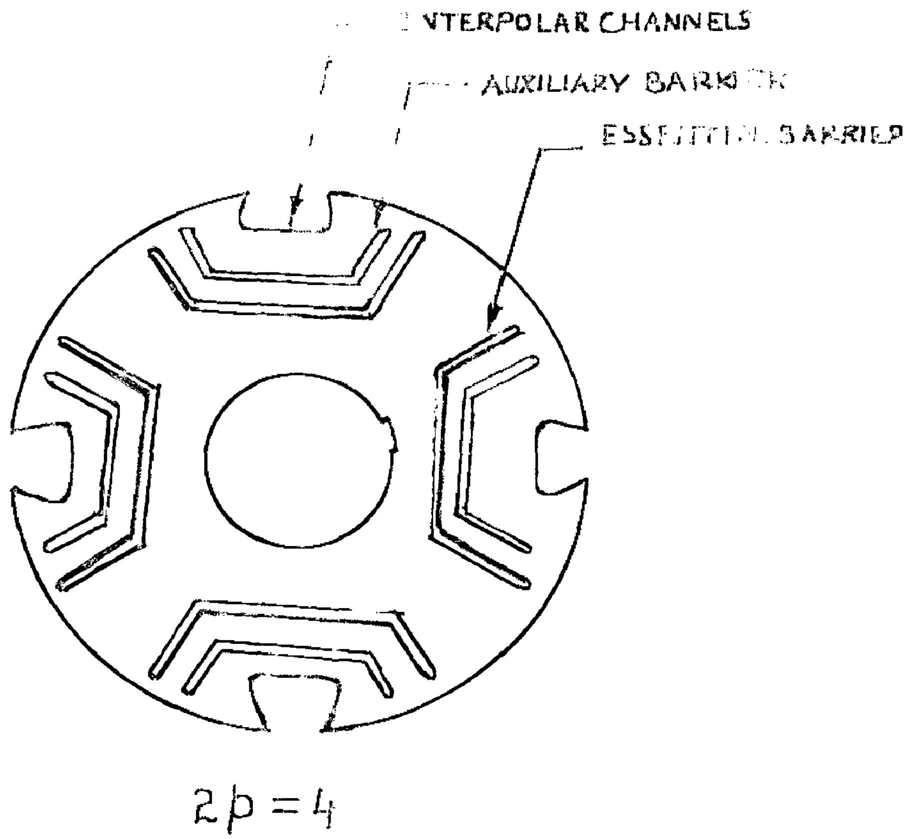

FIG 2.6. Rotor structure with one set of barriers per pole.

laminations employing barriers for single speed operation are shown in Figs. 2.4, 2.5, 2.6.

The latest approach has been to employ one system of flux-barriers per pole pair rather than per pole. The ends of each flux barrier always coincide with two direct-axes; and P flux barriers divided the periphery of the rotor into 2P equal parts (Fig. 3.P) . This approach changes the flux paths in such a way that there is no need for a stainless steel shaft. All materials used in the fabrication are standard and cost is expected to be equal to that of a squirrel-cage induction motor, if specially punched laminations can be made available.

2.5 EXTENSION OF PRINCIPLE TO TWO SPEED

The multi-speed operation of reluctance machine has been of interest for a long time due to the possibility of obtaining perfect constant speed from them without having the d.c. excitation in normal synchronous machines Among the notable contribution the earliest was the modification of the conventional machine (Fig. 2.1) to yield speeds in the ratio 2:1 . Two and more speeds were also derived from segmental rotor. But two poles on rotor and two or more poles excitation on stator, could not give satisfactory performance. It was observed from the derived expressions that higher X_d / X_q ratio can be achieved if number of channels, milled on rotor periphery are made equal to the higher number of poles for which stator is wound. A compromised rotor design is therefore essential for successful operation at two different speeds.To fulfil this requirement a rotor with unevenly spaced channels on its periphery (Fig. 3.5) was developed.

In the present work, theprinciple of flux-barriers is being incorporated with the above rotor with optimised pole widths and locations, for improved operation of the reluctance motor at two different speeds as the principle permits the combination of any one set of essential-barrier with another set to give a change-speed rotor.

CHAPTER III

ANALYSIS OF TWO SPEED ROTOR

3.1 SIMPLIFYING ASSUMPTIONS

The following assumptions are made in order to simplify the analysis:

1. Iron is infinitely permeable and hysteresis and eddy currents are negligible.
2. Effective flux-linkages are produced only by fundamental component of air-gap flux-density.
3. A sinusoidal space distribution of m.m.f is considered.

3.2 ANALYSIS WITH INTERPOLAR CHANNELS AND FLUX BARRIERS INCLUDED IN THE ROTOR STRUCTURE

3.2.1 Description of Lamination

Fig. 3.1 shows an eight pole rotor lamination with four auxiliary barriers enclosed within the four essential barriers. The interpolar channels of the earlier designs have been retained as such. The lamination also has peripheral slots punched out to accommodate the squirrel-cage winding in the usual manner for starting the motor and bringing its speed very near to synchronous speed of the motor (not shown in the Figure). Each flux-barrier is made up of three parts, a central channel, auxiliary barrier

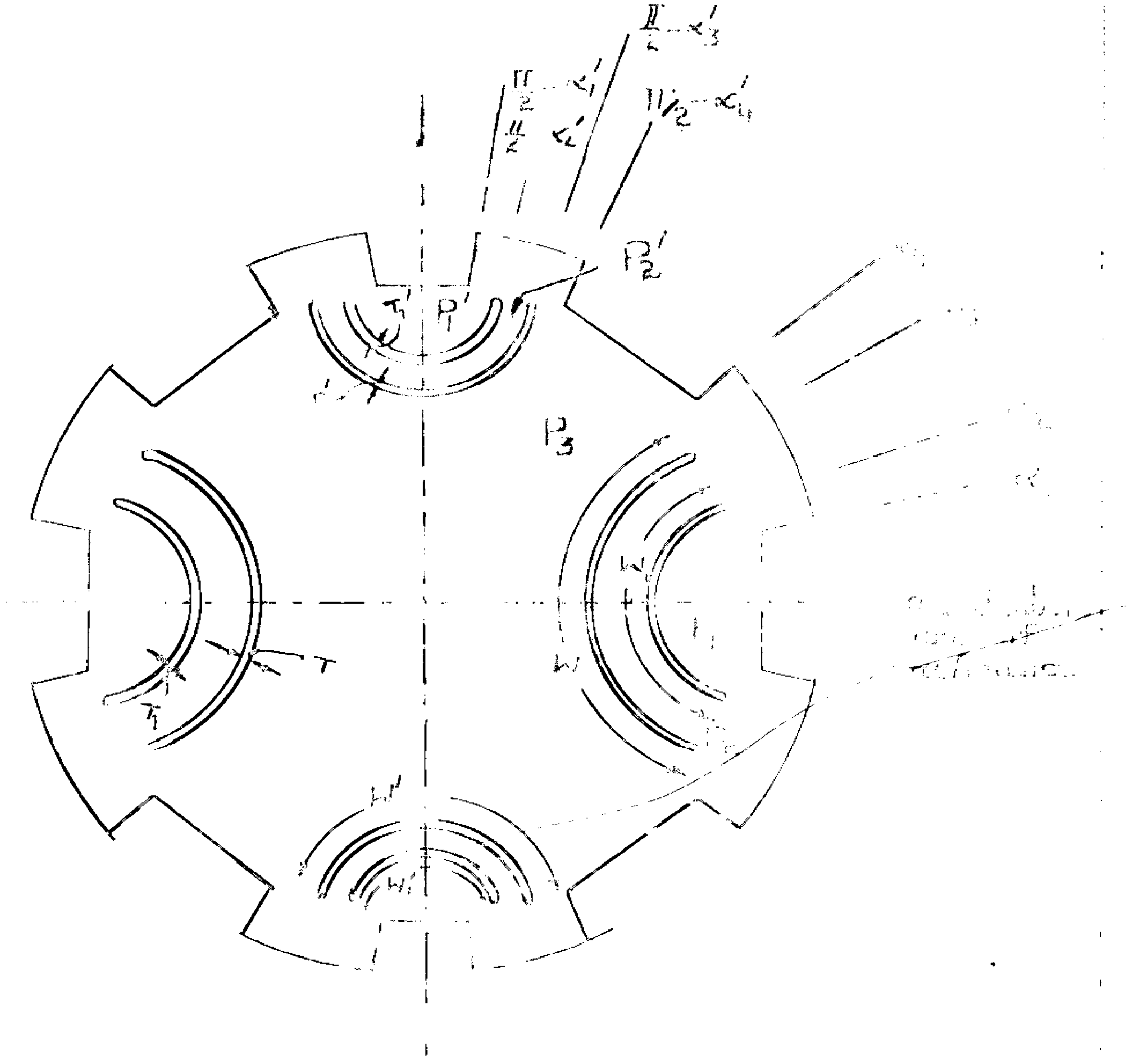

FIG 3.1. Rotor lamination [illegible]

and essential barrier.

Relative to the quadrature-axis, positioned at the centre of a channel , the peripheral location of the flux-barriers and the interpolar channels are defined as follows :

First pole-end is marked at an angle α_1 radians. The auxiliary-barrier o f W_1 width and T_1 Thickness is situated at α_2 radians. This auxiliary-barrier and an essential - barrier of width W and thickness T , situated at α_3 radians are symmetrically placed about the reference axis. The far-end of pole is at α_4 radians. Next pole starts at $\pi/2 - \alpha_4'$ and finishes at $\pi/2 - \alpha_3'$ radians. Essential-barrier with W' width and T' thickness is located at $\pi/2 - \alpha_3'$ radians while the auxiliary barrier with W_1' width and T_1' thickness is situated at $\pi/2 - \alpha_4'$. These two are also symmetrically placed about an axis at right angle to the original reference axis. If the angles (position) of second set of barriers and pole is referred to this axis then the angles will read : α_1' , α_4' for pole-ends, and α_2' , α_3' for auxiliary and essential-barrier respectively.

3.2.2. Direct-Axis Flux-density

This is the amplitude of the fundamental air-gap flux-density wave when the rotor direct-axis are coincident with the axes of the fundamental stator m.m.f. wave. It's amplitude is obtained by Fourier's analysis as :

$$B_{1d} = \frac{4}{\pi} \int_{0}^{\pi/2} (\text{m.m.f}) \, (\text{Permeance}) \sin P\theta \, d\theta$$

$$= \frac{4}{\pi} \int_{0}^{\pi/2} (H_{1d} \sin p\theta) \, . \, \lambda(\theta) . \sin p\theta \, d\theta \quad (3.1)$$

Where the value of $\lambda(\theta)$ keeps on changing with angle, as measured from the reference axis. Variation of permeance is defined by Table No. 3.1.

Table 3.1

Value of permeance $\lambda(\theta)$	Range with respect to reference axis.
μ_o/G	0 to α_1
μ_o/g	α_1 to α_2
μ_o/g	α_2 to α_3
μ_o/g	α_3 to α_4
μ_o/G	α_4 to $\frac{\pi}{2} - \alpha'_4$
μ_o/g	$\frac{\pi}{2} - \alpha'_4$ to $\frac{\pi}{2} - \alpha'_3$
μ_o/g	$\frac{\pi}{2} - \alpha'_3$ to $\frac{\pi}{2} - \alpha'_2$
μ_o/g	$\frac{\pi}{2} - \alpha'_2$ to $\frac{\pi}{2} - \alpha'_1$
μ_o/G	$\frac{\pi}{2} - \alpha'_1$ to $\pi/2$

Integration of eqn 3.1 after proper substitutions and simplifications (Appendix 9.2) gives the value of flux-density B_{1d} as :

$$B_{1d} = \frac{2\,\mu_0\,H_{1d}}{\pi\,g}\left[\left\{\frac{\pi}{2h} + \left(1 - \frac{1}{h}\right)(\alpha_b - \alpha_1 + \alpha'_b - \alpha'_1)\right\}\right.$$

$$- \frac{1}{2p}\left\{\sin 2p\,\alpha_b - \sin 2p\,\alpha_1 - \sin 2p\left(\frac{\pi}{2} - \alpha'_b\right)\right.$$

$$\left.\left. - \sin 2p\left(\frac{\pi}{2} - \alpha'_1\right)\right\}\left(1 - \frac{1}{h}\right)\right] \qquad (3.2)$$

In the above expression h is the ratio of maximum air-gap to minimum air-gap.

3.2.3 Direct-axis Magnetising Reactance

The value of unsaturated direct-axis magnetising reactance is given by :

$$X_{ad} = K\,(B_{1d} / H_{1d}) \qquad (3.3)$$

where

K = $24\,DL\,f(N\,K_w)^2$

D = Rotor diameter

L = Core length

N = Series turns/pole/phase

K_w = Winding factor

Substituting Eqn 3.2 in 3.3, the value of X_{ad} is determined. The expression for X_{ad} is :

$$X_{ad} = \frac{2\mu_0 K}{\pi\,g}\left[\left\{\frac{\pi}{2h} + \left(1 - \frac{1}{h}\right)(\alpha_b - \alpha_1 + \alpha'_b - \alpha'_1)\right\} - \frac{1}{2p}\left\{\sin 2p\alpha_b\right.\right.$$

$$\left.\left. - \sin 2p\alpha_1 - \sin 2p\left(\frac{\pi}{2} - \alpha'_b\right) + \sin 2p\left(\frac{\pi}{2} - \alpha'_1\right)\right\}\left(1 - \frac{1}{h}\right)\right]$$

(3.4)

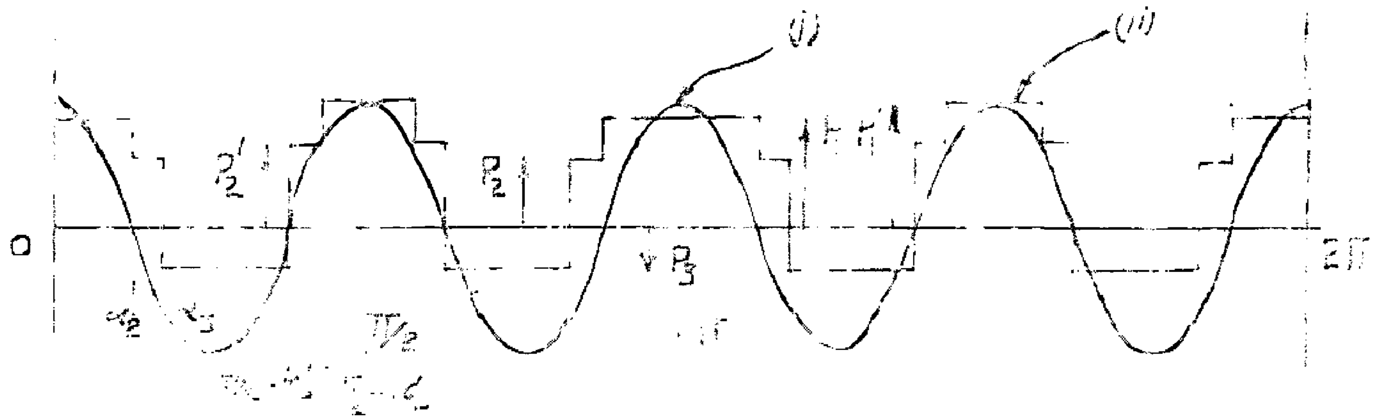

FIG. 3.7. M.M.F. of 8-pole ROTOR with auxiliary barriers.

(i) Stator m.m.f. $H_{1q} \cos p\theta$ $(p=4)$.

(ii) Rotor m.m.f.

3.2.4 Rotor Magnetic Potentials

The rotor lamination of Fig. 3.1 is supposed to be divided into three typical regions. First region has the interpolar channel, second is in between the auxiliary and essential-barrier and the third region extends beyond the essential barrier.

Owing to the presence of those flux-barriers the various regions in the rotor take up different magnetic potentials. The rotor magnetic potentials constitute an opposing rotor m.m.f. wave, set up under the influence of a fundamental stator m.m.f. wave. The rotor m.m.f. wave is of stepped form as shown in Fig. 3.2 To determine the height of the rotor m.m.f. wave in various regions, use can be made of the condition that the summation of the flux in any enclosed part of the rotor is zero.

Assuming P to be the general height of the rotor magnetic potential, its value in different regions is defined as given in Table 3.2.

Equating to zero, the summation of flux per unit length in the third, second and first region defined earlier, the following expressions are written :

$$2\left[\int_{\alpha_3}^{\alpha_4} \frac{\mu_o}{g}(H_{1q}\cos p\theta - P_3)\frac{D}{2}\,d\theta + \int_{\alpha_4}^{\pi/2-\alpha_4'} \frac{\mu_o}{G}(H_{1q}\cos p\theta - P_3)\cdot\frac{D}{2}\,d\theta + \int_{\frac{\pi}{2}-\alpha_4'}^{\frac{\pi}{2}-\alpha_3'} \frac{\mu_o}{g}(H_{1q}\cos p\theta - P_3)\frac{D}{2}\,d\theta + \mu_o(-P_3+P_2)\frac{W}{2T} + \mu_o(-P_3+P_2')\cdot\frac{W'}{2T'}\right] = 0 \qquad (3.5)$$

and

$$2\left[\int_{\alpha_2}^{\alpha_3} \frac{\mu_o}{g} (E_{1q} \cos p\theta - P_2)\frac{D}{2}\, d\theta + \mu_o(P_1 - P_2)\frac{W_1}{2T_1} + \mu_o(P_3 - P_2)\frac{W}{2T}\right] = 0 \qquad (3.6)$$

and

$$2\left[\int_{0}^{\alpha_1} \frac{\mu_o}{G}(E_{1q} \cos p\theta - P_1)\frac{D}{2}\,d\theta + \int_{\alpha_1}^{\alpha_2} \frac{\mu_o}{g}(E_{1q} \cos p\theta - P_1)\frac{D}{2}\, d\theta + \mu_o(P_2 - P_1)\frac{W_1}{2T_1}\right] = 0 \qquad (3.7)$$

Table 3.2

Value of P	Range with respect to the reference axis.
P_1	0 to α_1
P_1	α_1 to α_2
P_2	α_2 to α_3
P_3	α_3 to α_4
P_3	α_4 to $\frac{\pi}{2} - \alpha_4'$
P_3	$\frac{\pi}{2} - \alpha_4'$ to $\frac{\pi}{2} - \alpha_3'$
P_2'	$\frac{\pi}{2} - \alpha_3'$ to $\frac{\pi}{2} - \alpha_2'$
P_1'	$\frac{\pi}{2} - \alpha_2'$ to $\frac{\pi}{2} - \alpha_1'$
P_1'	$\frac{\pi}{2} - \alpha_1'$ to $\pi/2$

Solution of these equations (Appendix 9.3.1 to 9.3.3) gives values of P_3, P_2 and P_1 as follows :

$$P_3 = \frac{A + P_2 \frac{U}{T} + P_2' \cdot \frac{U'}{T'}}{B} \qquad (3.8)$$

$$P_2 = \frac{A_1 + P_1 \cdot \frac{U_1}{T_1}}{B_1} \qquad (3.9)$$

and
$$P_1 = \frac{H_{1q}\left[\frac{\sin p\alpha_1}{p\delta/D} + \frac{\sin p\alpha_2 - \sin p\alpha_1}{p\delta/D}\right] + \frac{A_1}{B_1}\cdot\frac{U_1}{T_1}}{\frac{\alpha_1}{\delta/D} + \frac{\alpha_2 - \alpha_1}{\delta/D} + \frac{U_1}{T_1} - \frac{1}{B_1}\left[\frac{U_1}{T_1}\right]^2} \qquad (3.10)$$

where

$$A_1 = H_{1q}\left[\frac{\sin p\alpha_3 - \sin p\alpha_2}{p\delta/D}\right] + \frac{A}{B}\cdot\frac{U}{T} \qquad (3.11)$$

$$B_1 = \frac{\alpha_3 - \alpha_2}{\delta/D} + \frac{U_1}{T_1} + \frac{U}{T} - \frac{1}{B}\left(\frac{U}{T}\right)^2 \qquad (3.12)$$

$$A = H_{1q}\left[\frac{\sin p\alpha_4 - \sin p\alpha_3}{p\delta/D} + \frac{\sin p(\pi/2 - \alpha_4') - \sin p\alpha_4}{p\delta/D} + \frac{\sin p(\pi/2 - \alpha_3') - \sin p(\pi/2 - \alpha_4')}{p\delta/D}\right] \qquad (3.13)$$

$$B = \frac{\alpha_4 - \alpha_3}{\delta/D} + \frac{\pi/2 - \alpha_4' - \alpha_4}{\delta/D} + \frac{\alpha_4' - \alpha_3'}{\delta/D} + \frac{U}{T} + \frac{U'}{T'} \qquad (3.14)$$

Similarly, the expressions for rotor magnetic potentials P_2' and P_1' can be derived (Appendix 9.3.4, 9.3.5) as:

$$P'_2 = \frac{A'_1 + D'_1 \cdot \dfrac{U'_1}{T'_1}}{B'_1} \qquad (3.15)$$

and

$$P'_1 = \frac{H_{1q}\left[\dfrac{\sin p(\pi/2 - \alpha'_1) - \sin p(\pi/2 - \alpha'_2)}{pG/D} + \dfrac{\sin p\beta/2 - \sin p(\pi/2 - \alpha'_1)}{pG/D}\right] + \dfrac{A'_1}{B'_1} \cdot \dfrac{U'_1}{T'_1}}{\dfrac{\alpha'_1}{G/D} + \dfrac{\alpha' - \alpha'}{G/D} + \dfrac{U'_1}{T'_1} - \dfrac{1}{B'_1}\left(\dfrac{U'_1}{T'_1}\right)^2} \qquad (3.16)$$

where,

$$A'_1 = H_{1q}\left[\frac{\sin p(\pi/2 - \alpha'_2) - \sin p(\pi/2 - \alpha'_3)}{pG/D}\right] + \frac{A}{B} \cdot \frac{U'}{T'} \qquad (3.17)$$

$$B'_1 = \frac{\alpha'_3 - \alpha'_2}{G/D} + \frac{U'_1}{T'_1} + \frac{U'}{T'} - \frac{1}{B}\left(\frac{U'}{T'}\right)^2 \qquad (3.18)$$

Thus the values of P_2, P_3 and p'_2 can be determined by proper substitutions.

3.2.5 Quadrature-axis flux -density

This is the amplitude of the fundamental air-gap flux-density wave when the rotor quadrature-axes are coincident with the axis of the fundamental stator m.m.f. wave. It is equal to the difference between the stator m.m.f. and the rotor m.m.f's multiplied by the permeance. By Fourier's analysis the amplitude of the fundamental air-gap flux-density wave can be obtained from the expression.

$$B_{1q} = \frac{4}{\pi} \int_0^{\pi/2} \left[B_{1q} \cos p\theta - P(\theta) \right] \cdot \lambda(\theta) \cdot \cos p\theta \, d\theta$$

(3.19)

where $P(\theta)$ and $\lambda(\theta)$ take the values given by table 3.1 and 3.2 respectively.

The expression for B_{1q} is derived in Appendix 9. and is shown as :

$$B_{1q} = \frac{2\mu_0}{\pi g} \left[B_{1q} \left\{ \frac{\pi}{2h} + (\alpha_4 - \alpha_1 + \alpha_4' - \alpha_1') (1 - \frac{1}{h_1}) \right. \right.$$

$$+ \frac{1}{2p} \left\{ \sin 2p\alpha_4 - \sin 2p\alpha_1 - \sin 2p(\pi/2 - \alpha_4') + \sin 2p(\pi/2 - \alpha_1') \right\} (1 - \frac{1}{h})$$

$$- \frac{2}{p} \left\{ \left\| -P_1 \sin p\alpha_1 + P_3(\sin p\alpha_4 - \sin p(\pi/2 - \alpha_4')) + P_1' \sin P(\pi/2 - \alpha_1') \right\| (1 - \right.$$

$$+ (P_1 - P_2) \sin p\alpha_2 + (P_2 - P_3) \sin p\alpha_3 + (P_3' - P_2') \sin p(\pi/2 - \alpha_3')$$

$$\left. \left. + (P_2' - P_1') \sin p(\pi/2 - \alpha_2') + \frac{P_1' \sin p\,\pi/2}{h} \right\} \right] \qquad (3.20)$$

3.2.6 Quadrature-axis Magnetising Reactance

The value of quadrature-axis magnetising reactance is given by:

$$X_{aq} = K \left(\frac{B_{1q}}{B_{1q}} \right) \qquad (3.21)$$

Substituting equation 3.20 in 3.21, the final expression for X_{aq} can be written as :

$$X_{aq} = \frac{2\mu_0 K}{\pi g}\left[\frac{\pi}{2h} + (\alpha_4 - \alpha_1 + \alpha'_4 - \alpha'_1)\left(1 - \frac{1}{h}\right)\right.$$

$$+ \frac{1}{2p}\left\{\sin 2p\alpha_4 - \sin 2p\alpha_1 - \sin 2p(\pi/2 - \alpha'_4) + \sin 2p\left(\frac{\pi}{2} - \alpha'_1\right)\right\}$$

$$\left(1 - \frac{1}{h}\right) - \frac{2}{pH_{1q}}\left\{\left[-P_1 \sin p\alpha_1 + P_3\left(\sin p\alpha_4 - \sin p\left(\frac{\pi}{2} - \alpha'_4\right)\right) + P'_1 \sin p\left(\frac{\pi}{2} - \alpha\right.\right.\right.$$

$$\cdot\left(1 - \frac{1}{h}\right) + (P_1 - P_2)\sin p\alpha_2 + (P_2 - P_3)\sin p\alpha_3 + (P'_3 - P'_2)\sin p\left(\frac{\pi}{2} - \alpha'_3\right)$$

$$\left.\left.+ (P' - P')\sin p(\pi/2 - \alpha') + \frac{P'_1 \sin p\frac{\pi}{2}}{h}\right\}\right] \qquad (3.22)$$

3.3 ANALYSIS OF TWO SPEED ROTOR WITH INTERPOLAR CHANNELS (Without Flux-barriers, employing the Conventional Method of Analysis).

3.3.1 Permeance Distribution

The rotor of a reluctance motor has salient poles on its periphery. Each pole corresponds to a complete cycle in permeance and the air-gap permeance distribution for a 2p - pole reluctance motor of this type can thus be expressed in terms of the angular displacement θ around the rotor periphery as $\lambda_0 + \lambda_{4p} \cos 2p\theta$ + higher order harmonics, where p is the fundamental number of pole pairs i.e. by a constant term λ_0, together with a dominant second-harmonic (4 p - pole), component and higher order harmonics of

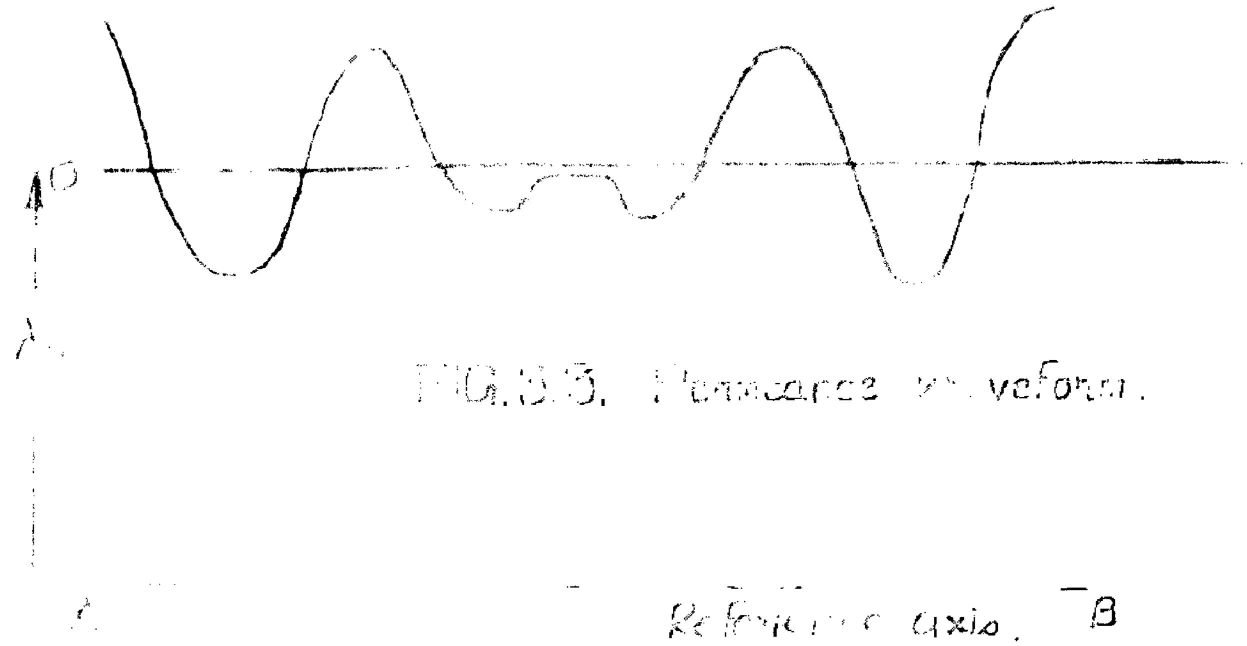

FIG. 3.3. Permeance waveform.

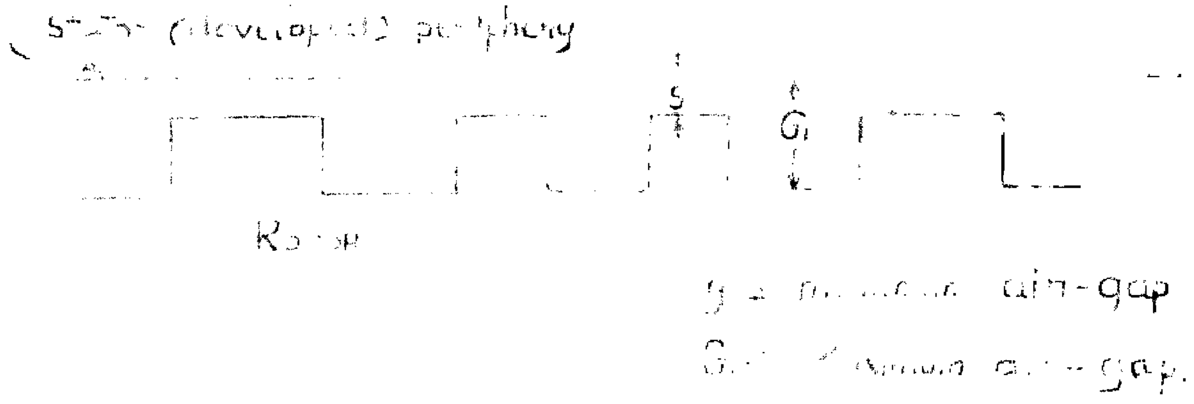

FIG. 3.4. Bivalued function representing the permeance distribution of Fig. 3.3.

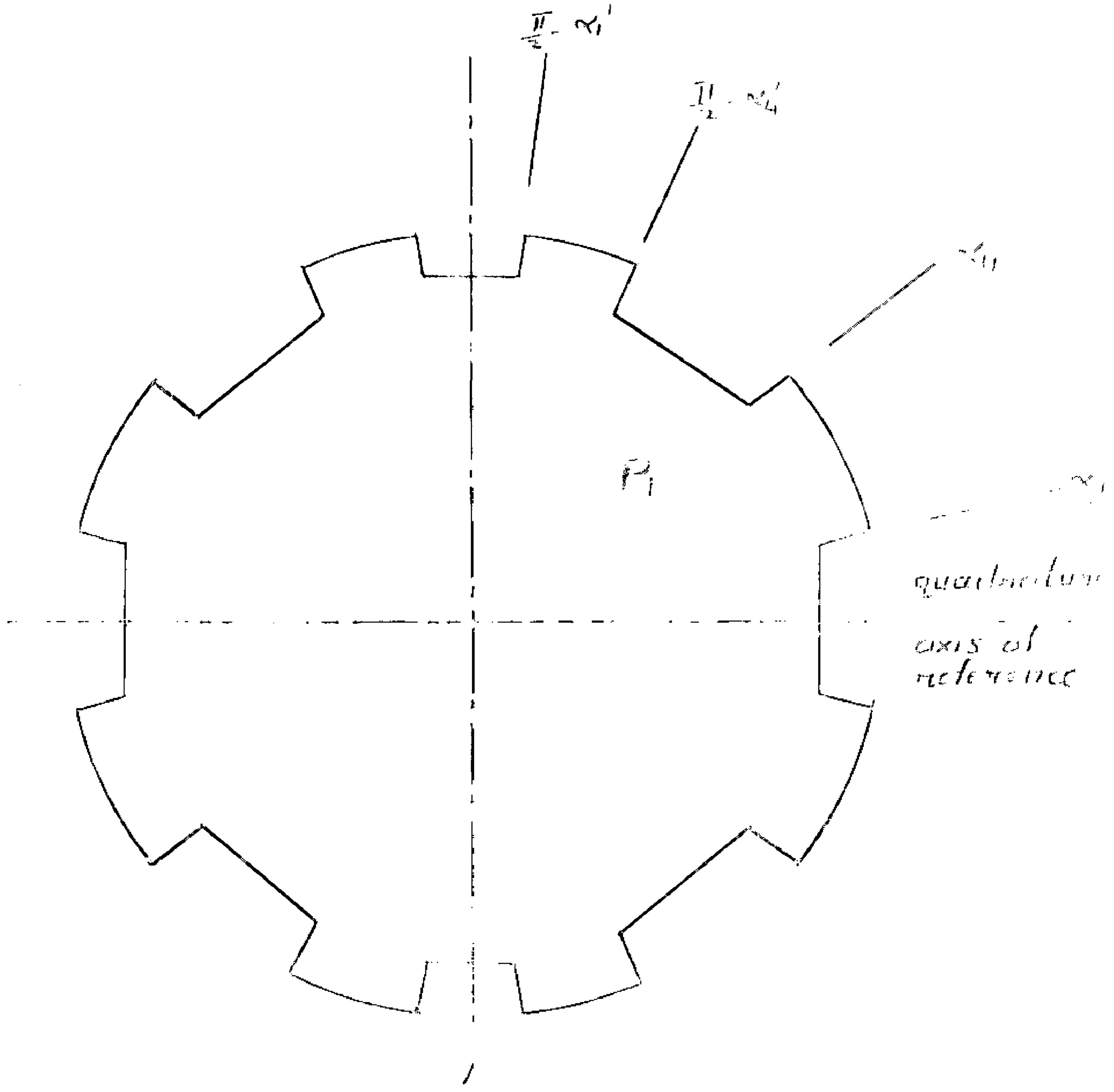

FIG 5.5. Rotor lamination with [illegible]
interpolar [illegible]

comparatively small magnitude.

If the air-gap permeance distribution of a squirrel-cage rotor can be made to be approximately represented by

$\Lambda_0 \pm \lambda_{2y} \cos y\theta \pm \lambda_{2z}(\cos z\theta)$ + other harmonics it will become possible to obtain synchronous operation for either y-poles or z-poles, when the rotor is used in conjunction with a p.a.m. stator winding for y/z poles.

For reasons explained in Section 4.2 λ_{2y} is taken equal to $\lambda 2z$. A graph of the permeance terms, varying with angle θ, is plotted with y = 6 and z = 8 for a 6/8 pole motor (Fig. 3.3.). The graph with the horizontal axis through O, contains no constant component. If however, a line AB, whose position is defined by value of λ_0, is taken as abscissa, an ideal permeance distribution containing no other harmonic results. An approximation to the ideal permeance distribution, taking the line AB as abscissa, can be obtained, in the simplest form by the bivalued function of Fig. 3.4.

3.3.2 Description of Rotor Lamination

A practical embodiment of such a permeance distribution, as is represented by Fig. 3.4 is obtained by using rotor punching of the shape shown in Fig. 3.5. Plainly the new rotor is a compromise between independent single speed rotors used for six and eight pole operation. Excluding the flux barriers this lamination resembles that described in Fig. 3.1 The permeance for such a rotor lamination can be defined by table 3.3.

Table 3.3

Permeance $\lambda(\theta)$	Range with respect to reference axis		
μ_o/G	0	to	α_1
μ_o/B	α_1	to	α_4
μ_o/G	α_4	to	$\frac{\pi}{2} - \alpha'_4$
μ_o/B	$\frac{\pi}{2} - \alpha'_4$	to	$\frac{\pi}{2} - \alpha'_1$
μ_o/G	$\frac{\pi}{2} - \alpha'_1$	to	$\frac{\pi}{2}$

3.3.3 Expression for Permeance Distribution

The bivalued function of Fig.3.4 can be represented by a Fourier series as:

$$P = \lambda_o + \sum_{n=1}^{\infty} \lambda_{4p} \cos \frac{n\pi X}{C} \qquad (3.23)$$

Since the function of Fig. 3.4 is symmetrical along two perpendicular axes, the term (eqn 3.23)C is equated to $\frac{\pi}{2}$ Then for α to be the angular displacement round the air-gap and (θ) the instantaneous rotor position Eqn 3.23 can be rewritten as :

$$P = \lambda_0 + \sum_{n=1}^{\infty} \lambda_{4p} \cos 2\,nP(\alpha - \theta) \qquad (3.24)$$

The expression for λ_0 and λ_{4p} have been established in Appendix 9.4 and are given by :

$$\lambda_0 = \frac{2\mu_0 R\, L}{\pi\, g}\left[\frac{\pi}{2h} + (B+C)\left(1 - \frac{1}{h}\right)\right] \qquad (3.25)$$

and

$$\lambda_{4p} = \frac{4\mu_0 RL}{\pi g n(2p)}\left[\left\{\sin 2pA - \sin 2p(A+B) - \sin 2p\left(\frac{\pi}{2} - \overline{C+D}\right) + \sin 2p\left(\frac{\pi}{2} - D\right)\right\}\left(1 - \frac{1}{h}\right)\right] \qquad (3.26)$$

Thus the expression for permeance can be written (for n=1) as :

$$P = \frac{2\mu_0\, RL}{\pi\, g}\left[\frac{\pi}{2h} + (B+C)\left(1 - \frac{1}{h}\right) + \frac{1}{p}\left\{\sin 2pA - \sin 2p(A+B) - \sin 2p\left(\frac{\pi}{2} - \overline{C+D}\right) + \sin 2p\left(\frac{\pi}{2} - D\right)\right\}\left(1 - \frac{1}{h}\right)\right]\cos 2p(\alpha - \theta) \qquad (3.27)$$

3.3.4 <u>Axis Reactances</u>

Referring to Appendix 9.5, the direct and quadrature axis magnetising reactances due to armature reaction are, respectively,

$$X_{ad} = K\left(\lambda_o + \frac{1}{2}\lambda_{bp}\right) \qquad (3.28)$$

and $$X_{aq} = K\left(\lambda_o - \frac{1}{2}\lambda_{bp}\right) \qquad (3.29)$$

where, $$K = \frac{2b\,v}{\pi}(N K_v)^2$$

Hence the ratio of direct and quadrature axis magnetising reactances is given by:

$$\frac{X_{ad}}{X_{aq}} = \frac{\lambda_o + \frac{1}{2}\lambda_{bp}}{\lambda_o - \frac{1}{2}\lambda_{bp}} \qquad (3.30)$$

3.4 ANALYSIS OF TWO SPEED ROTOR WITH INTERPOLAR CHANNELS

(Without flux-barriers, employing the principle of net flux accumulation).

3.4.1 Rotor Magnetic Potential

The shape of lamination is same as shown in Fig. 3.5 where, only one region can be realised. The permeance distribution is again defined by Table 3.1. Assuming the value of rotor magnetic potential in the rotor to be 'p_1' and using the condition that net flux accumulation in the region is equal to zero the following expression is solved for p_1:

$$2\Big[\int_0^{\alpha_1}\frac{\mu_o}{g}(H_{1q}\cos p\theta - P_1)\frac{D}{2}d\theta + \int_{\alpha_1}^{\alpha_4}\frac{\mu_o}{g}(H_{1q}\cos p\theta - P_1)\frac{D}{2}d\theta + \int_{\alpha_4}^{\frac{\pi}{2}-\alpha_4}\frac{\mu_o}{g}(H_{1q}\cos p\theta - P_1)\frac{D}{2}d\theta + \int_{\pi/2-\alpha_4'}^{\pi/2-\alpha_1'}\frac{\mu_o}{g}(H_{1q}\cos p\theta - P_1)\frac{D}{2}d\theta + \int_{\pi/2-\alpha_1'}^{\pi/2}\frac{\mu_o}{g}(H_{1q}\cos p\theta - P_1)\frac{D}{2}d\theta\Big] = 0 \qquad (3.31)$$

and its value (Appendix 9.6) is given by the expression

$$P_1 = \frac{H_{1q}\left[\sin p\alpha_4 - \sin p\alpha_1 - \sin p\left(\frac{\pi}{2} - \alpha'_4\right) + \sin p\left(\frac{\pi}{2} - \alpha'_1\right)\right]\left(1 - \frac{1}{h}\right)}{\frac{\pi}{2h} + \left(\alpha_4 - \alpha_1 + \alpha'_4 - \alpha'_1\right)\left(1 - \frac{1}{h}\right)}$$

Making substitutions $\alpha_1 = A$, $\alpha_4 - \alpha_1 = B$, $\alpha'_1 = D$ and $\alpha'_4 - \alpha'_1 = C$, the above expression can be rewritten in different form as :

$$P_1 = \frac{H_{1q}\left[\sin p(A+B) - \sin pA - \sin p\left(\frac{\pi}{2} - C + D\right) + \sin p\left(\frac{\pi}{2} - D\right)\right]\left(1 - \frac{1}{h}\right)}{\frac{\pi}{2h} + (B + C)\left(1 - \frac{1}{h}\right)}$$

(3.32)

3.4.2 Quadrature-axis flux-density

The expression for B_{1q} is :

$$B_{1q} = \frac{4}{\pi} \int_0^{\pi/2} \left(H_{1q} \cos p\theta - P_1 \right) \cos p\theta \, \lambda(\theta) \, d\theta$$

where variation of $\lambda(\theta)$ is given by Table 3.1.

With proper substitutions and simplifications, the expression for B_{1q} can be derived (Appendix 9.7) as :

$$B_{1q} = \frac{\dfrac{2\mu_o H_{1q}}{\pi g}\left[\dfrac{\pi}{2h} + (B+C)\left(1-\dfrac{1}{h}\right) + \dfrac{1}{2p}\left\{\sin 2p(A+D) - \sin 2pA - \sin 2p\left(\dfrac{\pi}{2} - \overline{C+D}\right) + \sin 2p\left(\dfrac{\pi}{2} - D\right)\right\}\left(1-\dfrac{1}{h}\right) - \dfrac{2}{p^2}\left\{\left|\sin p(A+D) - \sin pA - \sin p\left(\dfrac{\pi}{2} - \overline{C+D}\right) + \sin p\left(\dfrac{\pi}{2} - D\right)\right|\left(1-\dfrac{1}{h}\right)\right\}^2\right]}{\dfrac{\pi}{2h} + (B+C)\left(1-\dfrac{1}{h}\right)}$$

(3.33)

3.4.3 Quadrature-axis reactance

Substituting eqn 3.33 in the expression $X_{aq} = K\,(B_{1q} / H_{1q})$ the expression for quadrature axis reactance can be determined.

3.4.4 Direct-axis Reactance

As the presence or absence of flux-barriers in no way affect the direct-axis flux density, the direct axis reactance remains unchanged. Thus the expression for direct-axis reactance remains same as determined in Sec.3.2 and the substitutions of sec 3.4.1 yield:

$$X_{ad} = \frac{2\mu_o K}{\pi g}\left[\frac{\pi}{2h} + (B+C)\left(1-\frac{1}{h}\right) + \frac{1}{2P}\left\{\sin 2PA - \sin 2P(A+B) + \sin 2p\left(\frac{\pi}{2} - \overline{C+D}\right) - \sin 2p\left(\frac{\pi}{2} - D\right)\right\}\left(1-\frac{1}{h}\right)\right]$$

(3.34)

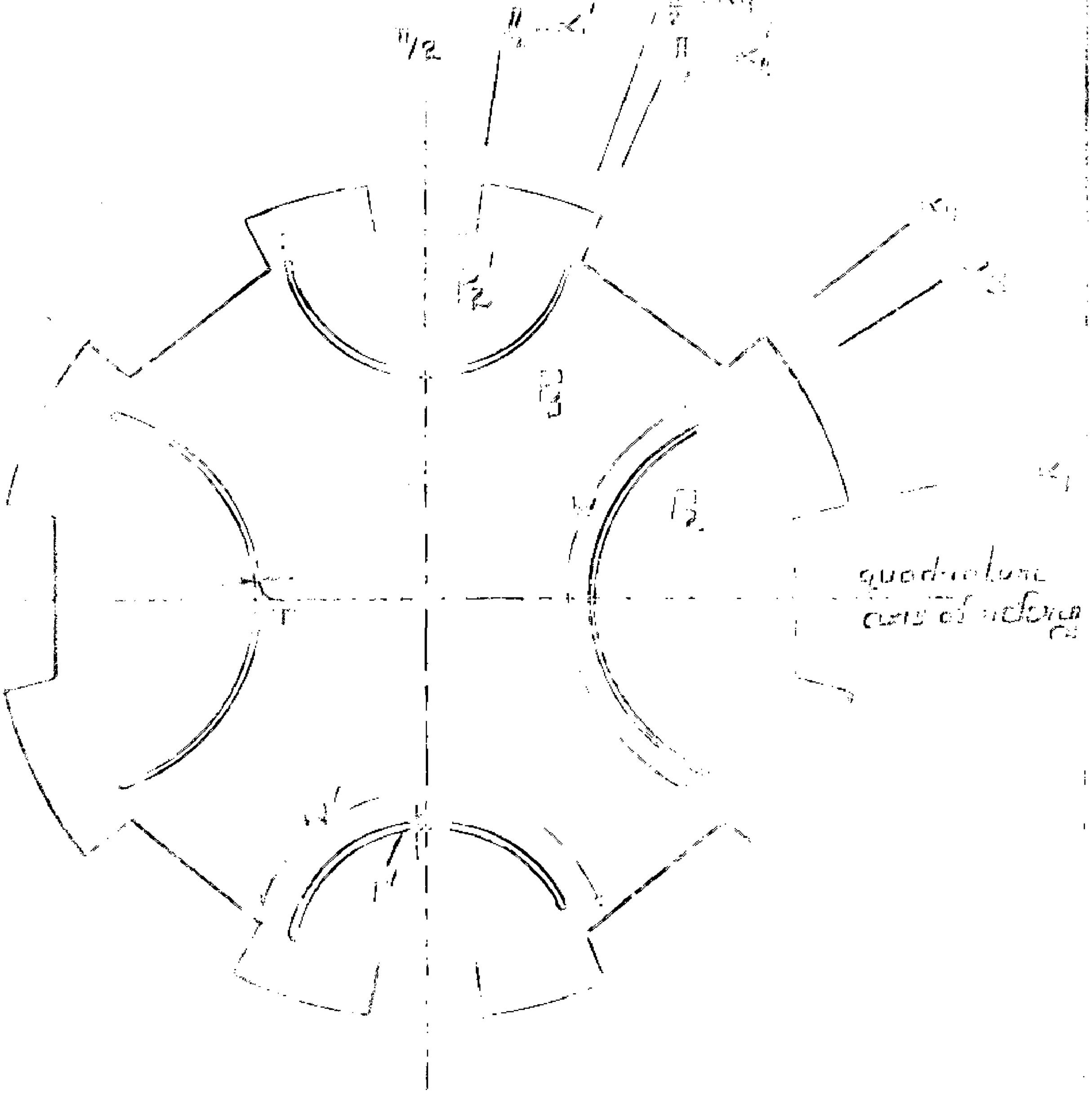

FIG. 3.6. Rotor lamination with essential flux barriers

3.5 ANALYSIS OF TWO SPEED ROTOR WITH INTERPOLAR CHANNELS AND ESSENTIAL BARRIERS

3.5.1 Description of Lamination

The shape of lamination is as shown in Fig. 3.6. Only the auxiliary barriers of Fig. 3.1(Sec. 3.2) have been omitted. Thus the lamination consists of two poles ends of which are situated at α_1, α_4, $\pi/2 - \alpha_4'$ and $\pi/2 - \alpha_1'$ radians with reference to a reference axis situated at the centre of a channel. At α_3 radians, a flux- barrier of width W and thickness T is included to guide the flux. This barrier is symmetrical about the reference axis. At $\pi/2 - \alpha_3'$ there is another barrier of width W' and thickness T' which is symmetrically placed about an axis at right angle to the original reference axis. The permeance distribution of Table 3.1 still holds good.

3.5.2 Rotor Magnetic Potentials

In the Fig. 3.6 , two regions are realised which have different magnetic potentials. Accordingly the variation of magnitude of rotor magnetic potential is defined by Table 3.4.

Equating to zero the summation of flux, per unit length in different regions, the expressions for rotor magnetic potentials have been derived (Appendix 9.8) which are expressed as :

Table 3.4

Rotor magnetic potential	Range with respect to the reference axis.
P_2	0 to α_1
P_2	α_1 to α_3
P_3	α_3 to α_4
P_3	α_4 to $\frac{\pi}{2} - \alpha_4'$
P_3	$\frac{\pi}{2} - \alpha_4'$ to $\frac{\pi}{2} - \alpha_3'$
P_2'	$\frac{\pi}{2} - \alpha_3'$ to $\frac{\pi}{2} - \alpha_1'$
P_2'	$\frac{\pi}{2} - \alpha_1'$ to $\frac{\pi}{2}$

$$P_3 = \frac{A + P_2 \cdot \frac{W}{T} + P_2' \cdot \frac{W'}{T'}}{B} \tag{3.35}$$

$$P_2 = \frac{H_{1q}\left[\frac{\sin p\alpha_1}{pG/D} + \frac{\sin p\alpha_3 - \sin p\alpha_1}{pg/D}\right] + \frac{A}{B} \cdot \frac{W}{T}}{\frac{\alpha_1}{G/D} + \frac{\alpha_3 - \alpha_1}{g/D} + \frac{W}{T} - \frac{1}{B}\left(\frac{W}{T}\right)^2} \tag{3.36}$$

and

$$P_2' = \frac{H_{1q}\left[\frac{\sin p(\pi/2 - \alpha_1') - \sin p(\pi/2 - \alpha_3')}{pg/D} + \frac{\sin p\frac{\pi}{2} - \sin p(\frac{\pi}{2} - \alpha_1')}{pG/D}\right] + \frac{AW}{BT}}{\frac{\alpha_1'}{G/D} + \frac{\alpha_3' - \alpha_1'}{g/D} + \frac{W'}{T'} - \frac{1}{B}\left(\frac{W'}{T'}\right)^2} \tag{3.37}$$

where,

$$A = H'_{1q}\left[\frac{\sin p\alpha_4 - \sin p\alpha_3}{pg/D} + \frac{\sin p(\frac{\pi}{2} - \alpha') - \sin p\,\alpha_4}{pG/D} + \frac{\sin p(\frac{\pi}{2} - \alpha'_3) - \sin p\,(\frac{\pi}{2} - \alpha'_4)}{pg/D}\right] \qquad (3.38)$$

$$B = \frac{\alpha_4 - \alpha_3}{g/D} + \frac{\frac{\pi}{2} - \alpha'_4 - \alpha_4}{G/D} + \frac{\alpha'_4 - \alpha'_3}{g/D} + \frac{W}{T} + \frac{W'}{T'} \qquad (3.39)$$

3.5.3 Quadrature-axis flux-density

The expression for B_{1q}, the quadrature - axis flux-density is :

$$B_{1q} = \frac{4}{\pi} \int_0^{\pi/2} (\, H_{1q} \cos p\theta - p(\theta))\, \lambda(\theta) \cos p\theta \, d\theta$$

where, variation of $\lambda(\theta)$ and $p(\theta)$ is given by table 3.1 and table 3.4.

The expression for B_{1q} can be solved (Appendix 9.9) and expressed as -

$$B_{1q} = \frac{2\mu_0}{\pi g}\Bigg[H_{1q}\Bigg\{ \frac{\pi}{2h} + (\alpha_4 - \alpha_1 + \alpha'_4 - \alpha'_1)\,.(1 - \frac{1}{h})$$

$$+ \frac{1}{2p}\left\{\sin 2p\alpha - \sin 2p\alpha - \sin 2p(\frac{\pi}{2} - \alpha'_4) + \sin 2p(\frac{\pi}{2} - \alpha'_1)\right\}(1 - \frac{1}{h})\Bigg\}$$

$$- \frac{2}{p}\Bigg\{\Big[-P_2 \sin p\alpha_1 + P_3(\sin p\alpha_4 - \sin p(\frac{\pi}{2} - \alpha'_4)) + P' \sin p(\frac{\pi}{2} - \alpha'_1)\Big](1 -$$

$$+ (P_2 - P_3)\sin p\alpha_3 \pm (P_3 - P'_2)\sin p(\frac{\pi}{2} - \alpha'_3) + P'_2 \frac{\sin p\ \pi/2}{h}\Bigg\}\Bigg]$$

(3.40)

3.5.4 Quadrature-axis Reactance

Substituting Eqn 3.40 in the expression $X_{aq} = K\,(B_{1q}/H_{1q})$ the value of quadrature axis reactance can be obtained.

3.5.5 Direct-Axis Reactance

Following the earlier discussion, the value of direct-axis magnetising reactance remains unchanged and hence rewritten as :

$$X_{ad} = \frac{2\mu_0 K}{\pi g}\left[\frac{\pi}{2h} + (\alpha_4 - \alpha_1 + \alpha_4' - \alpha_1')\left(1 - \frac{1}{h}\right) - \frac{1}{2p}\left\{\sin 2p\alpha_4 - \sin 2p\alpha_1 - \sin 2p\left(\frac{\pi}{2} - \alpha_4'\right) + \sin 2p\left(\frac{\pi}{2} - \alpha_1'\right)\right\}\left(1 - \frac{1}{h}\right)\right] \tag{3.41}$$

3.6 PERFORMANCE EQUATIONS

Now, that the expression for direct-axis and quadrature axis magnetising reactances have been established, the value of direct-axis and quadrature axis reactances can be determined as :

$$X_d = X_{ad} + X_1$$

$$X_q = X_{aq} + X_1$$

By substituting these values in the various performance equations listed below the performance of the motor can be predicted.

3.6.1 Torque

For line voltage V the output torque of a star connected reluctance motor is given in synchronous watts by

$$T = \frac{2V^2(X_d - X_q)\sin 2\delta_e}{\left[2r-(X_d-X_q)\sin 2\delta_e\right]^2 + \left[(X_d+X_q)+(X_d-X_q)\cos 2\delta_e\right]^2} \qquad (3.42)$$

By differentiating this equation with respect to δ_e, the condition for maximum output may be obtained :

$$\cos 2\delta_e = \frac{-(X_d^2 - X_q^2)}{2r^2 + X_d^2 + X_q^2} \qquad (3.43)$$

and substituting for it in Equation 3.42 gives the expression for pull-out torque T_{po} :

$$T_{po} = \frac{V^2}{2} \frac{(X_d - X_q)}{r(X_d - X_q) + \left[r^2(X_d - X_q)^2 + r^4 + 2r^2 X_d X_q + X_d^2 X_q^2\right]^{1/2}} \qquad (3.44)$$

If resistance is neglected, this equation reduces to

$$T_{po\,r=0} = \frac{V^2}{2} \frac{(X_d - X_q)}{X_d X_q} = \frac{V^2}{2} \left(\frac{1}{X_q} - \frac{1}{X_d} \right) \qquad (3.45)$$

3.6.2 Current

The equation for current is

$$I = \frac{V}{\sqrt{3}} \frac{2V^2(X_d - X_q)\sin 2\delta_e}{\left[\left\{2r-(X_d-X_q)\sin 2\delta_e\right\}^2 + \left\{(X_d+X_q)+(X_d-X_q)\cos 2\delta_e\right\}^2\right]^{1/2}}$$

(3.46)

At pull out the value of current becomes :

$$I_{po} = \frac{V}{\sqrt{6}} \quad \frac{(X_d^2 + X_q^2)^{\frac{1}{2}}}{X_d X_q} \tag{3.47}$$

3.6.3 Power Factor

The expression for power factor , is

$$\cos \phi = \frac{2r + (X_d - X_q) \sin 2\delta_o}{\left[\{2r + (X_d - X_q) \sin 2\delta_o\}^2 + \{(X_d + X_q) + (X_d - X_q) \cos 2\delta_o\}^2 \right]^{1/2}} \tag{3.48}$$

which gives the maximum power factor, $\cos \phi_{max}$, as

$$\cos \phi_{max} = \frac{(X_d - X_q)^2 - 4r^2}{X_d^2 - X_q^2 - 4r(X_d X_q + r^2)^{1/2}} \tag{3.49}$$

Neglecting the resistance r,

$$\cos \phi_{\substack{max \\ r=0}} = \frac{X_d - X_q}{X_d + X_q} = \frac{1 - X_q/X_d}{1 + X_q/X_d} \tag{3.50}$$

CHAPTER - 4

DESIGN PROCEDURE

4.1 GENERAL

The principal parameters to be obtained in the design of a two speed reluctance motor are :

a. The minimum and maximum air-gap reluctance factor pg/D and pg'/D respectively.

b. The essential barrier permeance factors W/T and W'/T'

c. The auxiliary-barrier permeance factors W_1/T_1 and W_1'/T_1'

d. The electrical angular displacements of interpolar channels $p\alpha_1$, $p\alpha_4$, $p\alpha_4'$ and $p\alpha_1'$.

e. The electrical angular displacements of auxiliary-barriers $p\alpha_2$ and $p\alpha_2'$

f. The electrical angular displacements of essential-barriers $p\alpha_3$ and $p\alpha_3'$.

The aim of design is to achieve as high a ratio X_{md}/X_{mq} as is possible for satisfactory operation at each speed. Small pg/D , W/T , W'/T' , W_1/T_1 , W_1'/T_1' , and a large pg'/D , in general , results in an increased X_{md}/X_{mq} ratio.

As there are a number of unknowns, their precise evaluation is a complicated task. In order to facilitate the design, the following steps are suggested:

1. The flux-barriers are omitted and optimum position and dimension of interpolar channels is determined.

2. To make the expressions obtained simpler for designing the rotor lamination, U/R, the permeance factor for essential barrier is neglected and airgap reluctance is made infinite. In the expression for X_{ad}/X_{aq} thus obtained, optimum values of step one are substituted. The resulting expression is again maximised, for both speeds of operation, with respect to essential barrier parameters.

3. Finally, in the expression for X_{ad}/X_{aq} (sec. 3.2) with essential and auxiliary barriers, both included along with the interpolar channels. The permeance factors U/R, U'/R', U_1/R_1, and U'_1/R'_1 are all equated to zero and maximum airgap reluctance factor is made infinite. Optimum values of step one and two are substituted and maximisation technique is applied with respect to the auxiliary-barrier parameters, for both speeds of operation. Thus the auxiliary-barrier parameters are also known and hence the complete design data for X_{ad}/X_{aq} to be maximum is obtained.

4.2 OPTIMISATION OF ROTOR PUNCHING WITH ONLY INTERPOLAR CHANNELS

4.2.1 Determination of Objective Function

The expression for X_{ad}/X_{aq} for P-pair of poles has been derived in Appendix 9.4 and is given by (Sec. 3.3.4)

$$\frac{X_{ad}}{X_{aq}} = \frac{\lambda_o + \frac{1}{2}\lambda_{4p}}{\lambda_o - \frac{1}{2}\lambda_{4p}} \qquad (4.1)$$

or

$$\frac{X_{ad}}{X_{aq}} = \frac{A_o + k\,A_{4p}}{A_o - k\,A_{4p}} \quad \text{(say)} \qquad (4.2)$$

where,

$$k = \left(1 - \frac{1}{h}\right) \qquad (4.3)$$

$$A_o = \frac{\pi}{2h} + (B + C)\left(1 - \frac{1}{h}\right) \qquad (4.4)$$

and

$$A_{4p} = \frac{1}{2p}\left[\sin 2pA - \sin 2p(A+B) + \sin 2p\left(\frac{\pi}{2} - \overline{C+D}\right) - \sin 2p\left(\frac{\pi}{2} - D\right)\right] \qquad (4.5)$$

For p = 3, $A_{4p} = A_{12} = 1/6 \cdot \left[\sin 6A - \sin 6(A+B) + \sin 6(\overline{C+D}) - \sin 6D\right]$ (4.6)

For p = 4, $A_{4p} = A_{16} = \frac{1}{8}\left[\sin 8A - \sin 8(A+B) - \sin 8(C+D) + \sin 8D\right]$ (4.7)

From Eqn 3.31 the expressions for ratio X_{ad}/X_{aq} for a 6/8 pole motor can easily be derived and written as.

$$\left.\frac{X_{ad}}{X_{aq}}\right|_{p=3} = \frac{A_o + k\,A_{12}}{A_o - k\,A_{12}} \qquad (4.8)$$

and

$$\left.\frac{X_{ad}}{X_{aq}}\right|_{p=4} = \frac{A_o + k\,A_{16}}{A_o - k\,A_{16}} \qquad (4.9)$$

Substituting Eqn 4.2 in eqns 3.45 and 3.50 the expressions for pull out torque and power factor are re-written as :

$$T_{p.o} = \frac{3V^2}{2\,X_{ad}} \left(\frac{X_{ad}}{X_{aq}} - 1 \right) \quad (\text{Assuming } X_1 = 0)$$

$$= \frac{3\,V^2}{2} \cdot \frac{1}{a(A_o + kA_{4p})} \cdot \left(\frac{A_o + kA_{4p}}{A_o - kA_{4p}} - 1 \right)$$

$$= \frac{3V^2}{2\,a} \left(\frac{k\,A_{4p}}{A_o^2 - k^2\,A_{4p}^2} \right) \qquad (4.10)$$

and $\cos \phi_{max} = \dfrac{(X_{ad}/X_{aq}) - 1}{(X_{ad}/X_{aq}) + 1}$

$$\text{or } \cos \phi_{max} = k \cdot \frac{A_{4p}}{A_o} \qquad (4.11).$$

To attain large values of pull-out torque and maximum power factor, from eqns 4.5 and 4.6, it is necessary to make A_{4p} maximum. A_{4p} possesses values

A_{12} and A_{16} for six and eight pole operation respectively Thus for a two speed motor the maximisation of A_{4p} virtually means simultaneous maximisation of A_{12} and A_{16}.

Hence the objective function F to be maximised is

$$F = A_{12} + A_{16} \qquad (4.12)$$

The variables in this function are A, B, C, and D.

There are two ways for maximising the function with respec t to these variables. First method is to maximise the function without putting any constraint on the value s of A, B, C ar D . Thus by suitable programming A, B, C, D is determined for which A_{4p} is maximum for both, six and eight pole operation. In the second method some constraint is put on the value of one or more variables. In the present problem, B and C are the widths of salient poles on the rotor periphery . In other words B+C is the amount of iron remaining on each quadrant after the interpolar channels have been milled out. If the value of B+C is suitably restricted, the magnitude of magnetising current can be controlled.

Both the possibilities have been considered. Subroutines given in Appendix 9.12 and 9.13 correspond to the case when there is no restriction placed on the values of the variables A, B, C and D while the subroutines

Appendix 9.14 and 9.15 correspond to the case where B+C is restricted to take a constant value 0.8 radians i.e. 51 per cent of the iron remains on the periphery after the channels have been milled out. Sign of objective function is reversed in the subroutines so that the minimization of $-F$ may maximise original F. For minimising $-F$, main programme (Appendix 9.11) and subroutine (Appendix 9.12) has been prepared which, with either subroutines of Appendix 9.12 and 9. 13 or of Appendix 9.14 and 9.15, give the optimum value of A,B,C and D.

4.2.2 Iteration Steps

The following iteration steps followed in preparing the programme:

1. Set $k = 0$ and evaluate $F(X^{(k)})$
2. Evaluate the gradient $g(X^{(k)})$
3. Initialise Hessian Matrix $H = I$
4. Calculate the descent direction
   $p^{(K)} = H^k g^{(k)}$
5. Find λ which minimizes $f(X^{(k)} + \lambda p^{(k)})$
6. Compute $dX^k = -\lambda H\ g(X^{(k)})$
7. Calculate values of $X^{(kH)}$
8. Compute $dg(X^{(k)}) = F(X^{k+1}) - F(X^k)$
9. If $g(X^{(k)})/F(X^{(k)})$ is less than the specified tolerance the minimum is found. If not the Hessian

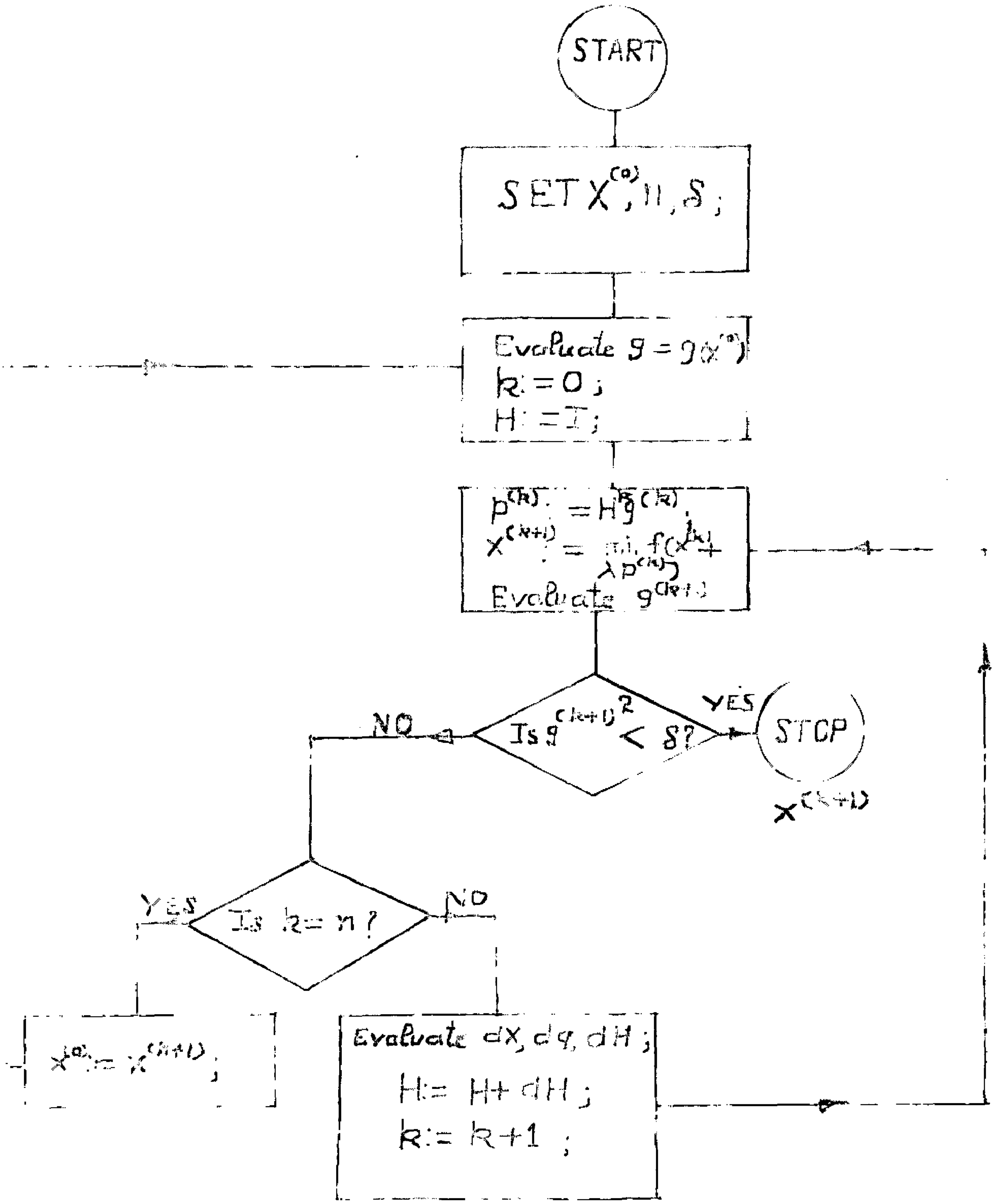

Fig. 4.1. Flow chart for the minimisation problem

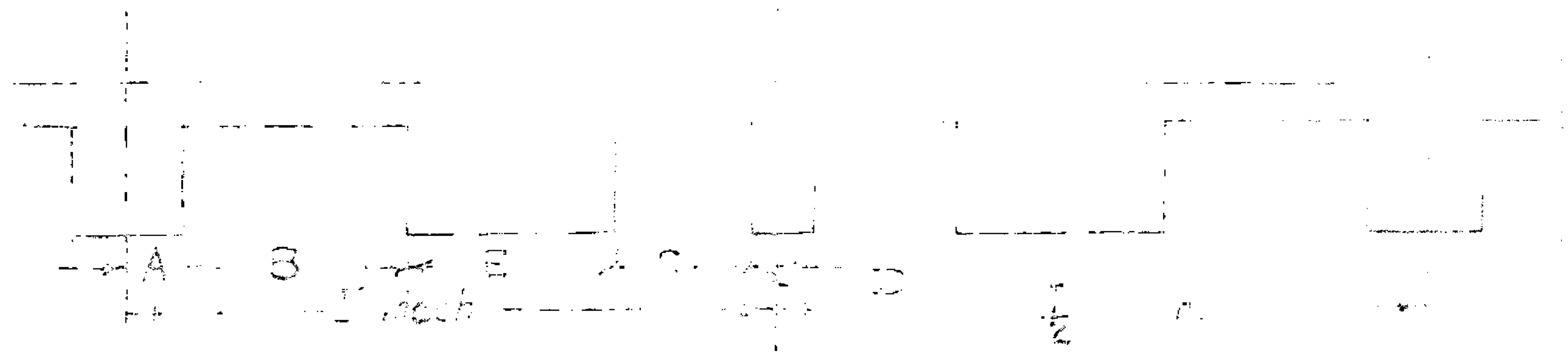

Fig. 1.2 Developed view of rotor periphery (for a span (II) radian. The [illegible] [illegible] about the axis of II radians the dimensions [illegible] shown only for half portion.)

is modified by the relation

$$H^{k+1} = H^K + \frac{dX^{(k)} \cdot dX^{(k)T}}{dX^{(k)T} \quad dg^{(k)}} - \frac{H^{(k)}\ dg^{(k)}\ fg^{(k)^T}\ H^{(k)}}{dg^{(k)^T}\ H^{(k)}\ dg^{(k)}}$$

and the above steps are repeated again. This is illustrated in the flow chart given in Fig. 4.1.

4.2.3 Results of Optimisation

The results obtained by successful execution of programmes listed in Appendix 9.10 to 9.15 are as Tabulated below (Refer Fig. 4.2 Sec. 4.2.2.)

Table 4.1

Optimised values	Without any constraint on width of poles	Width of poles restricted to 51% of whole rotor periphery.
A	0.232	0.22
B	0.421	0.44
E	0.458	0. 484
C	0.277	0.36
D	0.181	0.066
h	25	25
A_o (Eq 4.4)	.7328	.8308
kA_{12}(eq 4.6)	.222	.2955
kA_{16} (eq 4.7)	.400	.312
$\left.\frac{X_{ad}}{X_{aq}}\right\vert_{P=3}$ (eq.4.8)	1.875	2.1
$\left.\frac{X_{ad}}{X_{aq}}\right\vert_{P=4}$ (eq.4.9)	3.410	2.21

From the table 4.1 it can be observed that value of kA_{12} and kA_{16} tends to become equal for fixed pole widths . This satisfies the aim of obtaining simultaneously, maximum possible values of kA_{12} and kA_{16} hence the ratio X_{ad}/X_{aq} for 6/8 pole operation. This leads to operation at equal maximum power factors at speeds corresponding to 6 and 8 poles excitation. That is also the reason for taking equal values of $\lambda_2 y$ and $\lambda_2 z$ in the sec. 3.1 for determination of permeance wave shape.

Programme can also be prepared to determine the position of interpolar channels in such a way that equal torques are available at two speeds of operation.

4.3 DETERMINATION OF DIMENSION AND POSITION OF ESSENTIAL BARRIERS

Expressions for direct and quadrature-axis reactances for this case have already been determined in sec. 3.5.5 and 3.5.4 The simplifying substitutions (1) $W/T = 0$ (2) $G = \infty$ are made in eqns 3.36 to 3.38 and modified expressions for P_3, P_2 and P_2' are obtained as follows :

$$P_3 = \frac{H_{1q}}{p}\left[\frac{\sin p\alpha_4 - \sin p\alpha_3 + \sin p(\frac{\pi}{2} - \alpha_3') - \sin p(\frac{\pi}{2} - \alpha_4')}{\alpha_4 - \alpha_3 + \alpha_4' - \alpha_3'}\right] \tag{4.13}$$

$$P_2 = \frac{H_{1q}}{p}\left[\frac{\sin p\,\alpha_3 - \sin p\alpha_1}{\alpha_3 - \alpha_1}\right] \qquad (4.14)$$

$$P_2' = \frac{H_{1q}}{p}\left[\frac{\sin p(\frac{\pi}{2} - \alpha_1') - \sin p(\frac{\pi}{2} - \alpha_3')}{\alpha_3' - \alpha_1'}\right] \qquad (4.15)$$

From last column of table 4.1 the optimum values of parameters corresponding to interpolar channels are:

$\alpha_1 = A = 0.22$, $\alpha_4 = A+B = 0.66$, $\alpha_4' = C+D = 0.426$
$\alpha_1' = D = 0.066$ and $h = 25$.

Substitution of expressions for rotor magnetic potentials along with the above values in the expression for X_{aq} given in eqn 3.42 yields the value of quadrature-axis reactances in terms of essential-barrier position parameters α_3 and α_3'. Direct-axis reactance is independent of these parameters. The expression for X_{ad}/X_{aq} is of the form $\dfrac{K_1}{K_2 - F_p}$ where K_1 and K_2 are known constants constants. F_p is an expression dependent on α_3 and α_3' and is valid for 'p' pair of poles. Its value for Y and Z pair of poles is F_y and F_z respectively. For X_{ad}/X_{aq} to ve maximum for Y and Z. Pair of poles the expression F_p must be maximised with respect to α_3 and α_3' for both pole pairs. The objective function is therefore $F = -(F_y + F_z)$ and can be minimised for F_Y and F_z

to become maximum.

Subroutines can be programmed for calculating $-F$ for any general $\{\alpha_3, \alpha_3'\}$ and the derivatives of $-F$ with respect to α_3 and α_3' for the same $\{\alpha_3, \alpha_3'\}$.

Depending on the position of interpolar channels, restrictions can be imposed on the values of α_3 and α_3' in such a way that conditions $\alpha_1 < \alpha_3 < \alpha_4$ and $\alpha_1' < \alpha_3' < \alpha_4'$ are always satisfied. Then the two subroutines alongwith main programme (Appendix 9.11) and subroutine (Appendix 9.12) would give optimum values of α_3 and α_3'.

For clearity sake suitable values of α_3 and α_3' have been assumed and specimen design sheet is prepared as shown in Table 4.2.

This also gives the probable steps for programming the subroutine for determination of objective function F.

4.4 DETERMINATION OF DIMENSION AND POSITION OF AUXILIARY BARRIERS

In the expressions for rotor magnetic potentials (Eqns 3.8 to 3.18) the simplifying substitutions 1. $W/T = 0$, 2. $W_1/T_1 = 0$ 3. $W'/T' = 0$ 4. $W_1'/T_1' = 0$ and SO = ∞ are made. In the resulting expressions the optimum values of parameters corresponding to interpolar channels and essential-barriers are substituted. The ratio

TABLE 4.2a

DESIGN SHEET FOR ESSENTIAL BARRIER PARAMETERS

Configuration A3 for optimised channel parameters

$\alpha_1 = 0.22$, $\alpha_4 = 0.66$, $\alpha_1' = 0.066$, $\alpha_4' = 0.426$

Essential Barrier Parameters (assumed)

$\alpha_3 =$ 0.4 $\alpha_3' =$ 0.4

Value of	=
P_3	$-0.07 \; H_{1q}$
P_2	$0.59 \; H_{1q}$
P_2'	$-0.52 \; H_{1q}$
$X_q \Big\rvert_{X_1 = 0}$	$\dfrac{2 \mu_o K}{\pi g} (0.2493)$
$X_d \Big\rvert_{X_1 = 0}$	$\dfrac{2 \mu_o K}{\pi g} (1.126)$
X_d / X_q	4.5
T pull out	2020 watt
Maximum power factor	0.632

TABLE 4.2b

Configuration A3 for Optimised channel parameters

$\alpha_1 = 0.22$, $\alpha_4 = 0.66$, $\alpha'_1 = 0.666$, $\alpha'_4 = 0.426$

Essential Barrier Parameters (Assumed)

$\alpha_3 = 0.4$ $\alpha'_3 = 0.4$

Value of	=
P_3	$-0.43\ H_{1q}$
P_2	$0.32\ H_{1q}$
P'_2	$0.57\ H_{1q}$
X_q $X_1 = 0$	$\frac{2\mu_o K}{\pi g}(0.165)$
X_d $X_1 = 0$	$\frac{2\mu_o K}{\pi g}(1.1428)$
X_d / X_q	6.95
T pull out	2000 watt
Maximum power factor	0.75

X_{ad}/X_{aq} obtained is of the same form as obtained in the preceding section 4.4 i.e.

$$\frac{X_{ad}}{X_{aq}} = \frac{K_1}{K_2 - F'_p}$$

Constants K_1 and K_2 are same but F'_p is a function of auxiliary -barrier parameters and attains values F_y for Y-pair of poles and F_z for z pair of poles so to find optimum values of auxiliary barrier parameters α_2 and α'_2 this has to be maximised with respect to α_2 and α'_2 for both speeds of operation, corresponding to Y and Z pair of poles respec tively. This would mean maximisation of ratio X_{ad}/X_{aq} with respect to α_2 and α'_2. Thus the subroutines of sec 4.3 when replaced by subroutines for determining the new objective function $F = -(F'_y + F'_z)$ and corresponding derivatives with respect to α_2 and α'_2. The main programme of Appendix 9.11 and subroutine of Appendix 9.12 , modified to suit the conditions $\alpha_1 < \alpha_2 < \alpha_3$ and $\alpha'_1 < \alpha'_2 < \alpha'_3$ For positioning the auxiliary barrier, would provide the optimum value of α_2 and α'_2 .

This completes the positioning of flux-barrier. The value of permeance factors W/T , W_1/T_1, W'/T' and W'_1/T'_1 can now be fixed in accordance with electrical and mechanical considerations . Once the final value of all parameters is known effective value of ratio X_{ad}/X_{aq} for two pole pairs can be determined.

CHAPTER - V

PULL IN CRITERION FOR RELUCTANCE MOTOR

5.1 GENERAL

Apart from the running performance of reluctance motor, the pulling in phenomenon plays an important role in the design of reluctance motor. It presents difficulties, particularly when the moment of inertia of the connected load is appreciable. The following are some important factors which influence the pulling-into step of reluctance motors.

1. The pulling into step requires that the slip should be as small as possible. Thus the induction motor action should bring the rotor and the coupled load to near synchronous speed. But the slip required to supply the load increases as the load increases and for a particular load the speed reached at by induction motor action may not be sufficient for pulling in to take place.
2. The moment of inertia of connected load combined with that of reluctance motor rotor also effects the pulling into step.

3. The reluctance torque which varies with width of poles i.e. X_d/X_q ratio, is also a factor effecting the pulling in phenomenon. Particularly in modern machines where X_d/X_q is quite large, this has pronounced effect on pull in phenomenon.

5.2 ANALYSIS FOR PULLIN PHENOMENON

A general description of the system under study includes the salient pole rotor of the reluctance motor rigidly attached to the shaft and the load connected to the shaft. The electromagnetic torque T acts on the rotor, which has a moment of inertia equal to J_1, viscous damping, characterised by the coefficient B_1, acts on the rotor whose position is fixed by the angular displacement θ_1. The load with a moment of inertia equal to J_2 is connected to the shaft through a coupling which is characterised by the spring constant k, viscous friction B_2, and a speed independent component T_L constitute the load.

The system equations can be written as:

$$T = J_1\ddot{\theta}_1 + B_1\dot{\theta}_1 + k(\theta_1 - \theta_2) \qquad (5.1)$$

$$k(\theta_1 - \theta_2) = J_2\ddot{\theta}_2 + B_2\dot{\theta}_2 \qquad (5.2)$$

The torque T has got three components-

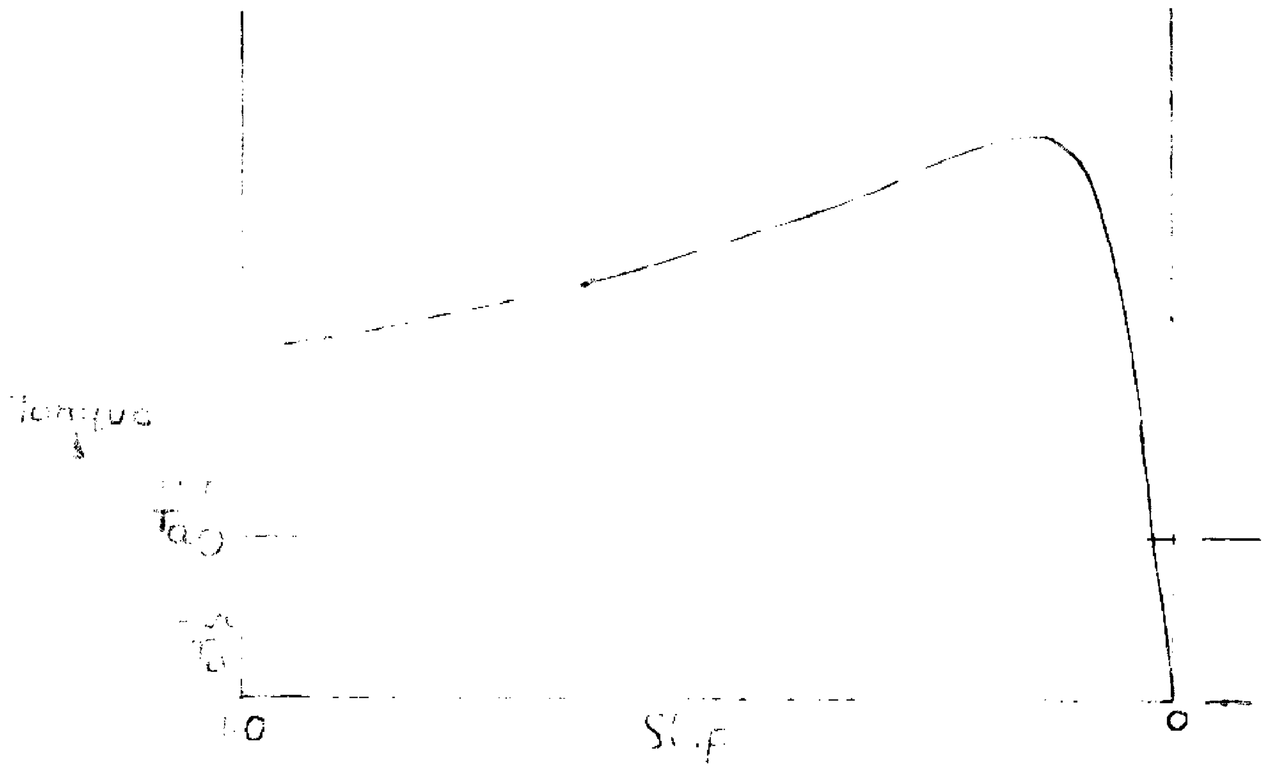

FIG 5.1 Induction Motor Characteristics.

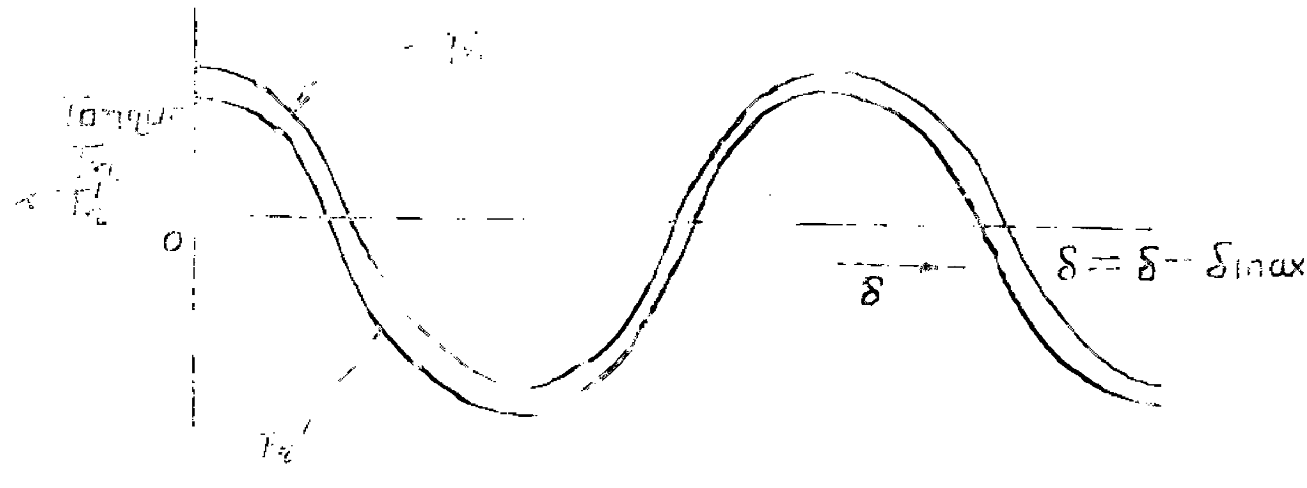

FIG 5.2 Reluctance Torque variation.

1. That produced by induction motor action, called the asynchronous torque and is denoted by T_a.
2. That produced by sunchronous motor action, called the reluctance torque and is denoted by T_R.
3. That consisting of mechanical load and other retarding torque T_1.

So the net torque T is expressed as:

$$T = T_a + T_R - T_1 \tag{5.3}$$

Curve of Fig. 5.1 shows the characteristic for a typical induction machine. The most striking feature of this curve is that it cuts the slip axis below the synchronous speed and shows a negative torque at zero, slip. This negative intercept at zero slip leads to higher values of average slip in the critical region just below synchronous speed and makes the jump into synchronous mode appreciably more difficult. The presence of this negative intercept does not allow to represent the characteristic through the zero torque point by a linear curve. It is found that a parabolic expression is more suited to such a characteristic. Thus the expression for asynchronous torque T_a is taken to be

$$T_a = AS^2 + BS - C \tag{5.4}$$

where s is slip and A,B are constants determined in Appendix 9.16 .

The variation of reluctance torque T_r with load angle δ is shown in Fig. 5.2 . A convenient form of expression for T_r is

$$T_r = D \cos 2\delta + E \sin 2\delta - C \qquad (5.5)$$

where,

$$D = \frac{V^2}{2} \frac{(X_d - X_q)}{(X_d X_q + r^2)^2} \left[r (X_d + X_q) \right] \qquad (5.6)$$

$$E = \frac{V^2}{2} \frac{(X_d - X_q)}{(X_d X_q + r^2)^2} \left[X_d X_q - r^2 \right] \qquad (5.7)$$

$$C = \frac{V^2 r}{2} \frac{(X_d - X_q)^2}{(X_d X_q + r^2)^2} \qquad (5.8)$$

Another form for T_r is

$$T_r = K \cos 2 (\delta - \delta_{max}) - C \qquad (5.9)$$

where,

$$K = \sqrt{D^2 + E^2}$$

$$\delta_{max} = \frac{1}{2} \tan^{-1} E/D$$

With the above values of T_r and T_a the value of negative intercept is accounted for twice . Therefore to avoid this the value of expression for net torque T is modified to

$$T = T_a + T_r' - T_e \qquad (5.10)$$

where $T_r' = T_r + C$

$$= K \cos 2 (\delta_{max} - \delta)$$

In Eqn. given above δ is the electrical load angle and is positive for motoring action. In the limit, as slip tends to zero the average torque at zero slip is obtained by integrating equation (5.10) with respect to δ from zero to π. The expression is :

$$T_{s=0} = \frac{-V^2 r (X_d - X_q)^2}{2 (X_d X_q + r^2)}$$ which is always negative

except when there is no saliency ie., $X_d = X_q$ and when resistance 'r' is negligible. Under these conditions Torque T becomes zero.

Evidently it is necessary to supply shaft torque at small positive slip. As the effect of resistance of stator winding is to increase the value of negative intercept at zero slip, at speeds approaching synchronous, asynchronous torque of a reluctance motor may, as far as synchronisation is concerned, be regarded as an equivalent effective load torque. The increasing value of this torque with increasing saliency and increasing stator resistance acts to the detriment of the synchronising performance. It is because of the stator resistance that the pull in torque is different for the same machine with different resistances inserted in the stator cirtuit. But if the effective load on the motor is considered it is observed that it is almost same whatever may be the value of resistance of stator winding. It can thereforebe concluded that the pull in performance will be worsened with decreasing motor size, since the stator resistance is normally more for small machines.

5.3 VARIOUS CONDITIONS OF PULLING -IN

At subsynchronous speed, $\dot{\delta}$ increases continuously so that $P\delta$ is positive slip and $P^2\delta$ is deacceleration. An attempt to pull-in starts (from subsynchronous speed corresponding to slip S_o) when, owing to T_r, T_t begins to increase even though T_a is decreasing. This attempt (not the synchronisation attempt), terminates when T_t becomes zero ~~at~~ and is successful or not depending on

(a) Wheather the speed reached is less than the synchronous speed.

(b) the load angle when T_t becomes equal to zero.

If speed remains less than synchronous speed, pull-in cannot occur otherwise the possibilities are there which are now discussed.

Let δ_1 be the angle at which the torque T_r attains value $-C$. Thereforefrom Equation

$$\delta_1 = \frac{\pi}{4} - \delta_{max}$$

Let δ_f be the stable load point at which the reluctance and load torque becomes equal. This value is obtained as follows :

$$T_1 = T_r = K \cos 2 (\delta_{max} - \delta_f) - C$$

$$\text{or } T_1 + C = K \cos 2 (\delta_{max} - \delta_f)$$

$$\text{or } \delta_{max} - \delta_f = \frac{1}{2} \tan^{-1} \frac{\sqrt{K^2 - (T_1 + C)^2}}{T_1 + C}$$

$$\delta_f = \delta_{max} - \frac{1}{2} \tan^{-1} \frac{\sqrt{K^2 - (T_1 + C)^2}}{T_1 + C} \tag{5.11}$$

Same value of T_r can be obtained at another angle δ_f' with the condition that

$$\frac{\delta_f + \delta_f'}{2} = \delta_{max}$$

δ_{max} is the angle at which maximum torque $T_{r.max}$ is available. Thus $\delta_f' = 2\,\delta_{max} - \delta_f$

$$= \frac{\pi}{2} - 2\,\delta_1 - \delta_f$$

If the load angle δ is less than δ_f or greater than δ_f', synchronous speed is never reached and so pull-in cannot occur. If value of δ lies in between these two angles, synchronous speed is reached and pull-in may or may not occur.

Of the possible load angles consider first the case for which T_t becomes zero. δ would then lie between δ_f and δ_{max} . If $T_r \gg T_l$ pull-in will occur with termina tion at the steady state load angle δ_f.

Next case is when T_t becomes zero, δ lies between δ_{max} and δ_f' . This meets the condition for synchronization but, as δ increases, $T_r - T_l$ also increases and thus instead of deceeleration acceler tion takes place and it takes some time before final stabilisation takes place with $\delta = \delta_f$.

The limiting case when δ just equals δ_f' , there exists two possibilities. If operating conditions tend to reduce δ below δ_f , then $T_r > T_l$ and synchronisation takes place in a similar way to that of case where δ lies between δ_{max} and δ_f . If , however, the system conditions tend to increase, δ then $T_r < T_l$ and a pole slip occurs.

5.4 PULL-IN CRITERION

It is apparent from preceding discussions that operational modes is class when slip becomes zero are the crucial cases for the establishment of a pull-in criterion.

It is also observed that net acceleration is larger in case when δ is equal to δ_f' , than in case when δ lies between δ_f' and δ_{max} . It is therefore the mode most likely to lead to synchronism , so that the terminal conditions for successful pull in are :

1. $S = 0$
2. $\delta = \delta_f' = \frac{\pi}{2} - \delta_f - 2\,\delta_1'$

Let the slip, at the moment when this synchronisation process starts, be equal to S_o and an approximation is made at this stage which assumes that S can be represented as a simple cosine function of δ . This is represented by

$$S = S_o \cos (\delta + \delta_f + 2\,\delta_1) \qquad (5.12)$$

So that at an angle $\delta = \frac{\pi}{2} - \delta_f - 2\,\delta_1$. S becomes zero. S will equal S_o when

$$\delta = \delta_o = - \delta_f - 2\,\delta_1$$

It is zero at this moment when the attempt of synchronisation starts. From Eqn.5.10 S_o is obtained as (Appendix 9.17)

$$S_o = \frac{1}{2A} \left[- B + \left\{ B^2 + 4\,A\,(T_1 + C - T_{ro}') \right\}^{1/2} \right] \qquad (5.13)$$

Finally the Eqn 5.1 is integrated. Using Eqn 5.2 and 5.12 substituting for initial and final conditions, yields pull-in criterion for inertia J which can be syn synchronised, against a load torque T_1. This J includes the inertia of reluctance machine rotor also.

The expression for J as derived in Appendix 9.18) is

$$J = \frac{-2}{S_o^2} \left[-D \sin 2\delta_o + E \cos 2\delta_o + (B - B_M) S_o - (T_1 + C - \frac{AS_o^2}{2} + K S_o + \frac{K\pi}{4}) \frac{\pi}{2} \right] \qquad (5.14).$$

CHAPTER 6
EXPERIMENTAL RESULTS

6.1 EXPERIMENTAL MACHINE

6.1.1 Stator

Number of stator slots	=	36
Outside diameter	=	22.2 cm
Stator bore diameter	=	14 cm
Stator core length	=	8.2 cm
Voltage	=	400 volt

6.1.2 Stator Winding

The principle of pole amplitude modulation has been applied in designing the two speed winding. Modulation is effected in practice by changing the direction of current flow in certain coils of the winding, thus resulting in the modulation of the ampere conductor distribution of the winding . The winding for single speed is modified in such a way that the operation at the second speed approaches normally without detriment to the performance at initial speed. The winding however, in the process, does not remain absolutely standard at either pole number. The scheme of connections at the terminal board where 72 ends are brought out is as shown in Fig. 6.1a The winding particulars are :

PHASE A SLOT NO.	PHASE C SLOT NO	PHASE B SLOT NO.
1 → A_2	C_1 — 8	B_1 — 4
6	9 → C_2	5 → B_2
7 → A_4	C_3 — 13 → C_4	B_3 — 10 → B_4
11	C_5 — 16 → C_6	B_5 — 15 → B_6
12 → A_6	C_7 — 20	B_7 — 17
14 → A_8	21 → C_8	18 → B_8
19 → A_{10}	C_9 — 26	B_9 — 22
24	27 → C_{10}	23 → B_{10}
25 → A_{12}	C_{11} — 31 → C_{12}	B_{11} — 28 → B_{12}
29	C_{13} — 34 → C_{14}	B_{13} — 33 → B_{14}
30 → A_{14}	C_{15} — 2	B_{15} — 35
32 → A_{16}	3 → C_{16}	36 → B_{16}

8-pole star connection:

(i) A_2-A_4; A_3-A_5, A_6-A_8; A_7-A_9; $A_{10}-A_{12}$, $A_{11}-A_{13}$, $A_{14}-A_{16}$; C_2-C_4, C_3-C_5, C_6-C_8, C_7-C_9; $C_{10}-C_{12}$, $C_{11}-C_{13}$, $C_{14}-C_{16}$; B_2-B_4, B_3-B_5, B_6-B_8, B_7-B_9, $B_{10}-B_{12}$, $B_{11}-B_{13}$, $B_{14}-B_{16}$; $A_{15}-C_{15}-B_{15}$.

Supply $A_1-C_1-B_1$.

6-pole delta connection:

(ii) A_2-A_4, A_3-A_5, A_6-A_7; A_8-A_{10}; A_9-A_{11}; $A_{12}-A_{13}$, $A_{15}-A_{14}$; B_2-B_4, B_3-B_5, B_6-B_7, B_8-B_{10}; B_9-B_{11}, $B_{12}-B_{13}$; $B_{15}-B_{14}$; C_2-C_4; C_5-C_6, C_3-C_7, C_8-C_{10}, C_9-C_{11}; $C_{12}-C_{13}$; $C_{14}-C_{16}$; A_1-C_{16}, C_1-B_{16}, B_1-A_{16}.

Supply $A_1-C_1-B_1$.

FIG. 6.a Connection diagram of 6/8 pole P.A.M. wdg.

Number of turns per phase = 954

Number of conductors per slot = 159

6.1.3 Rotor

In the present dissertation work it is the rotor design which has been emphasised in the overall design of reluctance motor . It is because the stator of the reluctance motor is same as that of an induction motor, which has already been standardised and does no more pose a problem.

Analysis has been done for a number of rotor structures in chapter 3 followed by listing a suitable design procedure . But before the optimisation method can be applied it is necessary to obtain approximate value of rotor parameters which could be supplied as the data for the optimisation programmes listed in Appendix 9.10 to 9.15.

For this the variation of X_d/X_q and hence the performance was studied by varying one of the four unknown variables keeping other three constant. The prodedure was repeated till variation of performance with respect to each unknown variable was obtained. The values of unknown variables at which these unknowns were kept constant, were decided on the basis of experimental results . By careful observation of the trend of variation of X_d/X_q suitable set of variables were chosen. The rotor periphery was accordingly milled out . This lead to the testing of the motor for different rotor designs. But only significant testing results are plotted and considered for comparison.

On the basis of above test results obtained data to be supplied for the optimisation problem was fixed. The successful execution of the programme lead to optimised values of rotor interpolar channel parameters which have been listed in Table 4.1 Accordingly a new rotor was fabricated and tested. The performance of this rotor and two other typical rotor designs have been plotted and compared. Rotor structures incorporating flux-barriers have also been considered. The

6.2 TESTING OF THE MACHINE

This section is concenred with the testing of reluctance motor for different rotor dimensions.

The ratio of main air-gap length and the interpolar channel depth was kept approximately 25 in all cases except for the newly fabricated rotor in which, because of width of the copper end ring welded to the copper bars, it was not possible to increase this ratio beyond about 20. But this does not very much effect the performance.

The results obtained on the basis of testing done on the reluctance motor are recorded in a series of curves. The variation of power factor with output for specified rotor dimensions, is shown in Fig. 6.1 for 6-pole and 8 pole operation. For the same rotor the efficiency is also plotted against the output as shown in Fig. 6.2.

Similarly for other two rotor designs Fig. 6.3 to 6.6 show the variation of power factor and efficiency with pull out torque measured in synchronous watts.

The testing indicated that the starting performance of the motor gets worsened as the pole width is decreased. This is because with the milling out of channels some copper bars are also excluded resulting in high rotor resistance leading to low induction motor asynchronous torque. At one stage beca use of this the motor actually did not pull-in-to- step even when no load was connected to the shaft . To establish that it was because of low induction motor torque that the motor could not pull into step, copper bars, milled out during the removal of iron, were pl replaced by welding them to the end rings. Testing of this rotor resulted in successful pulling in and the motor synchronous performance was as predicted on the basis of X_d/X_q ratio obtainable from that particular rotor design.

To avoid such failure in pulling in the milling was performed on the new rotor in such a way that maximum number of bars possible, were left on the rotor. This avoided the welding of copper bars to the end rings to bring down the rotor resistance in order to increase the asynchronous torque.

6.3 COMPARISON OF RESULTS

Tables 6.1 to 6.3 compare the ratio X_d/X_q , power factor (maximum), pull-out torque and effec tive load being supplied by the motor as determined from analytical and experimental results.

The performance calculated by using results of conventional analysis, can be observed to be very much deviated from the experimental results. This means simply and not surprising that the method of analysis (conventional), based on the p-ermeance distribution' and the use of Fourier series, is inadequqte, to deal with the problem . If, to obtain better results from the same analysis, the higher order harmonics are considered, it will not be without the introduction of mathematics of complexity that the accurate results could be obtained.

The performance obtained from the analysis, employing the principle of flux-accumulation, its very much closer to the experimental results. Thus it is established that the results given for direct axis and quadrature axis reactances in sec. 3.4 are simple and accurate as well when compared with the conventional analysis. The term 'effective load', determined alongwith pull out torque, maximum power factor and efficiency, is the sum of net load being supplied through the shaft and the torque needed to supply the negative intercept at zero slip which is

$$T_{s=0} = \frac{V^2 r \ (X_d - X_q)^2}{2(X_d X_q + r^2)}$$

As the value of expression increases with increasing saliency and stator resistance, the amount of actual load that can be supplied through the shaft, can be increased by decreas-ing the value of stator resistance for a parti-cular machine.

The effective load being the value of pull-out torque at zero stator winding resistance, it is easily concluded that its value would remain constant for all values of stator resistance . But the external load that can be supplied will reduce with increasing stator resis-tance . Table 6.4 compares the ratio of torques available at two speeds obtained from experimental as well as analyti-cal results. Table 6.5 compares the magnitude of stator input current for the three rotor structures whose perfor-mance is being discussed.

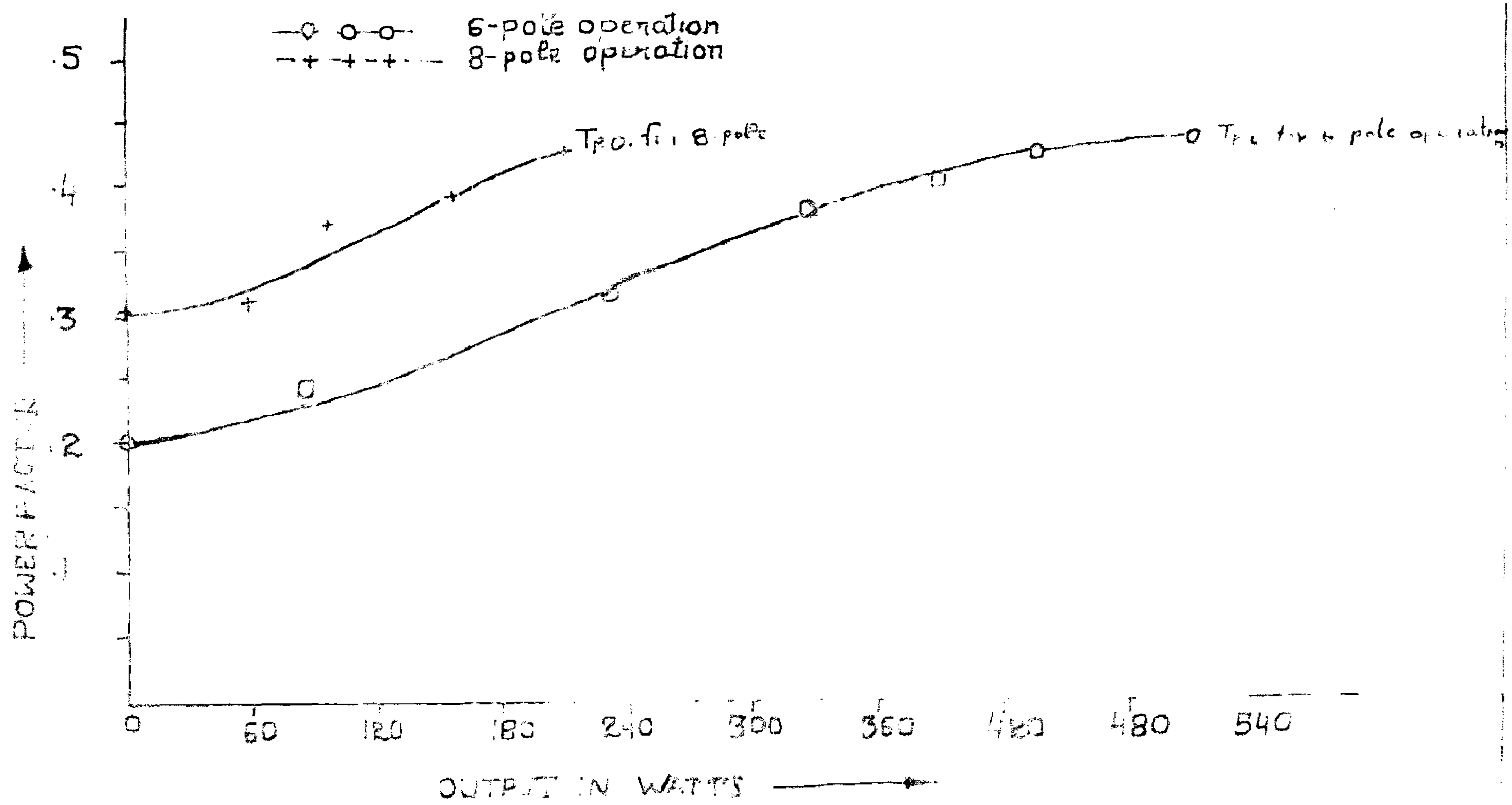

configuration A-1 : $A = 0.25$, $B = 0.486$, $E = 0.389$, $C = 0.295$, $D = 0.15$, $n = 25$

FIG.6.1. PERFORMANCE CHARACTERISTICS for the configuration A-1

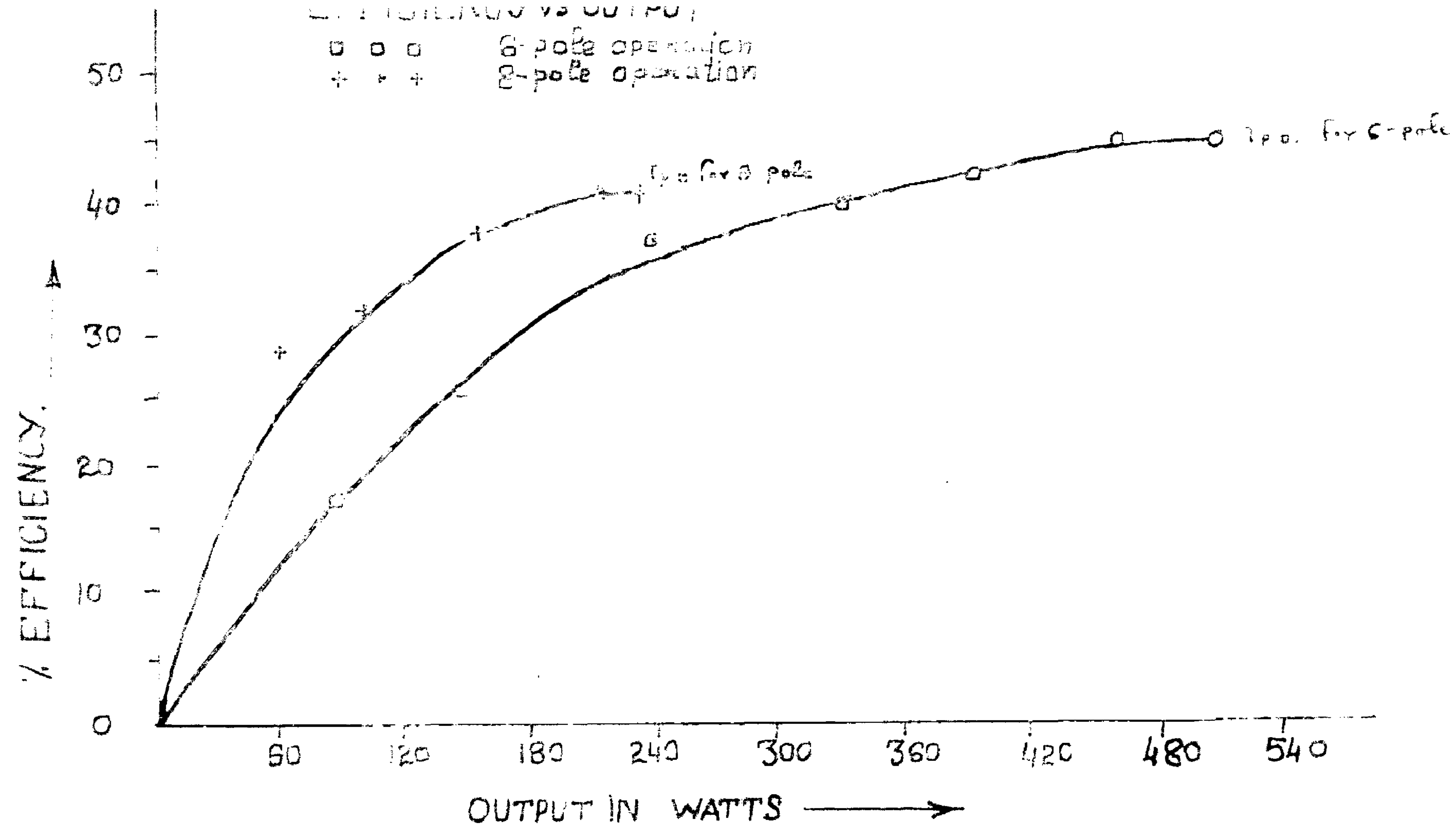

configuration A-2 ; A= 0.25 , B = 0.486, E=0.389 , C = 0.295, D= 0.15 , h = 25

FIG.6.2. PERFORMANCE CHARACTERISTICS for the configuration A-2

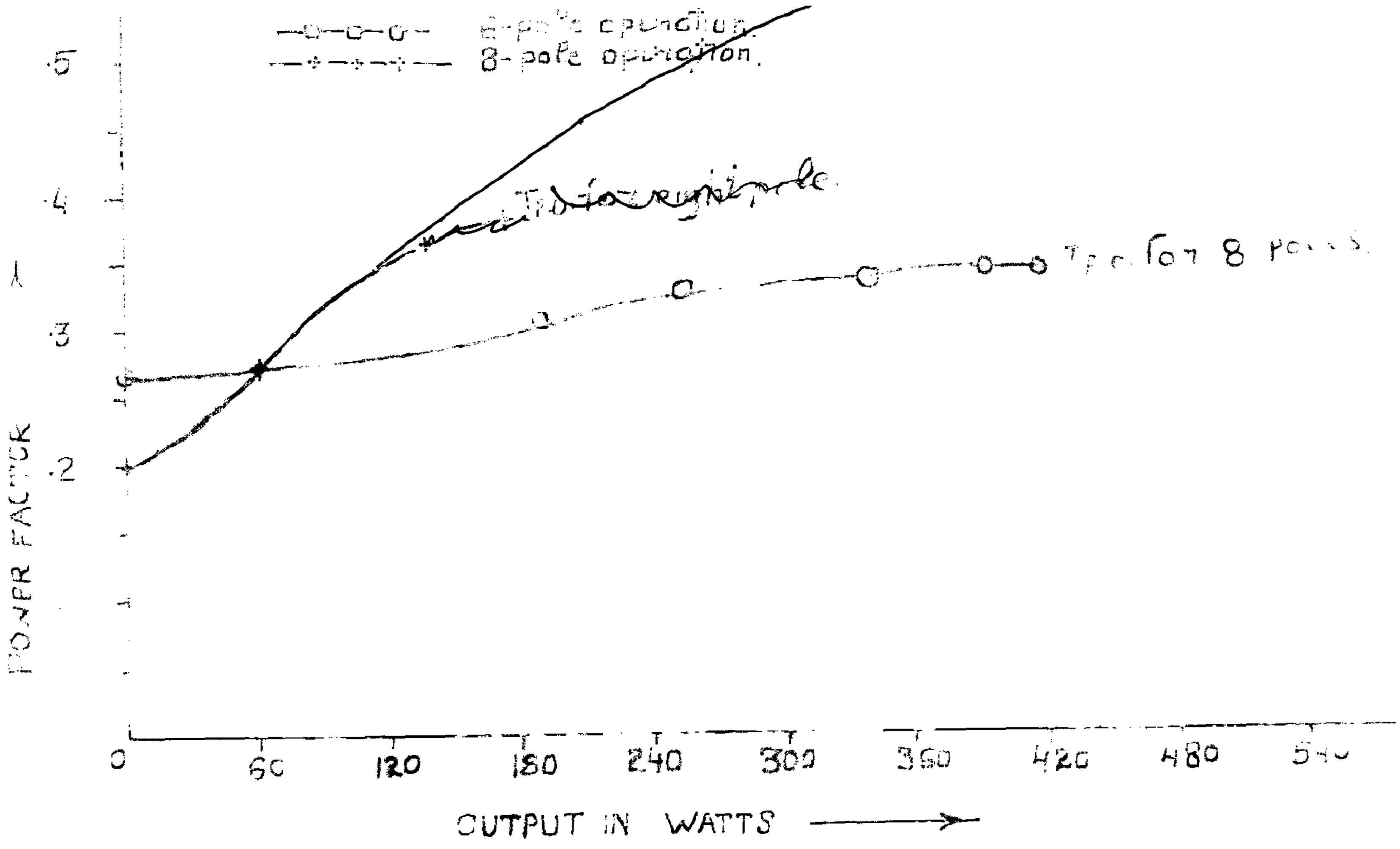

configuration A-2 : A= 0·262, B= 0·382, C= 0.264, E= 0·487, D= 0·175 , h= 20.

FIG.6.3. PERFORMANCE CHARACTERISTICS for the configuration A-2

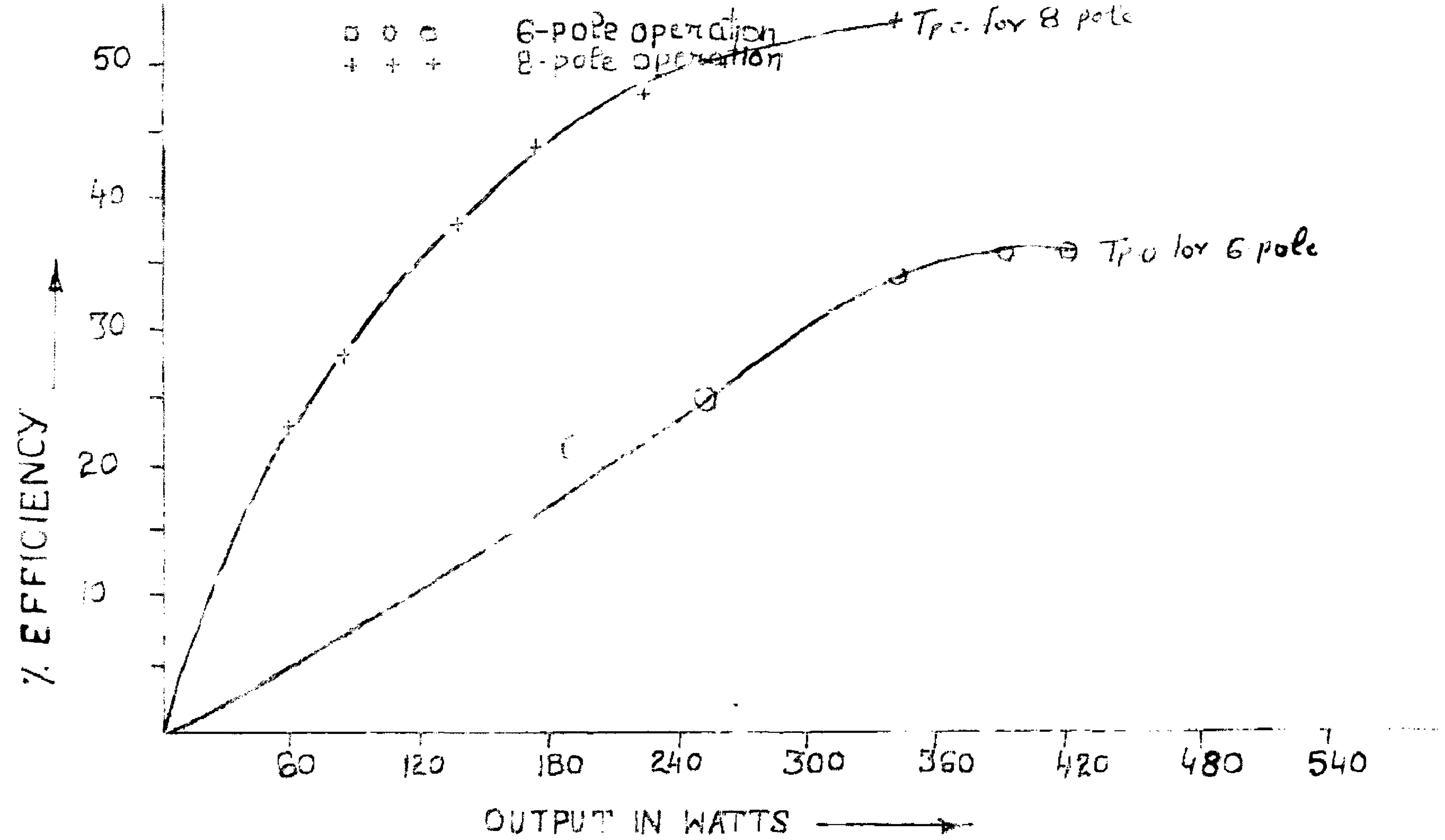

configuration A-2 : A= 0.262, B= 0.382, E=0.487 , C=0.264, D= 0.175 , h= 25

FIG.6.4. PERFORMANCE CHARACTERISTICS for the configuration A-2

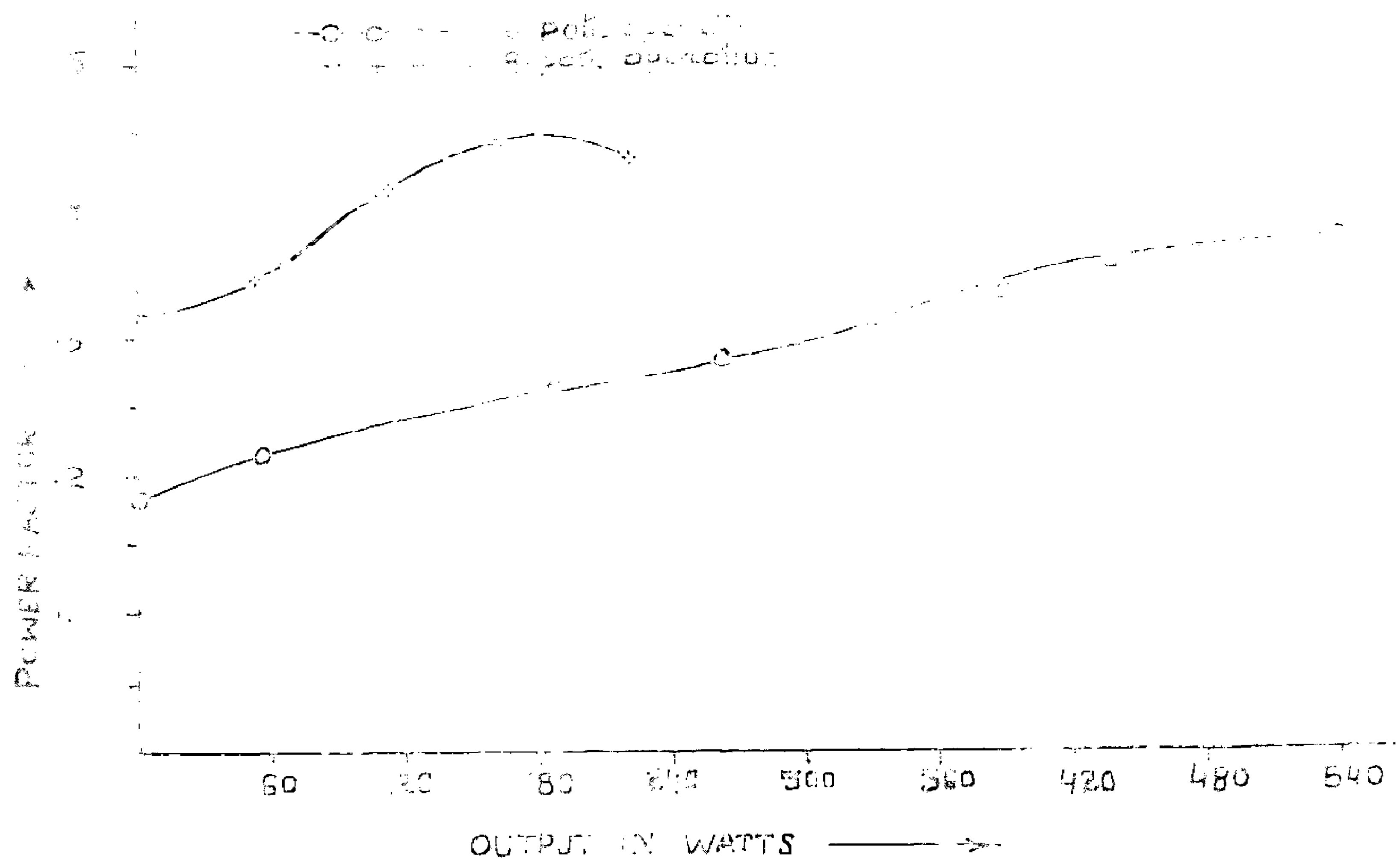

configuration A-3 : $A = 0.22$, $B = 0.44$, $E = 0.484$, $C = 0.36$, $D = 0.066$, $h = 20$.

FIG.6.5. PERFORMANCE CHARACTERISTICS for the configuration A-3

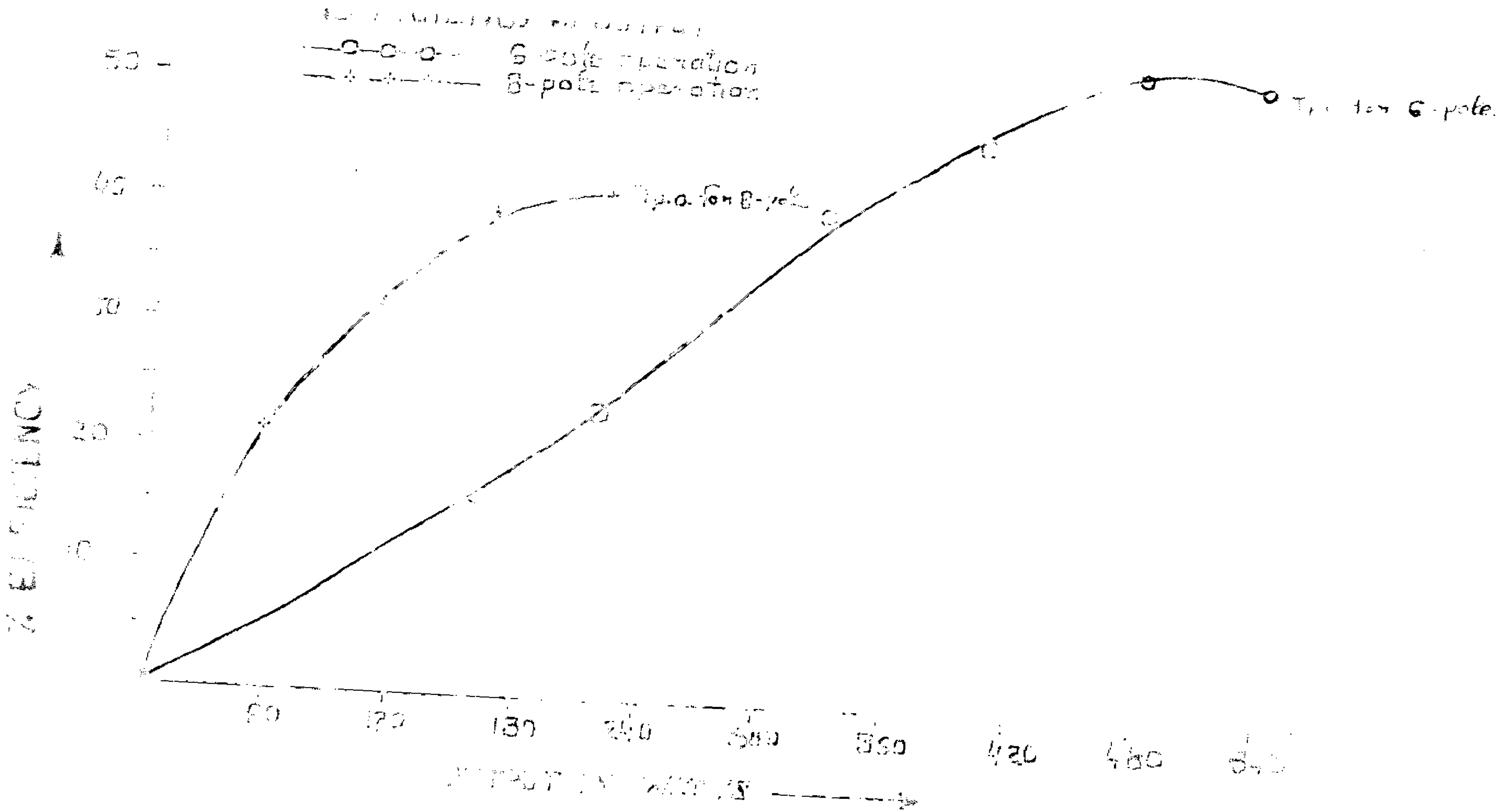

configuration A-3 : A=0.22 , B=0.44 , E=0.484 , C=0.36 , D=0.066 , h=20

FIG. 36 PERFORMANCE CHARACTERISTICS for the configuration A-3

TABLE 6.1

Configuration A1 for interpolar channels		$A = 0.25$, $B = 0.486$ $E = 0.389$, $C = 0.295$, $D = 0.15$, $h = 25$			
Performance to be compared	No. of poles	X_d / X_q	Effective load being supplied in syn. watts.	Pull out torque	Maximum power factor
Experimental Results	6		520		.434
	8		228		.432
Analytical Results for $r = 13\Omega$, $X_1 = 0$ % Following conventional analysis of sec. 3.3	6	1.93	653	653	0.31
	8	2.24	435	435	0.436
Analytical Results for $r = 13\Omega$, $X_1 = 10\%$. Following the conventional analysis of sec. 3.3	6	1.78	470	457	0.276
	8	2.02	324	300	0.412
Analytical results for $r = 13\Omega$ $X_1 = 10\%$, following the suggested analysis, employing the net flux accumulation principle of Sec. 3.4	6	2.7	1000	937	0.435
	8	2.13	356	330	0.433

TABLE 6.2

Configuration A2 for interpolar channels		A = 0.262, B = 0.382 , R = 0.487 , C = 0.264 D = 0.175 , h = 25			
Performance to be compared	No. of poles.	X_d / X_q	Effective load being supplied in syn. watts.	Pull out torque	Maximum power factor
Experimental Results	6		420		0.342
	8		345		0.46
Analytical results for $r = 13\Omega$, $X_1 = 0\%$, Following conventional analysis of sec. 3.3	6	1.85	670	670	0.288
	8	3.37	969	860	0.475
Analytical results for $r=13\Omega$, $X_1 = 10\%$, Following the conventional analysis of sec. 3.3	6	1.72	515	500	0.256
	8	2.78	600	542	0.463
Analytical results for $r=13\Omega$ $X_1 = 10\%$, following the suggested analysis, employing the net flux accumulation principle of sec. 3.4	6	2.06	760	739	0.342
	8	2.77	596	539	0.462

TABLE 6.3

Configuration A3 for interpolar channels

$A = 0.22$, $B = 0.44$, $E = 0.484$, $C = 0.36$, $D = 0.066$, $h = 20$

Performance to be compared	No.of poles	X_d/X_q	Effective load being supplied in syn. watts.	Pull out torque	Maximum power factor
Experimental Results	6		532		0.378
	8		220		0.43
Analytical results for r=133, X_1 = 0% , following conventional analysis of sec.3.3	6	2.13	705	705	0.4
	8	2.2	406	406	0.33
Analytical results for r=133 X_1 = 10%, Following the conventional analysis of Sec. 3.3	6	1.95	540	526	0.354
	8	1.98	305	287	0.434
Analytical results for r=133, X_1 = 10%, following the suggested analysis, employing the net flux accumulation principle of sec. 3.4	6	2.23	710	690	0.413
	8	2.19	371	350	0.44

TABLE 6.4

Rotor configuration	Analytical T_6/T_8	Experimental T_6/T_8
A_1	2.84	2.28
A2	1.37	1.21
A_3	2.0	2.4

TABLE 6.5

Rotor Configuration	Current for 6 pole operation	Current for 8 pole operation
A1	4.2 A	1.8 A
A2	4.8 A	2.0 A
A3	4.15 A	1.6 A

CHAPTER - VII

CONCLUSIONS, APPLICATIONS AND SCOPE FOR FUTURE WORK

The test results of Sec. 6.3 prove that the permeance distribution fundamental component obtained by Fourier's analysis is quite inadequate to predict the performance. The analysis, based on the principle of net flux accumulation, gives results which tally favourably with the experimental results. The expression for X_d/X_q obtained from this analysis is simple to handle and is capable of giving accurate results. The results further establish that the reluctance motor with optimised rotor draws lesser current from the supply and runs at almost equal power factors at the two speeds, which was aimed at in designing the rotor. The ratios of pull-out torque are also found to be approximately same as determined from analysis and experimental results.

Analysis has been done to incorporate the flux barriers for causing asymmetry in the magnetic circuit amounting to high X_d/X_q ratio. As effect of flux-barriers when employed with the channels, is much more pronounced than the channels, it is suggested to further decrease the channel width by keeping the amount of iron to be milled out at 30% or so. This would lead to lower stator input current and increased efficiency as well.

Sufficiently high X_d/X_q ratio can be achieved, for a particular set of optimised channel parameters by suitable placement of flux-barriers.

The study of pullin phenomenon was also carried out at various stages of experimental work. Except for the case when extra copper bars, were welded to the end rings, the motor failed to pullin with a connected load equivalent to nearly 50% of the pull-out torque in synchronous mode. This suggests that removal of copper bars alongwith the iron , during the milling out leads to low induction motor torque which is still lower at the slip corresponding to the load to be synchronised.

The great merit of reluctance motor is its ability to maintain a constant speed within normal fluctuations in supply voltage. Reluctance motors of rating as high as hundred and fifty horse power are being used in variety of industrial applications. Three outstanding applications, that can be categori-sed are in the field of :

1. Constrant speed drive. e.g. for Motor alternator sets to keep the frequency variation to that of mains e.g. computer and buffer supply sets, drive for electric clocks, tape decks, cine projector and synchronising switches etc.

2. Group drives, particularly multispeed drives are more important. (e.g. they have been used to provide precisely controllable and completely synchronised multiple drives of textile machinery and in synthetic fibre processing machines).

3. Position control systems. (e.g. They have been used to position precisely and reliably the control rods in nuclear reactors and in multimachine systems requiring exact synchronisation of all elements at all times.)

In general, an obvious field of application for reluctance motor is where any divergence in the speed would amount to variation in the desired work to be obtained from the drive.

The motor is lower in cost than the existing constant speed drives. It requires comparatively little maintenance which is a major consideration in continuous 24 hours process work. In comparison to induction motor the reluctance motor has the advantage of having synchronous speed operation, corresponding to the supply frequency and the number of poles for which it is wound.

Applications in which reluctance motors are required to work from variable frequency supply, are also increasing and thyristor invertors are becoming the most popular form of supply . These give square wave output voltages which are quite acceptable to these machines even down to frequency below 15 c/s . The performance with regard to power factor and efficiency on square wave input, however will always be somewhat lower than on sine wave input.

In order to attain the advantages of using thyristor invertors for variable frequency operation, it is suggested to analyse the performance of the machine when switched on to such supply sets.

As it was not possible to fabricate rotor with flux-barriers due to nonavailability of necessary facilities the analysis for multispeed operation could not be tested. It is therefore suggested to fabricate such multispeed rotors with optimum dimensions. The attempt, if successful will lead to the better utilisation of stator frame, a power factor equal to that of industrial induction motors and increased pull out torque, which would enable the reluctance motor to outclass the other machines in a large number of industrial applications.

VIII

REFERENCES.

1. LAURENSON, P.J., AGU, A.L., "Theory and Performance of Polyphase reluctance machines", IEE-Proc., Vol. 111, No.11, 1964, pp 1435-45.

2. KOSTKO, J.K., "Polyphase Reaction Synchronous Motor," J.A.I.E.E., 1923, p 1162.

3. FONG, W., " Change speed reluctance motors", IEE-Proc., Vol.114, No. 6, 1967, pp 797-801

4. LAWRENSON, P.J., GUPTA, S.K., VAMARAJU, S.R.M., "Multi speed performance of segmental-rotor reluctance machines, IEE- Proc. (GB) V. 114, N5, May 1968, pp. 695-702.

5. FONG, W., " New Type of Reluctance Motor" IEE-Proc. V. 117, No.3, 1970, p. 545-551.

6. LAWRENSON, P.J., "Synchronizing performance of Reluctance Motors", IEEE Proc. (GB), V. 115, 1968.

7. STEPHENSON, J.M. and LAWRENSON, P.J., "Average asynchronous torque of a synchronous machine with particular reference to reluctance machine, "Proc. IEE, 1969, 116, (6), p. 1049.

8,10. LAWRENSON, P.J., "PULL in Criterion for Reluctance motors," IEE, Proc. Vol. 120, No. 9, 1973, p.982.

9. BURIAN, K., "Pulling into Step of Reluctance Motors," IEE, Trans., 1965, PAS, 84, p. 349-352.

11. LAWRENSON, P.J., and GUPTA, S.K., " Developments in the performance and theory of segmental rotor reluctance motors", Proc. IEE, 1967, V. 114 (5) p 645.

12. LAWRENSON, P.J., "Two speed Operation of Salient Pole reluctance machines", IEE-Proc. (GB), Vol. 112, No. 12, 1965, pp. 2311-2316.

13. GREENWOOD, P.B., "Synchronous Reluctance Motors", Electric Review (GB), March, 1968 Vol. 182, No.12, p. 432-434.

14. RAWCLIFFE, G.H., "A New Type of Reluctance Motor" Electric Review (GB), Vol. 183, 1968, p.129-30.

15. LAWRENSON, P.J., GUPTA, S.K., " Developments in the performance and theory of segmented rotor reluctance motors", IEE-Proc., V. 114, No.5, May 1967, pp. 645-653.

16. "Non Linear Optimisation" - L.C.W. Dixon.

CHAPTER - 9

APPENDICES.

9.1 EXPRESSION FOR THE RELUCTANCE TORQUE

Fig. 9.1 shows the basic conventional feature of a simple single phase reluctance motor. The essential requirement is that the rotor should be shaped so that the reluctance of the magnetic circuit is a function of the angular position of the rotor. Referring to figure, it can be seen that reluctance H is a periodic function of the angle θ_o between the long axis of the stator poles and of the rotor.

When the rotor is direction in line with the axis of the stator poles (i.e. $\theta = 0, \pi, 2\pi, \ldots$) the reluctance has a minimum value, H_d, called the direct axis reluctance. when the axis of rotor is at right angles to the axis of the stator poles (i.e. $\theta = \frac{\pi}{2}, \frac{3\pi}{2}, \ldots$), the reluctance has a maximum value, H_q, called the quadrature axis reluctance. The excitation is provided by connecting the winding on the stator to a single phase source of alternating voltage. Fig. (9.2) shows that the flux ϕ is alternatin According to equation (2.1)

$T = -\frac{1}{2} \phi^2 \frac{dH}{d\theta_o}$, where T is the instantaneous torque acting in the direction so as to increase the angle θ_o. The curve of ϕ^2 and $dH/d\theta_o$ corresponding to ϕ and H respectively are shown in Fig. 9.3.

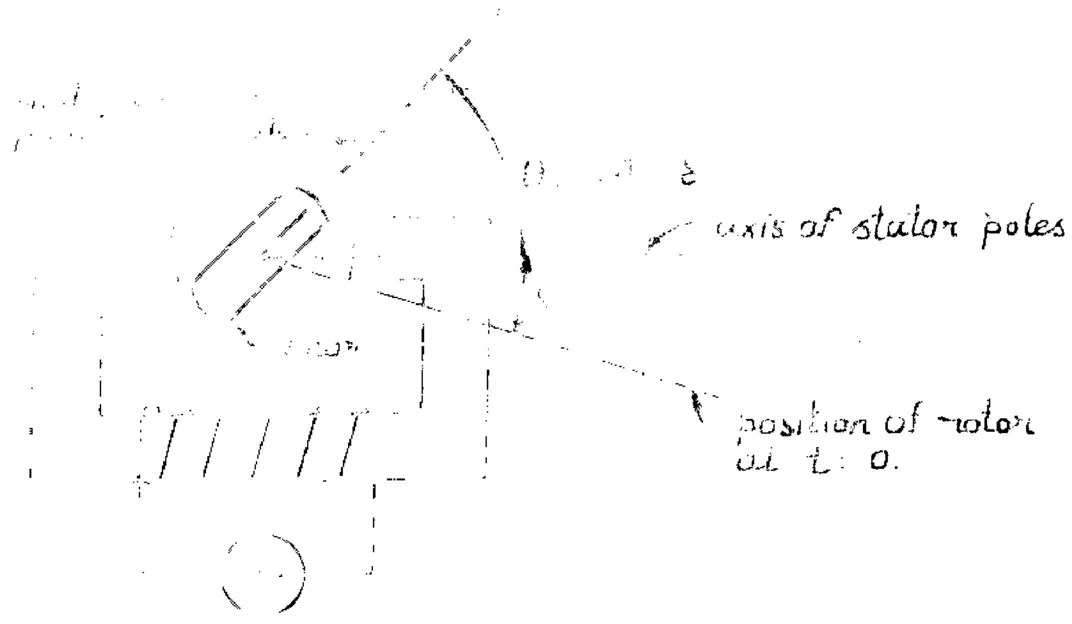

FIG. 6 [illegible] MOTOR

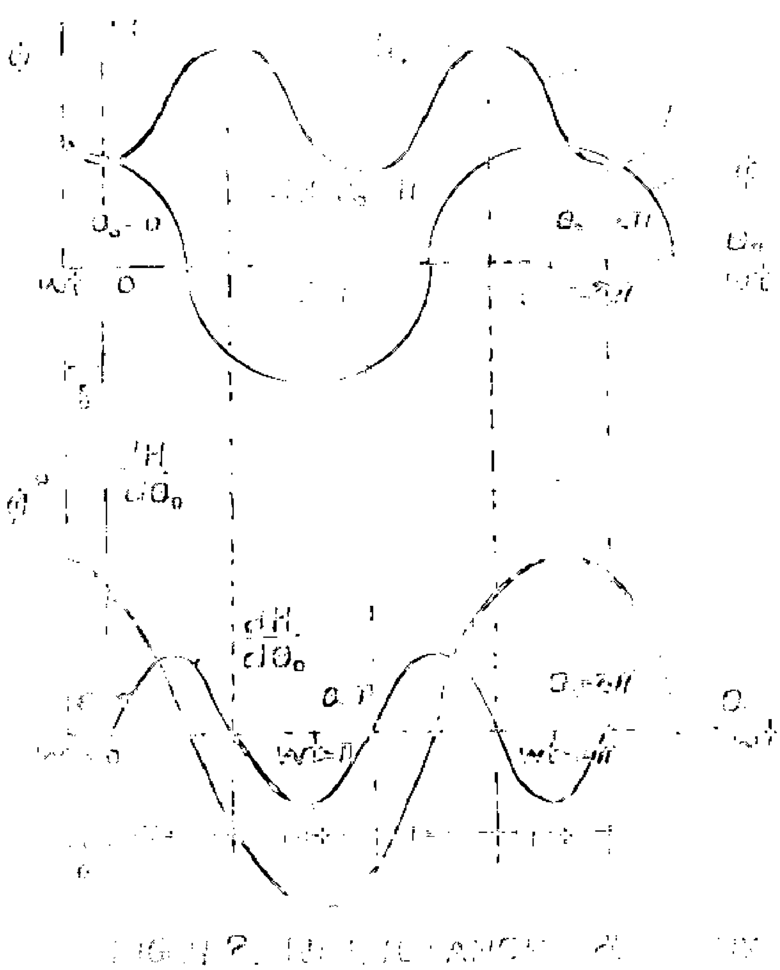

FIG. 8 [illegible] VARIATIONS

FIG. 9 [illegible] VARIATIONS

The direction of torque in equation (2.1) is determined by the sign of $dH/d\theta_o$. Figure shows that torque is positive when the reluctance is decreasing and negative when the reluctance is increasing. The reluctance varies according to the geometry of magnetic circuit and the waveform of the flux depends upon the waveform of the applied voltage . For simplification, it is assumed that the flux and reluctance vary sinusoidally. This assumption of the sinusoidal waveform is a fairly realistic assumptions. If there is sufficient departure in waveform from sinusoidal, the flux and reluctance can be expressed in terms of Fourier series. The instantaneous value of ϕ of the flux will be

$$\phi = \phi_m \cos \omega t \qquad (9.1)$$

where ϕ_m is the maximum value of flux

ω is angular velocity

Hence $\phi^2 = \phi_m^2 \cos^2 \omega t = \frac{1}{2} \phi_m^2 (1 + 2 \cos \omega t)$ (9.2)

The instantaneous value H of the reluctance is the function of the variable angle θ_o. If sinusoidal reluctance variation is assumed, referring to reluctance curve shown in Fig. (9.3) the reluctance can be expressed as :

$$H = \frac{1}{2} (H_d + H_q) - \frac{1}{2} (H_q - H_d) \cos 2 \theta_o \qquad (9.3)$$

$$\therefore \quad \frac{dH}{d\theta_o} = (H_q - H_d) \sin 2\theta_o \qquad (9.4)$$

It is to be assumed that the rotor has been started by auxiliary device and is running at a constant angular velocity ω_o radians per second.

Neglecting torque pulsations, the instantaneous position of the rotor is given by

$$c\theta_o = (\omega_o t - \delta) \tag{9.5}$$

where δ is its instantaneous position at zero time when the flux is passing through its maximum value. For simplification in derivation δ is taken as a lag angle.

Substituting expression (9.5) in expression (9.4)

$$\frac{dH}{d\theta_o} = (H_q - H_d) \sin (2\omega_o t - 2\delta) \tag{9.6}$$

Substituting expression (9.2) and expression (9.6) in the basic torque equation (2.1).

$$T = -\frac{1}{4} \phi^2_{max} (H_q - H_d) \left[\sin(2\omega_o t - 2\delta) + \sin(2\omega_o t - 2\delta) \cos 2\omega_t\right] \tag{9.7}$$

which on further simplification takes the form -

$$T = -\frac{1}{4} \phi^2_{max} (H_q - H_d) \left[\sin (2\omega_o t - 2\delta) + \frac{1}{2} \sin \left\{2(\omega_o + \omega) t - 2\delta\right\} + \frac{1}{2} \sin\left\{2 (\omega_o - \omega) t - 2\delta\right\} \right] \tag{9.8}$$

If the time angular velocity ω of the flux wave i.e. applied voltage is not equal to the shaft angular velocity ω_o, the three terms in equation (9.8) are a function of time and the average value of each of them over a complete cycle reduces to zero. Hence no average torque is developed unless $\omega = \omega_o$.

When $\omega = \omega_o$, the torque becomes,

$$T = -\frac{1}{4}\phi^2_{max}(H_q - H_d) \left[\sin (2\omega t - 2\delta) + \frac{1}{2} \sin (4\omega t - 2\delta) + \frac{1}{2} \sin(-2\delta)\right] \tag{9.9}$$

The first two sine terms are functions of time and hence their average value are zero. The last sine term being independent of time, the average torque will be :

$$T = + \frac{1}{8} \phi_{max}^2 (H_q - H_d) \sin 2\delta \qquad (9.10)$$

The above equation is the characteristics of reluctance torque in all synchronous motor excited or non excited.

9.2 DETERMINATION OF DIRECT AXIS FLUX DENSITY

The equation 3.1 is rewritten as

$$B_{1d} = \frac{4}{\pi} \int_0^{\pi/2} H_{1d}\, \lambda(\theta) \sin^2 p\theta \, d\theta$$

$$= \frac{4}{\pi} \left[H_{1d}\, \lambda(\theta) \int_0^{\pi/2} \frac{1 - \cos 2p\theta}{2} d\theta \right]$$

$$= \frac{2 H_{1d}}{\pi} \left[\lambda(\theta) \left\{ \theta - \frac{\sin 2p\,\theta}{2P} \right\} \right]_0^{\pi/2}$$

$$= \frac{2H_{1d}}{\pi} \Big[\lambda(\theta)\; F(\theta) \Big]_0^{\pi/2}$$

$$= \frac{2H_{1d}}{\pi} \left[\frac{\mu_o}{G} \Big| F(\theta) \Big|_0^{\alpha_1} + \frac{\mu_o}{g} \Big| F(\theta) \Big|_{\alpha_1}^{\alpha_4} + \frac{\mu_o}{G} \Big| F(\theta) \Big|_{\alpha_4}^{\pi/2 - \alpha_4'} \right.$$

$$\left. + \frac{\mu_o}{g} \Big| F(\theta) \Big|_{\pi/2 - \alpha_4'}^{\pi/2 - \alpha_1'} + \frac{\mu_o}{G} \Big| F(\theta) \Big|_{\pi/2 - \alpha_1'}^{\pi/2} \right]$$

$$= \frac{2H_{1d}}{\pi}\left[\frac{\mu_o}{G}\left(\alpha_1 - \frac{\sin 2p\alpha_1}{2p}\right) + \frac{\mu_o}{g}\left(\alpha_4 - \alpha_1 - \frac{\sin 2p\alpha_4}{2p} + \frac{\sin 2p\alpha_1}{2p}\right)\right.$$

$$+ \frac{\mu_o}{G}\left(\pi/2 - \alpha'_4 - \alpha_4 - \sin 2p\left(\frac{\pi}{2} - \alpha'_4\right) + \sin 2p\alpha_4\right)$$

$$+ \frac{\mu_o}{g}\left(\alpha'_4 - \alpha' - \sin 2p\left(\frac{\pi}{2} - \alpha'_1\right) + \sin 2p\left(\frac{\pi}{2} - \alpha'_4\right)\right)$$

$$\left. + \frac{\mu_o}{G}\left(\alpha'_1 - \sin 2p\frac{\pi}{2} + \sin 2p\left(\frac{\pi}{2} - \alpha'_1\right)\right)\right]$$

$$= \frac{2H_{1d}\,\mu_o}{\pi\, g}\left[\frac{\pi}{2h} + (\alpha_4 - \alpha_1 + \alpha'_4 - \alpha'_1)\left(1 - \frac{1}{h}\right)\right.$$

$$- \frac{1}{2p}\left(\sin 2p\alpha_4 - \sin 2p\alpha_1 - \sin 2p\left(\frac{\pi}{2} - \alpha'_4\right) + \sin 2p\left(\frac{\pi}{2} - \alpha'_1\right)\right)(1-$$

(9.11)

where, $h = G/g$, the ratio of maximum to minimum airgap.

9.3 DETERMINATION OF ROTOR MAGNETIC POTENTIALS

9.3.1 Determination of P_3

For determining P_3 eqn 3.5 is rewritten after integration as :

$$\frac{D}{g}\left[H_{1q}\frac{\sin p\theta}{p} - P_3\theta\right]_{\alpha_3}^{\alpha_4} + \frac{D}{G}\left[H_{1q}\frac{\sin p\theta}{p} - P_3\,\theta\right]_{\alpha_4}^{\frac{\pi}{2} - \alpha'_4}$$

$$+\frac{D}{g}\left[H_{1q}\frac{\sin p\theta}{p} - P_3\theta\right]_{\pi/2 - \alpha'_4}^{\pi/2 - \alpha'_3} + (P_2 - P_3)\frac{W}{T} + (P'_2 - P'_3)\frac{W'}{T'} = 0$$

or $$H_{1q}\left[\frac{\sin p\alpha_4 - \sin p\alpha_3}{pg/D} + \frac{\sin p\left(\frac{\pi}{2} - \alpha'_4\right) - \sin p\alpha_4}{pG/D}\right.$$

$$\left. + \frac{\sin p(- - \alpha') - \sin p(- - \alpha')}{pg/D}\right] + \frac{P_2 W}{T} + \frac{P'_2 . W'}{T'}$$

$$= P_3 \left[\frac{\alpha_4 - \alpha_3}{g/D} + \frac{\frac{\pi}{2} - \alpha_4' - \alpha_4}{G/D} + \frac{\alpha_4' - \alpha_3'}{g/D} + \frac{W}{T} + \frac{W'}{T'} \right]$$

or

$$P_3 = \frac{A + P_2 \frac{W}{T} + P_2' \frac{W'}{T'}}{B} \qquad (9.12)$$

where,

$$A = H_{1q} \left[\frac{\sin p\alpha_4 - \sin p\alpha_3}{pg/D} + \frac{\sin p(\frac{\pi}{2} - \alpha_4') - \sin p\alpha_4}{PG/D} + \frac{\sin p(\frac{\pi}{2} - \alpha_3') - \sin p(\frac{\pi}{2} - \alpha_4')}{pg/D} \right] \qquad (9.13)$$

and

$$B = \frac{\alpha_4 - \alpha_3}{g/D} + \frac{\frac{\pi}{2} - \alpha_4' - \alpha_4}{G/D} + \frac{\alpha_4' - \alpha_3'}{g/D} + \frac{W}{T} + \frac{W'}{T'} \qquad (9.14)$$

9.3.2 <u>Determination of P_2</u>

For determination of P_2 Eqn. 3.6 is solved.

$$\frac{D}{g} \left[H_{1q} \frac{\sin p\theta}{P} - P_2 \theta \right]_{\alpha_2}^{\alpha_3} + (P_1 - P_2) \frac{W_1}{T_1} + (P_3 - P_2) \frac{W}{T} = 0$$

$$\text{or } H_{1q} \left[\frac{\sin p\alpha_3 - \sin p\alpha_2}{pg/D} \right] + P_1 \frac{W_1}{T_1} + \frac{A + P_2 \frac{W}{T} + P_2' \frac{W'}{T'}}{B} \cdot \frac{W}{T}$$

$$= P_2 \left[\frac{\alpha_3 - \alpha_2}{g/D} + \frac{W_1}{T_1} + \frac{W}{T} \right]$$

or

$$P_2 = \frac{A_1 + P_1 \cdot \frac{W_1}{T_1}}{B_1} \qquad (9.15)$$

In which the term $\dfrac{\frac{P_2'}{B} \cdot \frac{W}{T} \cdot \frac{W'}{T'}}{B_1}$ has been neglected because it is too small to be considered.

where,

$$A_1 = H_{1q}\left[\frac{\sin p\alpha_3 - \sin p\alpha_2}{pg/D}\right] + \frac{A}{B}\cdot\frac{W}{T} \tag{9.16}$$

and
$$B_1 = \frac{\alpha_3-\alpha_2}{g/D} + \frac{W_1}{T_1} + \frac{W}{T} - \frac{1}{B}\left(\frac{W}{T}\right)^2 \tag{9.17}$$

9.3.3 Determination of P_1

Equation 3.34 can be rewritten after integration as,

$$\frac{p}{G}\left[H_{1q}\frac{\sin p\theta}{p} - P_1\theta\right]_0^{\alpha_1} + \frac{D}{g}\left[H_{1q}\sin p\theta - P_1\theta\right]_{\alpha_1}^{\alpha_2} + (-P_1+P_2) = 0$$

or
$$H_{1q}\left[\frac{\sin p\alpha_1}{pG/D} + \frac{\sin p\alpha_2 - \sin p\alpha_1}{pg/D}\right] + \frac{W_1}{T_1}\left(\frac{A_1+P_1\cdot\frac{W_1}{T_1}}{B_1}\right)$$

$$= P_1\left[\frac{\alpha_1}{G/D} + \frac{\alpha_2-\alpha_1}{g/D} + \frac{W_1}{T_1}\right]$$

or
$$P_1 = \frac{H_{1q}\left[\frac{\sin p\alpha_1}{pG/D} + \frac{\sin p\alpha_2 - \sin p\alpha_1}{pg/D}\right] + \frac{A_1}{B_1}\cdot\frac{W_1}{T_1}}{\frac{\alpha_1}{G/D} + \frac{\alpha_2-\alpha_1}{g/D} + \frac{W_1}{T_1} - \frac{1}{B_1}\left(\frac{W_1}{T_1}\right)^2} \tag{9.18}$$

9.3.4 Determination of P_2'

Equating to zero the summation of flux, in region $\frac{\pi}{2} - \alpha_3'$ to $\frac{\pi}{2} - \alpha_2'$:

$$2\left[\int_{\pi/2-\alpha_3'}^{\pi/2-\alpha_2'} \frac{\mu_o}{g}\left(H_{1q}\cos p\theta - P_2'\right)\frac{D}{2}\,d\theta + \mu_o(P_1' - P_2')\frac{W_1'}{2T_1'} + \mu_o(P_3 - P_2')\frac{W'}{2T'}\right] = 0$$

$$\text{or}\quad \frac{D}{g}\left[H_{1q}\frac{\sin p\theta}{p} - P_2'\theta\right]_{\pi/2-\alpha_3'}^{\pi/2-\alpha_2'} + (P_1' - P_2')\frac{W_1'}{2T_1'} + (P_3 - P_2') = 0$$

$$\text{or}\quad H_{1q}\left[\frac{\sin p(\frac{\pi}{2}-\alpha_2') - \sin p(\frac{\pi}{2}-\alpha_3')}{pg/D}\right] + P_1'\frac{W_1'}{T_1'} + \left\{\frac{A + P_2\cdot\frac{W}{T} + P_2'\frac{W'}{T'}}{B}\right\}\cdot\frac{W'}{T'} = P_2'\left[\frac{\alpha_3' - \alpha_2'}{g/D} + \frac{W_1'}{T_1'} + \frac{W'}{T'}\right]$$

$$\text{Thus}\quad P_2' = \frac{A_1' + P_1'\cdot\frac{W_1'}{T_1'}}{B_1'} \qquad (9.19)$$

in which the term $\dfrac{\frac{P_2}{B}\cdot\frac{W}{T}\cdot\frac{W'}{T'}}{B_1'}$ has been neglected because it is too small to be considered.

where,

$$A_1' = H_{1q}\left[\frac{\sin p(\frac{\pi}{2}-\alpha_2') - \sin p(\frac{\pi}{2}-\alpha_3')}{pg/D}\right] + \frac{A}{B}\cdot\frac{W'}{T'} \qquad (9.20)$$

and

$$B_1' = \frac{\alpha_3' - \alpha_2'}{g/D} + \frac{W_1'}{T_1'} + \frac{W'}{T'} - \frac{1}{B}\left(\frac{W'}{T'}\right)^2 \qquad (9.21)$$

9.3.5 Determination of P_1^0

Lastly, equating to zero the summation of flux in region $\frac{\pi}{2} - \alpha_2^0$ to $\pi/2$.

$$2\left[\int_{\pi/2-\alpha_2^0}^{\pi/2-\alpha_1^0} \frac{\mu_0}{g}\left(H_{1q}\cos p\theta - P_1^0\right)\frac{D}{2}\,d\theta + \int_{\pi/2-\alpha_1^0}^{\pi/2} \frac{\mu_0}{g}\left(H_{1q}\cos p\theta - P_1^0\right)\frac{D}{2}\,d\theta + \mu_0\left(P_2^0 - P_1^0\right)\frac{W_1^0}{2T_1^0}\right] = 0$$

or
$$\frac{D}{g}\left[H_{1q}\frac{\sin p\theta}{p} - P_1^0\,\theta\right]_{\pi/2-\alpha_2^0}^{\pi/2-\alpha_1^0} + \frac{D}{g}\left[H_{1q}\frac{\sin p\theta}{p} - P_1^0\,\theta\right]_{\pi/2-\alpha_1^0}^{\pi/2} + \left(P_2^0 - P_1^0\right)\frac{W_1^0}{T_1^0} = 0$$

or,
$$H_{1q}\left[\frac{\sin p(\frac{\pi}{2}-\alpha_1^0) - \sin p(\frac{\pi}{2}-\alpha_2^0)}{p\,g/D} + \frac{\sin p\frac{\pi}{2} - \sin p(\frac{\pi}{2}-\alpha_1^0)}{p\,g/D}\right] + \frac{W_1^0}{T_1^0}\left(\frac{A_1^0}{D_1^0} + \frac{P_1^0}{D_1^0}\,\frac{W_1^0}{T_1^0}\right) = P_1^0\left[\frac{\alpha_2^0 - \alpha_1^0}{g/D} + \frac{\alpha_1^0}{g/D} + \frac{W_1^0}{T_1^0}\right]$$

or
$$P_1^0 = \frac{H_{1q}\left[\frac{\sin p(\frac{\pi}{2}-\alpha_1^0) - \sin p(\frac{\pi}{2}-\alpha_2^0)}{p\,g/D} + \frac{\sin p\frac{\pi}{2} - \sin p(\frac{\pi}{2}-\alpha_1^0)}{p\,g/D}\right] + \frac{W_1^0}{T_1^0}\cdot\frac{A_1^0}{D_1^0}}{\frac{\alpha_2^0-\alpha_1^0}{g/D} + \frac{\alpha_1^0}{g/D} + \frac{W_1^0}{T_1^0} - \frac{1}{D_1^0}\left(\frac{W_1^0}{T_1^0}\right)^2}$$

(9.22)

9.3.6 Determination of Quadrature - axis flux density

Expression for quadrature-axis flux density given in Eqn 3.19 of Sec. 3.2.5 is rewritten as:

$$B_{1q} = \frac{4}{\pi} \int_0^{\pi/2} (H_{1q} \cos^2 p\theta - P(\theta) \cos p\theta) \cdot \lambda(\theta) \cdot d\theta$$

$$= \frac{4}{\pi} \left[H_{1q} \lambda(\theta) \int_0^{\pi/2} \frac{1 + \cos 2p\theta}{2} d\theta - \left| P(\theta) . \lambda(\theta) \frac{\sin p\theta}{p} \right|_0^{\pi/2} \right] \quad (9.23)$$

Observing the expression for direct-axis flux density it is very much clear that as far as first two terms of equations 9.23 and 9.11A are conserned there is only a difference of sign and therefore eqn 9.23 becomes,

$$B_{1q} = \frac{2\mu_o}{\pi g} H_{1q} \left[\frac{\pi}{2h} + (\alpha_4 - \alpha_1 + \alpha_4' - \alpha_1') (1 - \frac{1}{h}) \right.$$

$$\left. + \frac{1}{2p} \left\{ \sin 2p\alpha_4 - \sin 2p\alpha_1 - \sin 2p(\frac{\pi}{2} - \alpha_4') + \sin 2p(\frac{\pi}{2} - \alpha_1') \right\} (1 - \frac{1}{h}) \right]$$

$$- \frac{4\pi}{\pi p} \left| P(\theta) \cdot \lambda(\theta) \cdot \sin p\theta \right|_0^{\pi/2} \quad (9.24)$$

After substituting for $\lambda(\theta)$ and $P(\theta)$ from Table 3.1 and 3.2 respectively, the last terms is

$$= \frac{4\mu_o}{\pi p} \left[\frac{P_1 \sin p\alpha_1}{G} + \frac{P_1 \sin p\alpha_2 - P_1 \sin p\alpha_1}{g} \right.$$

$$+ \frac{P_2 \sin p\alpha_3 - P_2 \sin p\alpha_2}{g} + \frac{P_3 \sin p\alpha_4 - P_3 \sin p\alpha_3}{g}$$

$$+ \frac{P_3 \sin p(\frac{\pi}{2} - \alpha_4') - P_3 \sin p\alpha_4}{6} + \frac{P_3 \sin p(\frac{\pi}{2} - \alpha_3') - P_3 \sin p(\frac{\pi}{2}}{6}$$

$$+ \frac{P_2' \sin p(\frac{\pi}{2} - \alpha_2') - P' \sin p(\frac{\pi}{2} - \alpha_3')}{6}$$

$$+ \frac{P_1' \sin p(\frac{\pi}{2} - \alpha_1') - P_1' \sin p(\frac{\pi}{2} - \alpha_2')}{6}$$

$$+ \frac{P_1' \sin p\frac{\pi}{2} - P' \sin p(\frac{\pi}{2} - \alpha_1')}{6} \Bigg]$$

$$= - \frac{4\mu_0}{\pi p 6} \Bigg[(- P_1 \sin p\alpha_1 + P_3 \sin p\alpha_4 - P_3 \sin p(\frac{\pi}{2} - \alpha_4')$$

$$+ P_1' \sin p(\frac{\pi}{2} - \alpha_1'))(1 - \frac{1}{h}) + (P_1 - P_2) \sin p\alpha_2 + (P_2 - P_1) \sin p\alpha_3$$

$$+ (P_3 - P_2') \sin p(\frac{\pi}{2} - \alpha_3') + (P_2' - P_1') \sin p(\frac{\pi}{2} - \alpha_2') + \frac{P_1' \sin p\frac{\pi}{2}}{h} \Bigg]$$

Therefore substituting for last term in Eqn 9.24 the expression for B_{1q} is written as :

$$B_{1q} = \frac{2\mu_0 H_{1q}}{\pi 6} \Bigg[\frac{\pi}{2h} + (\alpha_4 - \alpha_1 + \alpha_4' - \alpha_1')(1 - \frac{1}{h})$$

$$+ \frac{1}{2p} \Big\{ \sin 2p\alpha_4 - \sin 2p\alpha_1 - \sin 2p(\frac{\pi}{2} - \alpha_4') + \sin 2p(\frac{\pi}{2} - \alpha_1') \Big\}$$

$$.(1 - \frac{1}{h}) - \frac{2}{p H_{1q}} \Big\{ \Big[- P_1 \sin p\alpha_1 + P_3 \sin p\alpha_4 - P_3 \sin p(\frac{\pi}{2} - \alpha_4')$$

$$+ P_1' \sin p(\frac{\pi}{2} - \alpha_1') \Big] (1 - \frac{1}{h}) + (P_1 - P_2) \sin p\alpha_2 + (P_2 - P_3) \sin p\alpha_3$$

$$+(P_3 - P_2')\sin p\left(\frac{\tau}{2} - \alpha_3'\right) + (P_2' - P_1')\sin p\left(\frac{\tau}{2} - \alpha_2'\right) + \frac{P_1' \sin p \frac{\tau}{2}}{h} \Bigg\} \Bigg] \qquad (9.25)$$

9.4 Determination of Constants of Permeance Equation for a Rotor, having interpolar Channels

9.4.1 General

The expression for permeance is given by

$$P = \lambda_0 + \sum_{n=1}^{\infty} \lambda_{kp} \cos \frac{n\pi X}{C} \qquad (3.24)$$

where, λ_0 and λ_{kp} are given by

$$\lambda_0 = \frac{1}{2C} \int_{-C}^{C} f(X)\, dX$$

and $$\lambda_{kp} = \frac{1}{C} \int_{-C}^{C} f(X) \cos \frac{n\pi X}{C}\, dX$$

in the interval $-C \leq X \leq C$.

The above expressions on simplification become:

$$\lambda_0 = \frac{1}{C} \int_{0}^{C} f(X)\, dX$$

$$\lambda_{kp} = \frac{2}{C} \int_{0}^{C} f(X) \cos \frac{n\pi X}{C}\, dX$$

where, $$f(X) = \frac{\mu_0 RL}{g(X)}$$

L = Length of core

R = Radius of rotor

μ_0 = Permeability of free space.

C = $\tau/2$ (Sec. 3.3.3).

9.4.2 Determination of λ_o

λ_o is rewritten after substituting $C = \pi/2$ in Equation 9.23a as,

$$\lambda_o = \frac{2}{\pi} \int_0^{\pi/2} \frac{\mu_o RL}{g(x)} \, dx$$

$$= \frac{2 \mu_o RL}{\pi} \left[\frac{1}{G} \left| x \right|_0^{\alpha_1} + \frac{1}{g} \left| x \right|_{\alpha_1}^{\alpha_4} + \frac{1}{G} \left| x \right|_{\alpha_4}^{\frac{\pi}{2} - \alpha'_4} + \frac{1}{g} \left| x \right|_{\pi/2 - \alpha'_4}^{\pi/2 - \alpha'_1} + \frac{1}{G} \left| x \right|_{\pi/2 - \alpha'_1}^{\pi/2} \right]$$

$$= \frac{2\mu_o RL}{\pi} \left[\frac{\alpha_1}{G} + \frac{\alpha_4 - \alpha_1}{g} + \frac{\frac{\pi}{2} - \alpha'_4 - \alpha_4}{G} + \frac{\alpha'_4 - \alpha'_1}{g} + \frac{\alpha'_1}{G} \right]$$

$$= \frac{2\mu_o RL}{\pi g} \left[\frac{\pi}{2h} + (\alpha_4 - \alpha_1 + \alpha'_4 - \alpha'_1)\left(1 - \frac{1}{h}\right) \right] \qquad (9.24)$$

This can be written in another form, after making the substitutions $\alpha_1 = A$, $\alpha_4 - \alpha_1 = B$, $\alpha'_1 = D$ and $\alpha'_4 - \alpha'_1 = C$ as,

$$\lambda_o = \frac{2 \mu_o RL}{\pi g} \left[\frac{\pi}{2h} + (B+C)\left(1 - \frac{1}{h}\right) \right] \qquad (9.25)$$

9.4.3 Determination of λ_{4p}

After substituting $C = \pi/2$ in Eqn. 3.23b the expression for λ_{4p} for $n = 1$ becomes,

$$\lambda_{4p} = \frac{4}{\pi}\int_0^{\pi/2} \frac{\mu_0 RL}{g(X)} \cos 2pX \, dX$$

Taking direct axis as reference axis

$$\lambda_{4p} = \frac{-4\mu_0 RL}{\pi(2P)}\left[\frac{1}{G}\left|\sin 2pX\right|_0^{\alpha_1}\right] + \frac{1}{g}\left|\sin 2pX\right|_{\alpha_1}^{\alpha_4}$$

$$+ \frac{1}{G}\left|\sin 2pX\right|_{\alpha_4}^{\pi/2-\alpha_4'} + \frac{1}{g}\left|\sin 2pX\right|_{\pi/2-\alpha_4'}^{\pi/2-\alpha_1'}$$

$$\left. + \frac{1}{G}\left|\sin 2pX\right|_{\pi/2-\alpha_1'}^{\pi/2}\right]$$

$$= \frac{-4\mu_0 RL}{\pi(2P)g}\left[\frac{1}{h}\sin 2p\alpha_1 + \sin 2p\alpha_4 - \sin 2p\alpha_1\right.$$

$$+ \frac{(\sin 2p(\frac{\pi}{2}-\alpha_4') - \sin 2p\alpha_4)}{h} + \sin 2p(\frac{\pi}{2}-\alpha_1') - \sin 2p(\frac{\pi}{2}-\alpha_4')$$

$$\left. + \frac{\sin 2p\frac{\pi}{2} - \sin 2p(\frac{\pi}{2}-\alpha_1')}{h}\right]$$

$$= \frac{-4\mu_0 RL}{\pi g(2P)}\left[\left\{\sin 2p\alpha_4 - \sin 2p\alpha_1 - \sin 2p(\frac{\pi}{2}-\alpha_4') + \sin 2p(\frac{\pi}{2}-\alpha_1')\right\}\right.$$

$$\left. \cdot \left(1 - \frac{1}{h}\right)\right] \qquad (9.26)$$

After making substitutions of previous section λ_{4p} can be written in different form as :

$$\lambda_{4p} = \frac{4\mu_0 RL}{\sigma g(2p)}\left[\sin 2pA - \sin 2p(A+B) + \sin 2p\left(\frac{\sigma}{2} - \overline{C+D}\right) - \sin 2p\left(\frac{\sigma}{2} - D\right)\right]\left(1 - \frac{1}{n}\right) \qquad (9.27)$$

9.5 DETERMINATION OF AXIS REACTANCES

9.5.1 Stator M.M.F

By simple adaptation of well known results for the air-gap, it is possible, taking phase 1 to be the leading phase with current $i_1 = I\cos(\omega t - \theta)$, to write the stator M.M.F M for a three phase machine, neglecting winding harmonics

$$M = \frac{6NI}{\sigma} K_\omega \cos(p\alpha - \omega t + \phi) \qquad (9.28)$$

where α is the angular displacement round the air-gap and ϕ is the time lag between voltage and current vector.

9.5.2 Permeance Equation

The equation for permeance is :

$$P = \lambda_0 + \lambda_{4p}\cos^2 2(p\alpha - \theta) \quad (\text{for } n=1)$$

To be more precise in determining the axis reactances it is necessary to include the other terms corresponding to $n = 2, 3, 4 \ldots\ldots$

9.5.3 Flux Density

For the present analysis, continuing with the simpler expression for permeance, the resultant flux density component is :

$$M.F = \frac{6NI}{\pi}\left[K_w \cos(p\alpha - \omega t + \sigma)\right] \times \left[\lambda_0 + \lambda_{4p}\cos 2(p\alpha - \theta)\right]$$

Substituting $\theta = \frac{\omega t}{p} + \delta - \sigma$ and multiplying the M.M.F. and permeance fundamental components, B is obtained as :

$$B = \frac{6NI}{\pi} K_w \lambda_0 \cos(p\alpha - \omega t + \sigma) + \frac{6NI}{\pi} K_w \lambda_{4p} \cos(p\alpha - \omega t + \sigma) . \cos 2(p\alpha - \omega t - p\delta + \sigma)$$

$$= ID\, K_w \cos(p\alpha - \omega t + \sigma) + I\, E\, K_w \left[\cos(3p\alpha - 3\omega t - 2p\delta + 3\sigma) + \cos(p\alpha - \omega t - 2p\delta + \sigma)\right]$$

where $D = \frac{6N\lambda_0}{\pi}$

and $E = \frac{6N\lambda_{4p}}{2\pi}$

9.5.4 Reactive E.M.F's

The voltage generated by the flux density B in phase 1 is obtained by evaluating the time variation of the total flux linkage.

$$\therefore\ v_1 = -2pN\ K_\omega^2\ I\ \frac{d}{dt}\int_{-\pi/2p}^{\pi/2p} B\ d\alpha$$

$$= -2pN\ K_\omega^2\ I\frac{d}{dt}\left[\frac{D}{p}\sin\ (p\alpha - \omega t + \phi\ ) + \frac{E}{p}\sin\ (p\alpha - \omega t - 2p\delta + \phi\ )\right]_{-\pi/2p}^{\pi/2p}$$

$$= -4N\ I\ K_\omega^2\ \frac{d}{dt}\left[D\cos\ (\omega t - \phi\ ) + E\cos\ (\omega t + 2p\delta - \phi)\right]$$

$$= 4NI\ K_\omega^2\ \omega\left[D\sin\ (\omega t - \phi) + E\sin\ (\omega t + 2p\delta - \phi)\right]$$

or $$v_1 = -4N\ IK_\omega^2\ \omega\left[D\sin\ (\omega t - \phi) + E\sin(\omega t - \phi)\cos 2p\delta + E\sin 2p\delta\cos\ (\omega t - \phi)\right]$$

$$= 4\ N\ K_\omega^2\ \omega\left[D\frac{di_1}{dt} + E\cos\ 2\ p\delta\ \frac{di_1}{dt} - E\ \omega\ i_1\ \sin 2p\delta\right] \qquad (9.29)$$

9.5.5. Axis Reactances

Equation indicates the armature reaction at any general position of the rotor. The impedance component can now be separated into resistive and reactive parts.

Thus $R_{eff} = -4N\ K_\omega^2\ \omega\ E\sin 2p\delta$ (9.30)

and $X_{eff} = 4\ N\ K_\omega^2\omega\ (D + E\cos 2p\delta)$ (9.31)

The energy dissipated in R_{eff} is that converted to in R_{eff} mechanical output, and its dependence on load angle δ is very much apparent. But practically, in addition to the voltage represented by equation (9.29) there are also leakage reactance voltages due to slot and end turn fluxes which do not depend on the rotor position.

The net reactances along the d and q - axis are then obtained by putting $p\delta = 0, \frac{\pi}{2}$, respectively in equation 9.31 and adding leakage reactance to the resulting expressions which yields

$$X_d = X_{ad} + X_e$$
$$= 4 N K_\omega^2 \omega (D + E) + X_o$$

and

$$X_q = X_{aq} + X_o$$
$$= 4 N K_\omega^2 \omega (D - E) + X_o$$

If leakage reactance is neglected X_d and X_q can be written as,

$$X_d = \frac{24 N^2 K_\omega^2 \omega}{\pi} (\lambda_o + \frac{1}{2} \lambda_{4p}) \qquad (9.32)$$

$$X_q = \frac{24 N^2 K_\omega^2 \omega}{\pi} (\lambda_o - \frac{1}{2} \lambda_{4p}) \qquad (9.33)$$

9.6 DETERMINATION OF ROTOR MAGNETIC POTENTIAL (with interpolar channels)

Eqn 3.31 is rewritten as:

$$\frac{D}{G}\left[H_{1q}\frac{\sin p\theta}{p} - P_1\theta\right]_0^{\alpha_1} + \frac{D}{G}\left[H_{1q}\frac{\sin p\theta}{p} - P_1\theta\right]_{\alpha_1}^{\alpha_4}$$

$$+ \frac{D}{G}\left[H_{1q}\frac{\sin p\theta}{p} - P_1\theta\right]_{\alpha_4}^{\frac{\pi}{2}-\alpha_4'} + \frac{D}{G}\left[H_{1q}\frac{\sin p\theta}{p} - P_1\theta\right]_{\frac{\pi}{2}-\alpha_4'}^{\frac{\pi}{2}-\alpha_1'}$$

$$+ \frac{D}{G}\left[H_{1q}\frac{\sin p\theta}{p} - P_1\theta\right]_{\pi/2-\alpha_1'}^{\pi/2} = 0$$

$$\text{or } H_{1q}\left[\frac{\sin p\alpha_1}{pG} + \frac{\sin p\alpha_4 - \sin p\alpha_1}{pG} + \frac{\sin p(\frac{\pi}{2}-\alpha_4') - \sin p\alpha_4}{G}\right.$$

$$\left. + \frac{\sin p(\frac{\pi}{2}-\alpha_1') - \sin p(\frac{\pi}{2}-\alpha_4')}{pG} + \frac{\sin p(\frac{\pi}{2}) - \sin p(\frac{\pi}{2}-\alpha_1')}{pG}\right]$$

$$= P_1\left[\frac{\alpha_1}{G} + \frac{\alpha_4 - \alpha_1}{G} + \frac{\frac{\pi}{2} - \alpha_4' - \alpha_4}{G} + \frac{\alpha_4' - \alpha_1'}{G} + \frac{\alpha_1'}{G}\right]$$

$$\text{or } P_1 = \frac{H_{1q}\left[\left\{\sin p\alpha_4 - \sin p\alpha_1 - \sin p(\frac{\pi}{2}-\alpha_4') + \sin p(\frac{\pi}{2}-\alpha_1')\right\}(1 - \ldots\right.}{(\alpha_4 - \alpha_1 + \alpha_4' - \alpha_1')(1 - \frac{1}{h}) + \frac{\pi}{2h}} \tag{9.34}$$

9.7 DETERMINATION OF QUADRATURE AXIS FLUX DENSITY

The expression of Sec. 3.4.2 is rewritten as :

$$B_{1q} = \frac{4}{\pi}\left[\int_0^{\pi/2} (H_{1q}\,\lambda(\theta)\,\cos^2 p\theta - p_1)\,(\cos p\theta\,)\,d\theta\right]$$

$$= \frac{4}{\pi}\left[H_{1q}\,\lambda(\theta)\int_0^{\pi/2}\frac{p + \cos 2p\theta\,d\theta}{2} - \int_0^{\pi/2} p_1 .\,\lambda(\theta)\cos p\theta\,d\theta\right]$$

First term in this equation is same as Eqn in sec. 9.3 The substitution for this yields

$$B_{1q} = \frac{2\mu_0}{\pi g}\,H_{1q}\left[\frac{\pi}{2h} + (\alpha_4 - \alpha_1 + \alpha_4' - \alpha_1')\,(1 - \frac{1}{h}\,)\right.$$

$$+ \frac{1}{2p}\left\{\sin 2p\alpha_4 - \sin 2p\alpha_1 - \sin 2p\,(\frac{\pi}{2} - \alpha_4') - \sin 2p(\frac{\pi}{2} - \alpha_1')\right\}$$

$$\left. .\,(1 - \frac{1}{h}\,)\right] - \frac{4}{\pi\,p}\Big[p_1\lambda(\theta)\,\sin p\theta\Big]_0^{\pi/2}$$

Substituting for $\lambda(\theta)$ from Table 3.3. the last term becomes,

$$= \frac{-4}{\pi p}\;P_1\left[\frac{\mu_0}{G}\Big|\sin p\,\theta\Big|_0^{\alpha_1} + \frac{\mu_0}{g}\Big|\sin p\theta\Big|_{\alpha_1}^{\alpha_4} + \frac{\mu_0}{G}\Big|\sin p\theta\Big|_{\alpha}^{\frac{\pi}{2}}\right.$$

$$\left. + \frac{\mu_0}{g}\Big|\sin p\theta\Big|_{\frac{\pi}{2}-\alpha_4'}^{\frac{\pi}{2}-\alpha_1'} + \frac{\mu_0}{G}\Big|\sin p\theta\Big|_{\pi/2-\alpha_1'}^{\pi/2}\right]$$

$$= -\frac{4\mu_0}{\pi p}\,P_1\left[\frac{\sin p\alpha_1}{G} + \frac{\sin p\alpha_4 - \sin p\alpha_1}{g}\right.$$

$$+ \frac{\sin p(\frac{\pi}{2} - \alpha_4'\,) - \sin p\alpha}{G} + \frac{\sin p(\frac{\pi}{2} - \alpha_1') - \sin p(\frac{\pi}{2} - \alpha_4')}{g}$$

$$\left. + \frac{\sin p\,\frac{\pi}{2} - \sin p(\,\frac{\pi}{2} - \alpha_1')}{G}\right]$$

$$= \frac{-4\mu_o p_1}{\pi p}\left[\left(\sin p\alpha_4 - \sin p\alpha_1 - \sin p\left(\frac{\pi}{2} - \alpha_4'\right) + \sin p\left(\frac{\pi}{2} - \alpha_1'\right)\right)\left(1 - \frac{1}{h}\right)\right]$$

After substituting value of p_1 expression for B_{1q} can be written as ,

$$B_{1q} = \frac{2\mu_o H_{1q}}{\pi g}\left[\frac{\pi}{2h} + (\alpha_4 - \alpha_1 + \alpha_4' - \alpha_1')\left(1 - \frac{1}{h}\right) + \frac{1}{2p}\left\{\left[\sin 2p\alpha_1 - \sin 2p\alpha_4 - \sin p\left(\frac{\pi}{2} - \alpha_4'\right) + \sin 2p\left(\frac{\pi}{2} - \alpha_1'\right)\right]\right\}\left(1 - \frac{1}{h}\right) - \frac{\frac{2}{p}\left\{\left[\sin p\alpha_4 - \sin p\alpha_1 - \sin p\left(\frac{\pi}{2} - \alpha_4'\right) + \sin p\left(\frac{\pi}{2} - \alpha_1'\right)\right]\left(1 - \frac{1}{h}\right)\right\}}{\frac{\pi}{2h} + (\alpha_4 - \alpha_1 + \alpha_4' - \alpha_1')\left(1 - \frac{1}{h}\right)}\right]$$

(9.35)

9.8 DETERMINATION OF ROTOR MAGNETIC POTENTIALS

9.8.1 For determination of P_s the net flux in the region α_3 to $\frac{\pi}{2} - \alpha_3'$ is equated to zero. This has already been done in sec. 9.2.1 The same result holds good here also.

9.8.2 Determination of P_2

The flux in the region 0 to α_3 is equated to zero, which is,

$$2\left[\int_0^{\alpha_1} \frac{\mu_o}{G}(H_{1q}\cos p\theta + P_2)\frac{D}{2}d\theta + \int_{\alpha_1}^{\alpha_3} \frac{\mu_o}{g}(H_{1q}\cos p\theta - P_2)\frac{D}{2}d\theta + \frac{\mu_o}{1}\cdot(-P_2 + P_3)\frac{W}{2T}\right] = 0$$

or $\frac{D}{G}\left[H_{1q}\frac{\sin p\theta}{p}-P_2\theta\right]_0^{\alpha_1}+\frac{D}{g}\left[H_{1q}\frac{\sin p\theta}{p}-P_2\theta\right]_{\alpha_1}^{\alpha_3}$

$+(-P_2+P_3)\frac{W}{T}=0$

or

$$H_{1q}\left[\frac{\sin p\alpha_1}{pG/D}+\frac{\sin p\alpha_3-\sin p\alpha_1}{pg/D}\right]+P_3\frac{W}{T}$$

$$=P_2\left[\frac{\alpha_1}{G/D}+\frac{\alpha_3-\alpha_1}{g/D}+\frac{W}{T}\right]$$

or

$$P_2=\frac{H_{1q}\quad\frac{\sin p\alpha_1}{PG/D}+\frac{\sin p\alpha_3-\sin p\alpha_1}{pg/D}\quad+\frac{AW}{BT}+P_2'\frac{W'}{T'}\quad\frac{W}{T}}{\frac{\alpha_1}{pG/D}+\frac{\alpha_3-\alpha_1}{g/D}+\frac{W}{T}-\frac{1}{B}(W/T)^2}$$

Las-t ferm in the expression, when divided by denominator, becomes, too small to effect the value of P_2.

$$\text{Hence } P_2=\frac{H_{1q}\left[\frac{\sin p\alpha_1}{pG/D}+\frac{\sin p\alpha_3-\sin p\alpha_1}{pg/D}\right]+\frac{A}{B}\cdot\frac{W}{T}}{\frac{\alpha_1}{G/D}+\frac{\alpha_3-\alpha_1}{g/D}+\frac{W}{T}-\frac{1}{B}\left(\frac{W}{T}\right)^2}\tag{9.36}$$

9.8.3 For determination of P_2', flux in the region $\frac{\pi}{2}-\alpha_3'$ to $\pi/2$ is equated to zero, which gives the expression:

$$2\left[\frac{\mu_o}{g}\int_{\pi/2-\alpha_3'}^{\pi/2-\alpha_1'}(H_{1q}\cos p\theta - P_2')\frac{D}{2}\,d\theta + \right.$$

$$\left. + \int_{\pi/2-\alpha_1'}^{\pi/2}\frac{\mu_o}{G}(H_{1q}\cos p\theta - P_2')\,\frac{D}{2}\,d\theta + (P_3-P_2')\,\frac{W'}{2T'}\right] = 0$$

or

$$\frac{D}{g}\left[H_{1q}\,\frac{\sin p\theta}{P} - P_2'\theta\right]_{\frac{\pi}{2}-\alpha_3'}^{\frac{\pi}{2}-\alpha_1'} + \frac{D}{G}\left[H_{1q}\frac{\sin p\theta}{P} - P_2'\theta\right]_{\frac{\pi}{2}-\alpha_1'}^{\pi/2}$$

$$+ (P_3 - P_2')\,\frac{W'}{T'} = 0$$

$$\text{or}\quad H_{1q}\left[\frac{\sin P(\frac{\pi}{2}-\alpha_1') - \sin p(\frac{\pi}{2}-\alpha_3')}{Pg/D} + \frac{\sin p\frac{\pi}{2} - \sin p(\frac{\pi}{2}-\alpha_1')}{PG/D}\right]$$

$$+\frac{A}{B}\,\frac{W'}{T'} + \frac{P_2}{B}\;\frac{W}{T}\;\frac{W'}{T'} = P_2'\left[\frac{\alpha_3'-\alpha_1'}{g/D} + \frac{\alpha_1'}{G/D} + \frac{W'}{T_1'}\right.$$

$$\left. - \frac{1}{B}\left(\frac{W'}{T'}\right)^2\right]$$

or,

$$P_2' = \frac{H_{1q}\left[\dfrac{\sin p(\frac{\pi}{2}-\alpha_1') - \sin p(\frac{\pi}{2}-\alpha_3')}{pg/D} + \dfrac{\sin p\frac{\pi}{2} - \sin p(\frac{\pi}{2}-\alpha_1')}{PG/D}\right] + \dfrac{AW'}{B\,T'}}{\dfrac{\alpha_3'-\alpha_1'}{g/D} + \dfrac{\alpha_1'}{G/D} + \dfrac{W'}{T'} - \dfrac{1}{B}\left(\dfrac{W'}{T'}\right)^2}$$

9.9 QUADRATURE AXIS FLUX DENSITY

Expression for B_{1q} is given in Sec. 3.5.3 as

$$B_{1q} = \frac{4}{\pi}\left[\int_0^{\pi/2} \left(H_{1q}\, \lambda(\theta) \cos^2 p\theta - P(\theta)\, \lambda(\theta) \cos p\theta\right) d\theta\right]$$

$$= \frac{4}{\pi}\left[H_{1q}\, \lambda(\theta) \int_0^{\pi/2} \frac{1+\cos 2p\theta}{2}\, d\theta - \int_0^{\pi/2} P(\theta)\, \lambda(\theta) \cos p\theta\, d\theta\right]$$

First term is same as in Eqn. 9.23 of Section 9.3.6.
Therefore,

$$B_{1q} = \frac{2\mu_o H_{1q}}{\pi g}\left[\frac{\pi}{2h} + (\alpha_4 - \alpha_1 + \alpha'_4 - \alpha'_1)\left(1 - \frac{1}{h}\right) + \frac{1}{2p}\left\{\sin 2p\alpha_4 - \sin 2p\alpha_1 - \sin 2p\left(\frac{\pi}{2} - \alpha'_4\right) + \sin 2p\left(\frac{\pi}{2} - \alpha'_1\right)\right\}\left(1 - \frac{1}{h}\right)\right]$$

$$- \frac{4}{\pi p}\Big[P(\theta)\, \lambda(\theta) \sin p\theta\Big]_0^{\pi/2}$$

Last term can be expanded after substituting for $\lambda(\theta)$ and $P(\theta)$ as:

$$- \frac{4}{\pi p}\Bigg[\left|P_2 \frac{\mu_o}{g} \sin p\theta\right|_0^{\alpha_1} + \left|P_2 \frac{\mu_o}{g} \sin p\theta\right|_{\alpha_1}^{\alpha_3} + \left|P_3 \frac{\mu_o}{g} \sin p\theta\right|_{\alpha_3}^{\alpha_4}$$

$$+ \left|P_3 \frac{\mu_o}{g} \sin p\theta\right|_{\alpha_4}^{\frac{\pi}{2} - \alpha'_4} + \left|P_3 \frac{\mu_o}{g} \sin p\theta\right|_{\frac{\pi}{2} - \alpha'_4}^{\frac{\pi}{2} - \alpha'_3} + \left|P'_2 \frac{\mu_o}{g} \sin p\theta\right|_{\frac{\pi}{2} - \alpha'_3}^{\frac{\pi}{2} - \alpha'_1}$$

$$+ \left|P'_2 \frac{\mu_o}{g} \sin p\theta\right|_{\frac{\pi}{2} - \alpha'_1}^{\pi/2}\Bigg]$$

$$= -\frac{4\mu_o}{\pi p}\left[P_2\frac{\sin p\alpha_1}{G} + P_2\frac{(\sin p\alpha_3 - \sin p\alpha_1)}{g} + \frac{P_3(\sin p\alpha_4 - \sin p\alpha_3)}{g}\right.$$

$$+\frac{P_3(\sin p(\frac{\pi}{2} - \alpha_4') - \sin p\alpha_4)}{G} + \frac{P_3(\sin p(\frac{\pi}{2}-\alpha_3') - \sin p(\frac{\pi}{2}-\alpha_4'))}{g}$$

$$\left. + \frac{P_2'(\sin p(\frac{\pi}{2}-\alpha_1') - \sin p(\frac{\pi}{2}-\alpha_3'))}{g} + \frac{P_2'(\sin p(\frac{\pi}{2}) - \sin p(\frac{\pi}{2}-\alpha_1'))}{G}\right]$$

$$= -\frac{4\mu_o}{\pi p g}\left[\left[\left\{-P_2\sin p\alpha_1 + P_3\left\{\sin p\alpha_4 - \sin p(\frac{\pi}{2}-\alpha_4')\right\}\right.\right.\right.$$

$$\left.\left. + P_2'\sin p(\frac{\pi}{2}-\alpha_1')\right\}\right](1-\frac{1}{h}) + (P_2-P_3)\sin p\alpha_3 + (P_3-P_2')\sin p(\frac{\pi}{2}-\alpha_3')$$

$$\left. + \frac{P_2'\sin p\frac{\pi}{2}}{h}\right]$$

Than the final expression for B_{1q} becomes,

$$B_{1q} = \frac{2\mu_o H_{1q}}{\pi g}\left[\frac{\pi}{2h} + (\alpha_4 - \alpha_1 + \alpha_4' - \alpha_1')(1-\frac{1}{h}) + \frac{1}{2p}\left\{\sin 2p\alpha_4 - \sin 2p\alpha\right.\right.$$

$$\left. - \sin 2p(\frac{\pi}{2}-\alpha_4') + \sin 2p(\frac{\pi}{2}-\alpha')\right\}(1-\frac{1}{h}) - \frac{2}{pH_{1q}}\left\{\left[-P_2\sin p\alpha_1\right.\right.$$

$$\left. + P_3(\sin p\alpha_4 - \sin p(\frac{\pi}{2}-\alpha_4')) + (P_2')\sin p(\frac{\pi}{2}-\alpha_4')\right](1-\frac{1}{h})$$

$$\left.\left. + (P_2-P_3)\sin p\alpha_3 + (P_3-P_2')\sin p(\frac{\pi}{2}-\alpha_3') + P_2'\sin p\frac{\pi}{2}/h\right\}\right]$$

(9.38)

APPENDIX 9.10

```
MAIN PROGRAM
DIMENSIONGR(10),GR1(10),H1(10),H2(10),H3(10),H(10,10),X1(10),
1X(10),DGR(10),DXX(10)
READ 1000,K2
READ 2000,(X(I),I=1,K2)
READ 2000,RO,OX2,OXX,OX1
CALL FUN(X,F1)
ITER=0
DO 30 I=1,K2
DO 30 J=1,K2
IF(I-J)20,10,20
H(I,J)=1.0
GO TO 30
H(I,J)=0.0
CONTINUE
CALL GRAD(X,GR)
DO 40 I=1,K2
GRA=ABSF(GR(I))
IF(GRA-OX2)40,40,50
CONTINUE
GO TO 180
DO 60 I=1,K2
H1(I)=0.0
DO 60 J=1,K2
H1(I)=H1(I)-H(I,J)*GR(J)
SP=0.0
DO 62 I=1,K2
SP=SP+H1(I)*H1(I)
SP=SQRTF(SP)
DO 63 I=1,K2
H1(I)=H1(I)/SP
CALL GOLDSE(X,RO,GR,H1,OXX,ITER,F,K2,TP,X1)
FAB=(F-F1)
IF(FAB)71,5,5
FAB=ABSF(FAB)
IF(FAB-OX1)180,180,72
CALL GRAD(X1,GR1)
DO 75 I=1,K2
AGR=ABSF(GR1(I))
IF(AGR-OX2)75,75,78
CONTINUE
GO TO 180
DO 80 I=1,K2
DXX(I)=X1(I)-X(I)
DGR(I)=GR1(I)-GR(I)
SUM1=0.0
SUM2=0.0
DO 120 I=1,K2
H2(I)=0.0
```

```
      H3(I)=0.0
      DO 110 J=1,K2
      H2(I)=H2(I)-H(I,J)*DGR(J)
  110 H3(I)=H3(I)+DGR(J)*H(J,I)
      SUM1=SUM1+DXX(I)
  120 SUM2=SUM2+H3(I)*DGR(I)
      DO 130 I=1,K2
      DO 130 J=I,K2
      H(I,J)=H(I,J)+DXX(I)*DXX(J)/SUM1+H2(I)*H3(J)/SUM2
  130 H(J,I)=H(I,J)
      DO 170 I=1,K2
      GR(I)=GR1(I)
  170 X(I)=X1(I)
      PUNCH6000,ITER
      PUNCH5000,(GR(I),I=1,K2)
      PUNCH5000,(X(I),I=1,K2)
      ITER=ITER+1
      PUNCH5000,F
      F1=F
      GO TO 50
 6000 FORMAT(20X,14HITERATION NO =,I5,13HGRADIENTS ARE)
 2000 FORMAT(7F10.5)
 1000 FORMAT(2I5)
 5000 FORMAT((E13.6)
  180 STOP
      END
```

APPENDIX 9.11

```
      SUBROUTINE GOLDSE(X,STEP,GR,S,FTOL,ITER,FY,K2,DP,Y)
      DIMENSION X(10),Y(10),S(10),GR(10)
      IPRIT=1
      IEXIT=0
      NTOL=0
      FTOL2=FTOL/100.
      CALL FUN(X,FX)
      FA=FX        $    FB=FX    $    FC=FX
      DZ=0.     $    DB=0.      $     DC=0.
      KK=-2
      M=0
      DP=STEP
    1 DO 2 I=1,K2
    2 Y(I)=X(I)+DP*S(I)
      CALL FUN(Y,FF)
      IF(ITER-1)351,351,352
  351 PUNCH7000,FF,DP,(Y(I),I=1,K2)
  352 KK=KK+1
      IF(FF-FA)5,3,6
    3 DO 4 I=1,K2
    4 Y(I)=X(I)+DZ*S(I)
```

```
      FY=FA
      DP=DA
      PUNCH7000,DA
      IF(IPRIT-1)60,55,60
 55   PUNCH2100
 60   GO TO324
  5   FC=FB     $    FB=FA     $       FA=FF
      DC=DB     $    DB=DZ       $       DZ=DP
      DP=2.0*DP+STEP
      GO TO 1
   6  IF(KK)7,8,9
   7  FB=FF
      DB=DP     $    DF=-DP    $  STEP=-STEP
      GO TO 1
   8  FC=FB     $    FB=FA     $     FA=FF
      DC=DB     $    DB=DZ     $    DZ=DP
      GO TO 21
  9   DC=DB     $    DB=DZ     $   DZ=DP
      FC=FB     $    FB=FA     $    FA=FF
 10   DP=0.5*(DZ+DB)
      IF(ITER-4)353,353,354
353   PUNCH7000,FF,DP,(Y(I),I=1,K2)
354   DO 11 I=1,K2
 11   Y(I)=X(I)+DP*S(I)
      CALL FUN(Y,FF)
 12   DXY=(DC-DP)*(DP-DB)
      IF(DXY)15,13,18
 13   DO 14 I=1,K2
 14   Y(I)=X(I)+DB*S(I)
      FY=FB
      DP=DB
      IF(IEXIT-1)62,61,62
 61   GO TO32
 62   IF(IPRIT-1)64,63,64
 63   PUNCH2200
 64   GO TO325
 15   FC=FB     $   FB=FF
      DZ=DB      $    DB=DP
      GO TO21
 18   IF(FF-FB)19,13,20
 19   FA=FB     $     FB=FF
      DZ=DB      $      DB=DP
      GO TO 21
 20   FC=FF
      DC=DP
 21   AZ=FA*(DB-DC)+FB*(DC-DZ)+FC*(DZ-DB)
      IF(AZ)22,30,22
 22   DP=0.5*((DB*DB-DC*DC)*FA+(DC*DC-DZ*DZ)*FB+(DZ*DZ-DB*DB)*FC)/AZ
      DDA=(DZ-DP)*(DP-DC)
```

```
      IF(DDA)13,13,23
   23 DO 24 I=1,K2
   24 Y(I)=X(I)+DP*S(I)
      CALL FUN(Y,FF)
      IF(ABSF(FB)-FTOL2)25,25,26
   25 AZ=1.0
      GO TO 27
   26 AZ=1.0/FB
   27 ADX=ABSF(FB-FF)*AZ-FTOL
      IF(ADX)18,28,12
   28 IEXIT=1
      IF(FF-FB)29,13,13
   29 FY=FF
      GO TO 32
   30 IF(M)31,31,13
   31 M=M+1
      GO TO 10
   32 DO99I=1,K2
      IF(Y(I)-X(I))325,99,325
   99 CONTINUE
      GO TO 33
  325 IF(NTOL)328,326,328
  328 IF(IPRIT-1)326,330,326
  330 PUNCH3000,NTOL
  326 IF(FY-FX)345,335,335
  335 AGX=-GR(I)
      IF(S(I)-AGX)340,336,340
  336 IF(FY-FX)345,338,338
  338 PUNCH5000
   33 IF(NTOL-5)339,340,339
  339 IEXIT=0
      NTOL=NTOL+1
      FTOL=FTOL/10.
      GO TO 12
  340 PUNCH7000,DF
 7000 FORMAT(13F6.3)
 2100 FORMAT(13HSEARCH FAILED)
 2200 FORMAT(25HSEARCH FAILED BY ROUNDING)
 3000 FORMAT(17HTOLERANCE REDUCED,I2)
 5000 FORMAT(18HSEARCH FAILED GRAD)
  345 RETURN
      END
```

APPENDIX 9.12

```
      SUBROUTINE FUN(X,F)
      DIMENSION X(10)
      A12=SINF(6.*X(1))-SINF(6.*(X(1)+X(2)))
      A12=(A12-SINF(6.*X(4))+SINF(6.*(X(3)+X(4))))/6.
      A16=SINF(8.*X(1))-SINF(8.*(X(1)+X(2)))
      A16=(A16-SINF(8.*(X(3)+X(4)))+SINF(8.*X(4)))/8.
```

```
F=A12+A16
F=-F
RETURN
END
```

APPENDIX 9.13

```
SUBROUTINE GRAD(X,GR)
DIMENSION X(10),GR(10)
GR1=COSF(6.*X(1))-COSF(6.*(X(1)+X(2)))
GR(1)=GR1+COSF(8.*X(1))-COSF(8.*(X(1)+X(2)))
GR(1)=-GR(1)
GR(2)=-COSF(6.*(X(1)+X(2)))-COSF(8.*(X(1)+X(2)))
GR(2)=-GR(2)
GR(3)=COSF(6.*(X(3)+X(4)))-COSF(8.*(X(3)+X(4)))
GR(3)=-GR(3)
GR4=COSF(6.*(X(3)+X(4)))-COSF(6.*X(4))
GR(4)=GR4+COSF(8.*X(4))-COSF(8.*(X(3)+X(4)))
GR(4)=-GR(4)
RETURN
END
```

APPENDIX 9.14

```
SUBROUTINE FUN(X,F)
DIMENSION X(10)
A12=SINF(6.*X(1))-SINF(6.*(X(1)+X(2)))
A12=(A12-SINF(6.*X(3))+SINF(6.*(.80-X(2)+X(3))))/6.
A16=SINF(8.*X(1))-SINF(8.*(X(1)+X(2)))
A16=(A16-SINF(8.*(.80-X(2)+X(3)))+SINF(8.*X(3)))/8.
F=A12+A16
F=-F
RETURN
END
```

APPENDIX 9.15

```
SUBROUTINE GRAD(X,GR)
DIMENSION X(10),GR(10)
GR1=COSF(6.*X(1))-COSF(6.*(X(1)+X(2)))
GR(1)=GR1+COSF(8.*X(1))-COSF(8.*(X(1)+X(2)))
GR(1)=-GR(1)
GR2=-COSF(6.*(X(1)+X(2)))-COSF(6.*(.80-X(2)+X(3)))
GR(2)=GR2-COSF(8.*(X(1)+X(2)))+COSF(8.*(.80-X(2)+X(3)))
GR(2)=-GR(2)
GR3=-COSF(6.*X(3))+COSF(6.*(.80-X(2)+X(3)))
GR(3)=GR3-COSF(8.*(.80-X(2)+X(3)))+COSF(8.*X(3))
GR(3)=-GR(3)
RETURN
END
```

9.16 Determination of A and B

The expression for torque T_a is :

$$T_a = AS^2 + BS - C$$

At slip S_1 T_a will have some known value T_{a_1} and at slip S_2 T_a will be T_{a_2}.

So,

$$T_{a_1} = AS_1^2 + BS_1 - C$$

and $$T_{a_2} = A S_2^2 + BS_2 - C$$

or $$S_1^2 A + S_1 B - C - T_{a1} = 0$$

and $$S_2^2 A + S_2 B - C - T_{a_2} = 0$$

Solving two simultaneous equations in A and B

$$A = \frac{(T_{a1} S_2 - T_{a2} S_1) - C(S_1 - S_2)}{S_1 S_2 (S_1 - S_2)} \tag{9.39}$$

$$\text{and } B = \frac{1}{S_1} (T_{a_1} + C - S_1^2 A) \tag{9.40}$$

9.17 Determination of Slip S_a

S_o is the slip at the beginning of the synchronising attempt and net torque at this point is zero.

Therefore $T = 0 = T_a + T_r' - T_1$ (from Eqn. 5.10)

or $$AS_o^2 + BS_o - C + T_{r_o}' - T_1 = 0$$

where T_{r_o}' is the value of T_r' at S_o slip.

$$\text{or } AS_o^2 + BS_o - (T_1 + C - T'_{ro}) = 0$$

$$\therefore \quad S_o = \frac{-B \pm \sqrt{B^2 + 4A(T_1 + C - T'_{ro})}}{2A}$$

so

$$S_o = \frac{1}{2A}\left[-B + \left\{B^2 + 4A(T_1 + C - T'_{ro})\right\}^{1/2}\right] \tag{9.41}$$

The negative sign is not considered as it is not realised.

9.18 Determination of Criterion for Pull - in

The equation to be integrated as stated in Sec. 5.4 is

$$J\frac{d^2\delta}{dt^2} + B_M\frac{d\delta}{dt} + K\delta = T_t$$

$$\text{or } J\frac{dS^2}{dt^2} + B_M\frac{d\delta}{dt} + K\delta = AS^2 + BS - C + T_r + C - T_1$$

$$\text{or } JS\frac{dS}{d\delta} + B_M S + K\delta = AS_o^2\cos^2(\delta+\delta_f+2\delta_1) + BS_o\cos(\delta+\delta_f+2\delta_1)$$

$$-C + D\cos 2\delta + E\sin^2\delta - T_1$$

$$\text{or } JS\frac{dS}{d\delta} + B_M S + K\delta = AS_o^2\left[\frac{1 + \cos 2(\delta+\delta_f+2\delta_1)}{2}\right]$$

$$+ BS_o\cos(\delta+\delta_f+2\delta_1) - C + D\cos 2\delta + E\sin 2\delta - T_1$$

$$\text{or} \int_{S_{in},\delta_{in}}^{S_{fin.},\delta_{fin}} \left(JS\frac{dS}{d\delta} + B_M S + K\delta\right) = \int \frac{AS_o^2}{2} + \frac{AS_o^2}{2}\cos 2(\delta+\delta_f+2\delta_1)$$

$$+ BS_o \cos(\delta+\delta_f+2\delta_1) + D\cos 2\delta + E\sin 2\delta = (T_1 + C)$$

$$\text{or} \int_{S_{in},\, \delta_{in}}^{S_{fin.},\, \delta_{fin.}} JS\, dS + B_M S_o \cos(\delta + \delta_f + 2\delta_1)\, d\delta + K\delta\, d\delta$$

$$= \int \left[\frac{AS_o^2}{2} + \frac{AS_o^2}{2}\cos 2(\delta+\delta_f+2\delta_1) + B S_o \cos(\delta+\delta_f+2\delta_1)\right.$$

$$\left. + D\cos 2\delta + E\sin 2\delta = (T_1 + C)\right] d\delta$$

$$\text{or} \left[\frac{JS^2}{2} + B_M S_o \sin(\delta+\delta_f+2\delta_1) + \frac{K\delta^2}{2}\right]_{S_o,\, \delta_o}^{0,\, \pi/2 + \delta_o}$$

$$= \left[\frac{AS_o^2}{2}\delta + \frac{AS_o^2}{4}\sin 2(\delta_o+\delta_f+2\delta_1) + BS_o \sin(\delta+\delta_f+2\delta_1)\right.$$

$$\left. + \frac{D}{2}\sin 2\delta - \frac{E\cos 2\delta}{2} - (T_1 + C)\delta\right]_{S_o,\, \delta_o}^{0,\, \pi/2 + \delta_o}$$

$$- \frac{JS_o^2}{2} + B_M S_o + \frac{K}{2}\left\{\left(\frac{\pi}{2} + \delta_o\right)^2 - \delta_o^2\right\}$$

$$= \frac{AS_o^2}{2}\,\frac{\pi}{2} + BS_{Mo} - \frac{D}{2}\sin 2\delta_o - \frac{D}{2}\sin 2\delta_o + \frac{E}{2}\cos 2\delta_o$$

$$+ \frac{E}{2}\cos 2\delta_o - (T_1 + C)\frac{\pi}{2}$$

or $$-\frac{J\delta_o^2}{2} = \Big[-D\sin 2\delta_o + E\cos 2\delta_o + (B - B_M)\delta_o - \frac{K}{2}\left(\frac{\pi^2}{4} + \pi\,\delta_o\right) - \left(T_1 + C - \frac{A\delta_o^2}{2}\right)\frac{\pi}{2}\Big]$$

or $$J = -\frac{2}{\delta_o^2}\Big[-D\sin 2\delta_o + E\cos 2\delta_o + (B - B_M)\delta_o - \left(T_1 + C - \frac{A\delta_o^2}{2} + \frac{K\pi}{4} - K\delta_o\right)\frac{\pi}{2}\Big]$$

(9.42).